

ANALYTICAL ESTIMATION OF THERMAL  
PROPERTIES AND VARIATION OF  
TEMPERATURE IN ASPHALTIC PAVEMENTS

Thesis for the Degree of Ph. D.  
MICHIGAN STATE UNIVERSITY  
AKBAR KAVIANIPOUR  
1971

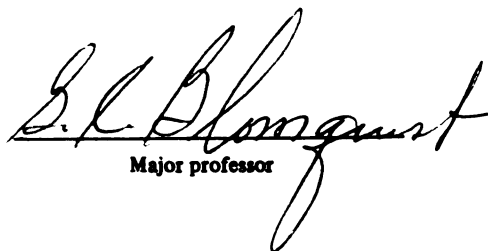


This is to certify that the  
thesis entitled  
"Analytical Estimation of Thermal  
Properties and Variation of  
Temperature in Asphaltic Pavements

presented by  
Akbar Kavianipour

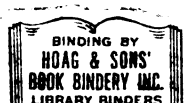
has been accepted towards fulfillment  
of the requirements for

Ph.D. degree in Civil Engineering

  
Major professor

Date Nov. 9, 1971

0-7639





## ABSTRACT

### ANALYTICAL ESTIMATION OF THERMAL PROPERTIES AND VARIATION OF TEMPERATURE IN ASPHALTIC PAVEMENTS

By

Akbar Kavianipour

The recent developments of full-depth asphaltic pavement for use in heavy duty highways and airports requires a more comprehensive study of thermal behavior and variation of temperature in the pavement structure. The consideration of variation of temperature at various depths of the pavement is necessary in the study of pavement deflection, load capacity, and rheological characteristics of asphaltic pavements during the winter and summer months.

The variation of temperature at various depths of a 19-inch full-depth pavement of Bishop Airport, Flint, Michigan, was recorded over a period of two years (1969-70). Similar data from a 7-inch asphaltic pavement was also employed in this study.

Daily and monthly variations of temperature at varying depths, due to the change in ambient temperature, are obtained for different seasons of the year. The



nonlinear estimation procedure, which is an extension of least-square analysis, is applied to calculate thermal properties of pavement material from recorded temperature data.

Laboratory experiments were performed on samples of asphaltic concrete and the measured temperature recorded as the function of time and position. A criterion is developed to determine the optimum experiment and the location of the thermocouple. A simple method is derived for calculating the thermal diffusivity of pavement material from recorded as well as experimentally measured temperature data.

A new method is proposed for directly calculating the thermal conductivity,  $K$ , and specific heat from temperature and heat flux boundary conditions. Calibrations of pavement temperature, as well as prediction of frost penetration, requires the knowledge of surface pavement temperature from air temperature which is related to the heat transfer coefficient  $h_c$  between the air and the pavement surface. A method of obtaining this heat transfer coefficient, is given, for the case of negligible radiant heat transfer. Thermal properties of asphaltic concrete are calculated by the nonlinear estimation method, as well as the simplified method, and the results are compared with each other.

Various methods of calculating temperature in the pavement are introduced. Temperature in the soil-pavement system is calculated by using a modified Crank-Nicolson difference approximation (49) applied to the heat-conduction equation. A comparison between the calculated and the measured temperatures at various depths of the pavement is given. Recommendations are made for the extension of this research.

ANALYTICAL ESTIMATION OF THERMAL PROPERTIES  
AND VARIATION OF TEMPERATURE IN  
ASPHALTIC PAVEMENTS

By

Akbar Kavianipour

A THESIS

Submitted to  
Michigan State University  
in partial fulfillment of the requirements  
for the degree of

DOCTOR OF PHILOSOPHY

Department of Civil Engineering

1971

## ACKNOWLEDGMENTS

The writer is greatly indebted to his major advisor, Dr. G. C. Blomquist, for his encouragement and guidance.

The writer wishes to express his deepest gratitude to Dr. J. V. Beck, for his supervision and suggestion of the basic concept for measurement of thermal diffusivity using the simplified method.

The writer is also indebted to the other members of his guidance committee: Dr. O. B. Andersland, Dr. M. M. Mortland, and Dr. J. W. Trow.

Appreciation must also be expressed to Mr. G. P. Manz, and the Asphalt Institute Association, whose sponsorship in providing the raw data made the investigation possible.

The writer also wishes to thank Maryellen Jones for her cooperation and assistance in typing the preliminary manuscript of this dissertation.

## TABLE OF CONTENTS

	Page
LIST OF TABLES . . . . .	vi
LIST OF FIGURES. . . . .	viii
INTRODUCTION. . . . .	1
PURPOSES . . . . .	4
 Chapter	
I. LITERATURE REVIEW. . . . .	6
1.1 Introduction. . . . .	6
1.2 Effect of Climate on Pavement Temperature and Frost Penetration. .	9
1.2.1 Solar Radiation . . . . .	10
1.2.2 Freezing Index. . . . .	11
1.2.3 Correlation Factor "n" . . . .	12
1.2.4 Pavement and Air Temperature .	13
1.3 Thermal Properties of Soils and Pavement Materials. . . . .	15
1.4 Estimated Thermal Properties Based on Published Data and Existing Prediction Equations . . . . .	16
1.4.1 Thermal Properties of Soils and Granular Systems. . . . .	16
1.4.2 Thermal Properties of Asphaltic Concrete . . . . .	27
1.4.2-1 Factors Influencing Thermal Properties of Asphaltic Concrete .	28
1.4.2-2 Changes in Volume and Density Due to Temperature. . . . .	30

Chapter	Page
1.4.2-3 Thermal Conductivity of Asphaltic Mixture . . .	32
1.4.2-4 Specific Heat Capacity of Asphaltic Mixture . . .	35
1.5 Estimated Thermal Properties of Pavement Materials Based on Field Temperature Measurement . . . . .	37
1.6 Temperature and Rheological Characteristics of Asphaltic Concrete. . . . .	43
II. DATA COLLECTION. . . . .	47
2.1 Site Location and Climate. . . . .	47
2.2 A Comparison Between the Recorded and the Long-Term Average Temperature . . . . .	47
2.3 Observation Period and Auxiliary Data. . . . .	49
2.4 Installation . . . . .	52
2.5 Thermocouples. . . . .	53
2.6 Data Analysis. . . . .	53
2.7 Daily Temperature Distribution . . . . .	57
2.8 Monthly Temperature Distribution . . . . .	63
2.9 The Effect of Snow . . . . .	69
2.10 Freezing Indices. . . . .	70
2.11 Correlation Factor "n". . . . .	73
2.12 Air and Surface Temperature . . . . .	75
III. EXPERIMENTATION. . . . .	77
3.1 Purpose of the Experiment. . . . .	77
3.2 Preparation of Test Specimen. . . . .	79
3.3 Facilities and Equipment . . . . .	81
3.4 Procedure . . . . .	83
3.5 Heat Flux Calculation . . . . .	85
3.6 Results. . . . .	86
IV. NONLINEAR ESTIMATION METHOD. . . . .	96
4.1 Nonlinear Estimation Method of Measuring Thermal Properties . . . . .	96
4.2 Nonlinear Estimation Procedure . . . . .	97
4.3 Computer Program. . . . .	100
4.3.1 Data Input . . . . .	101
4.3.2 Temperature Boundary Conditions . . . . .	101
4.3.3 Heat Flux Boundary Condition . . . . .	102
4.3.4 Other Variable Input . . . . .	103
4.4 Output and Results . . . . .	103

Chapter	Page
V. SIMPLIFIED METHOD . . . . .	112
5.1 Simplified Analysis for Estimation of Thermal Diffusivity Using the Laplace Transform . . . . .	112
5.2 Simplified Laplace Transform Method . . . . .	113
5.3 Laplace Transform Criteria . . . . .	118
5.4 The Optimum Experiment. . . . .	122
5.5 Optimum Location (x) . . . . .	123
5.6 Optimum "s" . . . . .	124
5.7 Heat Flux Condition. . . . .	129
5.8 Heat Transfer Coefficient. . . . .	131
5.9 Correction for Initial Condition . . . . .	135
5.10 Computer Program. . . . .	148
5.10.1 Input. . . . .	151
5.10.2 Output and Results . . . . .	151
VI. PAVEMENT TEMPERATURE . . . . .	156
6.1 Temperature Distribution in Pavement . . . . .	156
6.2 Exact Solution Based on Periodic Surface Temperature. . . . .	158
6.3 The Integration Method (Volterra Integral Equation) . . . . .	163
6.4 Finite Difference Method . . . . .	164
6.5 Computer Program. . . . .	169
6.5.1 Input . . . . .	170
6.5.2 Output and Results. . . . .	171
VII. RESULTS AND DISCUSSION . . . . .	176
7.1 Recorded Temperature Data. . . . .	176
7.2 Thermal Properties of Asphaltic Concrete . . . . .	180
7.3 Pavement Temperature . . . . .	190
CONCLUSIONS . . . . .	192
Recommendations for Further Research. . . . .	194
BIBLIOGRAPHY . . . . .	198
APPENDIX 1 . . . . .	203
APPENDIX 2 . . . . .	210

## LIST OF TABLES

Table		Page
1.6.1	Dynamic Modulus $E^*$ and Phase Lag $\phi$ for Bishop Airport Asphalt Concrete Wearing and Binder Courses, and Hot-Mix Asphalt Base Course, After The Asphalt Institute Laboratory . . . .	46
2.2.1	Annual Climatological Data of Flint, Michigan. . . . .	50
2.8.1	Duration of Warmest Temperature Levels at Various Depths for a 19-inch Asphalt Concrete Pavement During the Summer of 1969. . . . .	67
2.8.2	Duration of Coldest Temperature Levels at Various Depths of a 19-inch Asphalt Concrete Pavement During the Winter of 1969-70. . . . .	68
3.2.1	Composition and Density of Dynamic Modulus Test Specimens (Bishop Airport Asphalt Concrete Wearing and Binder Courses, and Hot-Mix Asphalt Base Course) After The Asphalt Institute Laboratory, July, 1970 . . . . .	78
3.6.1	Calculated Thermal Diffusivity of Asphaltic Concrete from Laboratory Data (Nonlinear Estimation Method) . .	89
3.6.2	Calculated Thermal Conductivity and Specific Heat of Asphaltic Concrete from Experimental Data (Nonlinear Estimation Method) . . . . .	90
3.6.3-A	Analysis of the Variance for the Representative Case. . . . .	93
3.6.3-B	Calculated Values of Root-Mean-Square and Thermal Diffusivity for the Representative Case . . . . .	93



Table		Page
4.4.1	Calculated Thermal Diffusivity of Asphaltic Concrete (Entire Pavement) from Recorded Temperature Data (Nonlinear Estimation Method) . . . .	110
4.4.2	Calculated Thermal Diffusivity of Wearing and Binder Courses from Recorded Temperature Data (Nonlinear Estimation Method) . . . . .	111
5.9.1	Correction Factor and Combined Effect of Temperature Pulses. . . . .	149
5.9.2	Calculated Thermal Diffusivity of Wearing and Binding Courses from Recorded Temperature Data ( $s = 4/t_{\max}$ ), Simplified Method . . . . .	153
5.9.3	Calculated Thermal Diffusivity of Asphaltic Concrete (Entire Pavement) from Recorded Temperature Data ( $s = 4/t_{\max}$ ) Simplified Method. . . .	154
5.9.4	Calculated Thermal Diffusivity of Wearing and Binder Courses from Laboratory Data ( $t_{\max} = 120$ seconds and $s = 4/t_{\max}$ ), Simplified Method . . . . .	155
6.5.1	Calculated Temperature at Various Depths of the Pavement During a Few Winter Days . . . . .	172
6.5.2	Calculated Temperature at Various Depths of the Pavement During a Few Summer Days . . . . .	173
7.2.1	Statistical Comparison Between the Calculated Thermal Diffusivity of Asphaltic Concrete (Analysis of the Variance and F-Test) . . . . .	188

## LIST OF FIGURES

Figure		Page
1.1.1	Intrinsic Factors Which Influence Frost Action (27) . . . . .	7
1.1.2	Extrinsic Factors Which Influence Frost Action (27) . . . . .	8
1.4.1	Moist-Soil Models. . . . .	18
1.4.2	Thermal Conductivity of Soils After Kersten (31). . . . .	24
1.4.3	Thermal Properties of Sandy Soils After Makowski and Mochlinski (33) .	25
2.1.1	Bishop Airport Temperature Study. . .	48
2.2.1	Average Monthly Temperatures During 1969-1970 Compared with Mean Temperatures of 1942-1969 . . . .	51
2.7.1	Full-Depth Asphaltic Pavement Temperature During a Summer Day (Sunny) . . . . .	54
2.7.2	Pavement Temperature During a Winter Day (1/5/70). . . . .	55
2.7.3	Temperature Distribution in 19" Full- Depth Asphaltic Pavement and a Gravel Section at Selected Times During a Winter Day . . . . .	56
2.7.4	Pavement Temperature During a Spring Day. . . . .	59
2.7.5	Temperature Distribution in a 7" Asphaltic Pavement and a Gravel Pavement During a Winter Day (1/13/65). . . . .	60

Figure		Page
2.7.6	Pavement Temperature During a Winter Day . . . . .	61
2.7.7	Pavement Temperature During a Summer Day (7/27/64). . . . .	62
2.8.1	Full-Depth Asphaltic Pavement Temperature During the July and August of 1969 . . . . .	64
2.8.2	Subgrade Temperatures Beneath the 19" Full-Depth Asphaltic Pavement and a Gravel Section (February 1970) . . .	65
2.10.1	Average Daily Temperature and Cumulative Degree Days (February 1970) . . . .	72
2.10.2	Cumulative Degree-Days Above and Below 32°F at Bishop Airport, Flint, Michigan . . . . .	74
3.2.1	Location of Thermocouples in the Asphaltic Sample. . . . .	80
3.5.1	Experimentally Measured Temperature at the Calorimeter Surface and Various Depths of the Asphaltic Sample (Solid and Dashed Lines Refer to First and Second Thermocouple Sets) .	87
3.6.1	Difference Between Calculated and Measured Temperature (Residuals) at 1/2-Inch and 1-Inch Below the Surface of the Specimen (Representative Case).	95
4.4.1	A Comparison Between Calculated and Measured Temperature at 1/2-Inch and 1-Inch Below the Surface of the Specimen (Representative Case) . . .	105
4.4.2	Variation of Thermal Diffusivity During One Iteration Process (Representative Case) . . . . .	106
4.4.3	Summation of Root-Mean-Square for the Representative Case. . . . .	107

Figure		Page
5.3.1	Laplace Transform Criteria . . . . .	119
5.6.1	Calculated Values of $[(\frac{S}{\omega})^2 + 1]^{-1}$ . . . . .	127
5.9.1	Temperature Distribution in 19-Inch Full-Depth Asphaltic Pavement at Selected Times During a Winter Day. . . . .	136
5.9.2	Temperature Profile in a 19-Inch Full-Depth Asphaltic Pavement During Winter and Summer . . . . .	137
5.9.3	Transient Temperature Distribution for Rectangular-Shaped Temperature Pulses. . . . .	142
5.9.4	Combination of Temperature Pulses and Correction Temperatures . . . . .	143
5.9.5	Correction Factor for a Single Rectangular-Shaped Temperature Pulse ( $y/a = 3.0$ ) . . . . .	146
6.2.1	Daily Variation of Temperature (Exact Solution) . . . . .	160
6.2.2	Annual Variation of Temperature (Exact Solution) . . . . .	161
6.4.1	Soil-Pavement System . . . . .	165
6.4.2	Location of Thermocouples, Regions and Nodes in the Soil-Asphalt System . . . . .	166
6.5.1	Calculated Pavement Compared with Measured Temperature During the Summer Days . . . . .	174
6.5.2	Calculated Pavement Temperature During Summer (Variable Initial Temperature). . . . .	175
7.2.1	Calculated Thermal Conductivity and Volumetric Specific Heat from Laboratory Data . . . . .	182
7.2.2	Calculated Thermal Diffusivity of Asphaltic Concrete from Recorded Field Data. . . . .	183

## INTRODUCTION

Frost is a major source of damage to the structure of highway and airfield pavements in the northern United States and the countries in the higher latitudes of the northern hemisphere. In order to withstand the detrimental effect of frost action, some estimate of frost penetration under the pavements is necessary. The current approach to the problem of determining the depth of frost penetration is based on a rational formula named "modified Berggren formula" (38), which is rooted in the theory of heat transfer. The data necessary for the solution of such an analytical equation must be realistic and accurate in order to properly predict the depth of frost penetration.

It is possible to utilize the analytical procedure for calculating temperature at various depths of the pavement and predict the depth of frost penetration provided the thermal properties of pavement elements and the ambient condition are known.

It was in recognition of the need for a reliable value of thermal properties that the major portion of this

research was devoted to determining estimates of the thermal properties of asphaltic concrete.

The thermal properties of soils have been the subject of numerous investigators, while little effort has been directed at evaluating the thermal properties of asphaltic concrete. Literature contains few references to the thermal property of asphaltic concrete. The traditional approach to property measurement is to create experimental conditions for which the system behavior is approximated by a limited form of a fabricated model in the laboratory. In practice, the application of the thermal properties obtained under the controlled condition may not be capable of predicting accurate thermal behavior and temperature distribution in the pavements under natural conditions. For these reasons, a method of estimating thermal property from recorded field temperature data is needed. The digital computer has made it possible to model complex physical systems and include numerous coupled phenomena, which are difficult to combine when conducting laboratory experiments, to measure individual properties.

In this study a review of various methods of property measurements in the laboratory or from field data are made and a method is introduced which embraces both the new concept and traditional methods.

Extensive available temperature data is utilized to evaluate the thermal properties of the asphaltic concrete and results are compared with laboratory values of thermal

properties. The recorded temperature data utilized in this research were obtained from an existing portion of pavement at Bishop Airport, Flint, Michigan. The thermocouples were installed to record the air temperature and the temperature in the pavement surface, base, subbase, and subgrade soils. Temperatures were recorded over a period of two years (1969-1970). Additional data employed in this study gave the temperature variation of a 7-inch thick asphalt pavement in Alger Road, Gratiot County, Michigan, recorded during the years 1964-1965 (34).

Data for evaluation of climatic factor and ambient condition was obtained from United States Weather Bureau records. The method of data collection and analysis is described, and the results of this study are presented in tabular and graphical form.

Current knowledge contained in the published literature is presented in the form of a brief literature review.

## PURPOSES

The primary purposes of this research are the following:

1. To obtain the temperature variations at various depths of the 19-inch full-depth asphaltic pavement and underlying subgrade soils. The available temperature data provide information verifying the range of temperature that an actual asphaltic pavement has in the central Michigan climate during various seasons of the year.
2. To approximate the actual pavement condition with those of the laboratory test and to determine whether the 140° F standard testing temperature of asphaltic concrete is applicable to the central Michigan climate.
3. To determine the ranges of temperature in various layers of the pavement (wearing course, binder course, and hot mix base course) which are necessary to consider in selecting the mechanical properties of asphaltic concrete.



4. To determine the minimum temperature in the subgrades beneath a 19-inch full-depth asphalt pavement, and a comparison between the temperature beneath this pavement and a gravel section during the freezing season.
5. To advance a method for determining thermal properties of pavement material through the field as well as the laboratory temperature data, with particular regard to asphaltic concrete.
6. To calculate temperature distribution at various depths of the pavement and compare the calculated temperature with the measured temperature.

## CHAPTER I

### LITERATURE REVIEW

#### 1.1 Introduction

In studying the pavement temperature and frost action, many influencing factors must be considered. The various factors which influence the pavement temperature are divided into two groups: extrinsic and intrinsic factors (27). Extrinsic factors are those which determine the ambient conditions. These factors are summarized in the block diagram of Figure 1.1.1. Intrinsic factors are those inherent to the pavement material. They include various components of a pavement system such as: paving materials, base, subbase, and subgrade soils, as well as physical and chemical properties of each component. More specifically, intrinsic factors include thermal properties of pavement elements such as thermal conductivity,  $K$ , specific heat,  $C$ , and thermal diffusivity,  $\alpha$ . These factors are given in Figure 1.1.2.

It is beyond the scope of this study to discuss each one of these factors separately. However, a systematic approach to increase the knowledge of the subject,

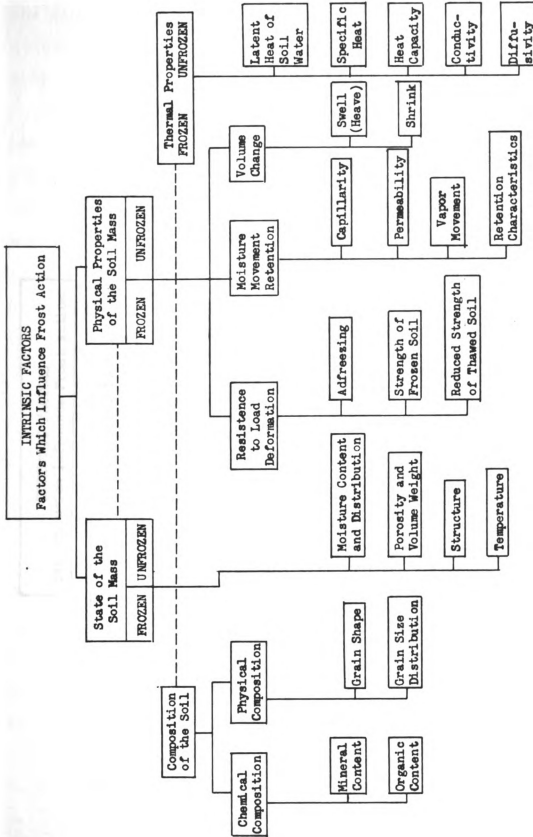


Figure 1.1.1 Intrinsic factors which influence frost action (27)

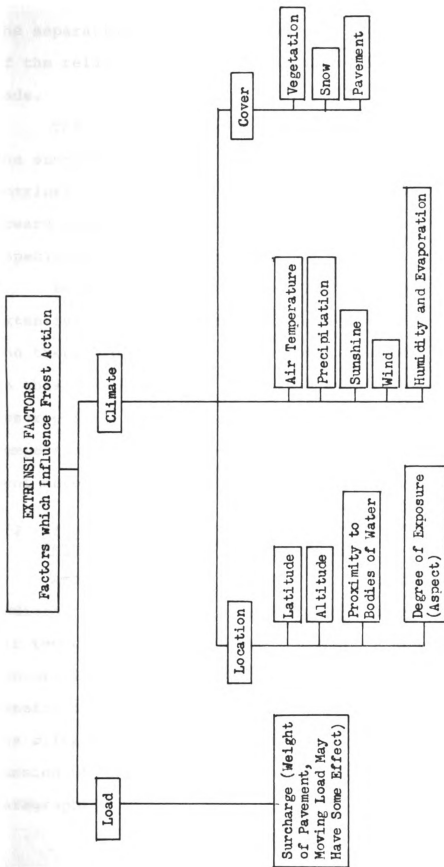


Figure 1.1.1.2 Extrinsic factors which influence frost action (27)

the separation of the major factors, and the determination of the relative influence of each one separately, has been made.

The effect of various extrinsic factors has been the subject of numerous investigators, but, among the intrinsic variables, little effort has been directed toward evaluating thermal properties of pavement materials, especially asphaltic concrete.

Because of the complexity of the subject matter, an extensive review is given of the literature dealing with the thermal properties of pavement material. The material in this chapter presents first, a brief discussion and description of governing factors influencing pavement temperature and finally, the thermal properties of pavement material will be presented in detail.

#### 1.2 Effect of Climate on Pavement Temperature and Frost Penetration

Among the climate factors, solar radiation, freezing indices, duration of freeze, and the relationship between air temperature and pavement temperature are of major concern in determining pavement temperature and frost penetration. The above mentioned factors are related to the climatic characteristic of an area. A brief discussion of the factors is presented in the following paragraphs.

### 1.2.1 Solar Radiation

Solar radiation consists of two types: (a) short-wave, and (b) longwave radiation. The shortwave type makes up the majority of received waves. Solar radiation has a greater heating potential than the air temperature on varying pavement temperature.

Scott (45) introduced an equivalent air temperature  $T'_a$  by:

$$T'_a = T_a + T_r \quad (1.2.1)$$

where  $T_a$  and  $T_r$  are air temperature and equivalent radiation temperature respectively. The influence of radiation effects on the pavement surface temperature is given by (45):

$$T_{pr} = M_r + B_r \cdot A_r \sin \frac{2\pi}{365} t \quad (1.2.2)$$

where  $M_r$  and  $A_r$  are the mean value and amplitude of the equivalent air temperature, respectively.  $B_r$  is the amplitude reduction factor defined by equation (1.2.4).

The amount of radiation received at the surface of the pavement depends upon the amount of water vapor, time of year, and location of the area (45). Methods of computing radiation quantities at the earth's surface are complicated by the presence of the atmosphere which tends to scatter, absorb, and reflect the radiation as it passes through.

Fowle (21) and Kimball (30) conducted studies on the relationship between the depletion of the incoming radiation and the quantities of agents in the atmosphere.

It is assumed that asphaltic pavement is a black mass and 10 per cent of the solar radiation is emitted from the pavement (43). Scott (45) presented methods of calculation and tabular solar radiation data from which the total radiation quantity could be determined for average atmospheric conditions for a black mass for any given latitude.

#### 1.2.2 Freezing Index

The general method of calculating frost penetration uses the air freezing index as a measure of the cold quantity to which the pavement is subjected (38). The freezing index is the difference between the maximum and minimum points of the cumulative degree-day plotted for one year (23).

Index values employed in design are the average air-freezing indices of the three coldest winters in the last thirty years of record (23). The design freezing index should be verified at least once every five years unless more recent temperature records indicate a significant change in thickness design requirements for frost (23).

The freezing index calculated from the recorded temperature data for Flint, Michigan, is given in Chapter II.

A value of the freezing index equal to 1,263 degree-days has been obtained by Oosterbaan et al. (41) for Midland, Michigan. Similar data, taken from the Tri-City Airport, Saginaw, Michigan, was equal to 1,622 degree-days.

### 1.2.3 Correlation Factor "n"

A correlation factor "n" which is the ratio of pavement surface freezing index to the air freezing index is referred to as the "n" factor (38):

$$n = \frac{\text{surface freezing index}}{\text{air freezing index}}$$

The freezing index determined for air temperature about five feet above the ground is commonly designated as the air-freezing index, while that determined for temperature immediately below a surface is known as the surface freezing index (23). Carlson (12), in a study of data obtained from a Corps of Engineer installation in Alaska, determined a correlation factor equal to 0.6, for both bituminous and portland cement concrete pavements.

Kersten (31) obtained a range of correlation of 0.6 to 0.8 for a bituminous pavement in Minnesota. Aldrich and Paynter (3) concluded that a value of the air-surface correlation factor "n", of 0.9 should be adapted for all pavements until further research has clarified the problem.



A value of "n"-factor approximately equal to 1.0 is given by Oosterbaan et al. (41) for Midland, Michigan. The "n"-factor calculated from the recorded temperature data for Flint, Michigan is given for comparison purposes in Chapter II.

#### 1.2.4 Pavement and Air Temperature

The relatively wide range of observed "n"-factors from references illustrates the complexity of the inter-relationship between the air and pavement surface temperature.

The depth of frost penetration, and all subsurface temperature, is governed by variation in the pavement surface temperature. The pavement surface temperature variations are generally unknown, however, while the air temperatures are available. In studies by Aldrich (2) and Carlson (12) it was found that the surface temperature was generally warmer than the air temperature during both summer and winter.

The relationship between air and pavement surfaces may only be obtained through careful theoretical and experimental consideration of the controlling variables. Scott (45) conducted a theoretical investigation into the factors affecting heat transfer at the air-earth interface with limited results. He assumed a sinusoidal variation of air temperature and derived the pavement surface temperature as:

$$T_p = M + \frac{S}{\sqrt{(S + \omega_1)^2 + \omega_1^2}} \cdot A \cdot \sin(\omega t - \delta) \quad (1.2.3)$$

where

$$S = \frac{S_1}{K}; \quad \omega_1 = \sqrt{\frac{\omega}{2\alpha}}; \quad \delta = \tan^{-1}\left(\frac{\omega_1}{\delta + \omega_1}\right);$$

and M and A are the mean value and amplitude of air temperature fluctuation, respectively.  $S_1$  is the heat transfer coefficient between the air and the pavement surface. Equation (1.2.3) indicates that variation of pavement surface temperature is also sinusoidal with a phase lag equal to:

$$B = \frac{S}{\sqrt{(S + \omega_1)^2 + \omega_1^2}} \quad (1.2.4)$$

In order to use Equation (1.2.3) the thermal properties of the paving material and the coefficient of heat transfer,  $s$ , must be known. The value of  $S_1$  and the thermal properties are assumed to be constant. Fewell (19) employed regression analysis to study the relationship between air and pavement surface temperature. The resulting equation describing the pavement surface temperature is given by the following expression:

$$T_p = C_1 + BT_a + C_2 \sin(\omega t + \theta) \quad (1.2.5)$$

where

$$C_1 = (1 - B)M + \frac{q_m}{S_1} \quad \text{and} \quad C_2 = B \frac{q_a}{S_1}$$

$q_m$  and  $q_a$  are the mean value and amplitude of the radiative heat flux, respectively, and  $\theta$  is the phase angle difference between the air temperature and radiation waves.

The results of the studies by Scott (45) and Fewel (19) indicate that some progress has been made in relating air and pavement temperature surfaces. However, most designers still employ the empirical correlation factor, "n," discussed earlier, to convert air freezing index to pavement surface freezing index.

### 1.3 Thermal Properties of Soils and Pavement Materials

Over the past few decades, many investigators have presented various techniques both in the laboratory and field to evaluate thermal properties of soils and pavement materials. These techniques may be grouped in two categories: (1) estimated thermal properties based on published data, laboratory and existing prediction equations; and (2) estimated thermal properties based on field temperature measurements. In the following, we review the literatures and researches dealing with each technique separately. The list is by no means complete, but points out that an extensive number of methods have been proposed

in the area of thermal properties of soils and pavement materials.

#### 1.4 Estimated Thermal Properties Based on Published Data and Existing Prediction Equations

##### 1.4.1 Thermal Properties of Soils and Granular Systems

Estimated thermal properties based on published data can only be used with caution. This is because the thermal properties of soils and pavement materials have a strong dependency on density, mineral type, grain size, and moisture content of the materials (31).

The analysis of the published data provides a general guide to the range of value of thermal properties. Accepted existing equations for prediction of the thermal properties frequently include questionable restrictions or assumptions, and hence the indiscriminate use of these equations leads to erroneous conclusions (see references 10, 35, and 50).

Many investigators have presented various techniques which eliminate one or more of these restrictions, but most of their contributions have been to present a new method of obtaining specific properties (e.g., thermal conductivity) rather than all the thermal properties (50).

Birth et al. (10) for calculating thermal resistivity of mixed aggregates assumed a series arrangement

(see Fig. 1.4.1A) for heat flow and effective conductivity  $K$  calculated from:

$$\frac{1}{K} = \frac{X_g}{K_g} + \frac{X_w}{K_w} + \frac{X_s}{K_s} \quad (1.4.1)$$

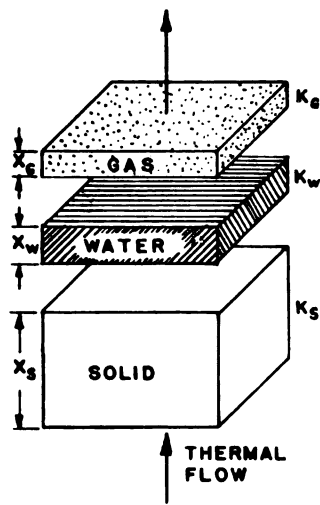
The effective conductivity for parallel treatment results in the equation:

$$K = K_g X_g + K_w X_w + K_s X_s \quad (1.4.2)$$

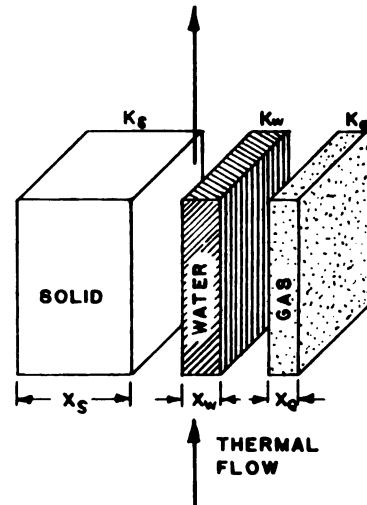
where  $K$  and  $X$  are the conductivity and volume fraction of each component and  $g$ ,  $w$ , and  $s$ , referred to gaseous matter, water, and solids, respectively. Mickley (35) introduced a method of determining thermal conductivity of a soil mass for moist, saturated, and dry conditions. Figure (1.4.1B) shows the picture of a three-component system which is assumed for the soil components.

The thermal property of soils has been related to its mechanical properties by a number of investigators. The experimental data obtained by Farouki (18) indicate that thermal conductivity of cemented granular materials increases linearly with the compressive strength. For a granular material Farouki used the following equation for conductivity,  $K$ , (cal/°C cm sec)

$$K = \beta (13,555 - 3,407f + 0.443 R_c) \quad (1.4.3)$$

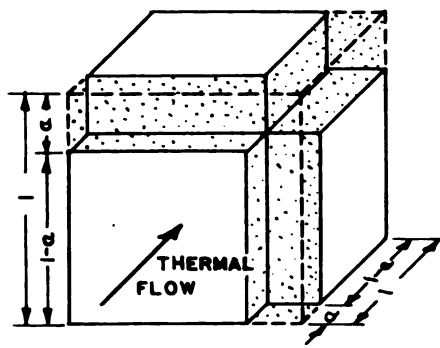


SERIES TREATMENT

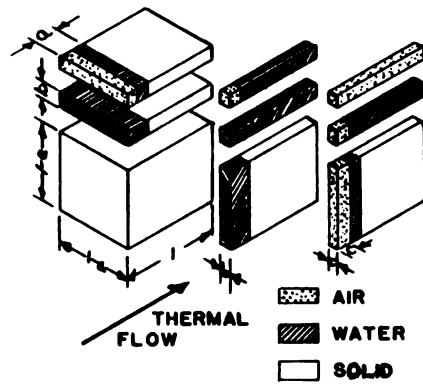


PARALLEL TREATMENT

(A.)



DRY SOIL



MOIST SOIL

MICKLEY'S MOIST-SOIL MODEL  
(B.)

Figure 1.4.1 Moist Soil Models

where

$R_c$  = compression strength of the soil (PSI)

$f$  = volume of clay/volume of granular material, and

$\beta$  depends on density, specific heat, and other mechanical properties of soil and varies from  $0.9 \times 10^{-6}$  to  $3.4 \times 10^{-6}$  gm/cm<sup>2</sup> sec per °C/cm.

Farouki (48) introduced a comprehensive equation for the thermal conductivity of a generalized soil in terms of partial volume of its components which has also included the effect of moisture migration in both the film and the vapor phase. The overall thermal conductivity,  $K$ , of unsaturated soils is given by:

$$K = K_s V_s + K_w (V_w - 10^{-5} S) + K_a V_a + h_L + h_V + h_w + 10^{-5} S K_0 \quad (1.4.4)$$

where  $V_s$ ,  $V_w$ , and  $V_a$  are the partial volumes of the solids, water, and air in a given soil;  $S$  cm<sup>2</sup>/cm<sup>3</sup> is the specific surface of the soils;  $K_0$  is the thermal conductivity of oriented water;  $h_L$ ,  $h_V$ , are the heat transferred by migrated moisture in liquids and vapor phase; and  $h_w$  is the amount of heat conducted by static moisture in liquid phase.

Equation (1.4.4) is written in a simple form as:

$$K = K' + h_L + h_V + h_w \quad (1.4.5)$$

where  $K'$  contains the terms which consider the effect of oriented water and volumic fraction of soil components.

Farouki (18) studied the effect of moisture content on thermal resistivity of a back-fill material and concluded that saturated materials have lower thermal resistivity than those which have been mixed and densified in the air-dry state. He concluded that, when the material dries out, the thermal resistivity increases linearly as the logarithm of the moisture content decreases. However, the thermal conductivity increases linearly as the logarithm of the moisture content increases.

Farouki (18) obtained the following relation between the thermal resistivity,  $\rho = 1/K$ , and the moisture content  $\omega$ :

$$\log \omega = a - \frac{\rho}{b} \quad (1.4.6)$$

where  $a$ , and  $b$  are positive constants for a given soil.

The binding effect between soil particles has been also mentioned by Farouki (18) as a cause for variations of  $K$  (Equation 1.4.5) at low moisture content.

Farouki (18) concluded that at high moisture contents, binding effect does not exist while as the material decreases its moisture content this effect increases, reaching a maximum in the dry state.

The oriented water around the soil particles has also been considered as an additional contributor by



Farouki (18) in obtaining a relation between the thermal conductivity of soils at various moisture contents.

This review shows the relative significance of mineral constituents and the strong dependency of phase composition on the thermal property of a soil system.

The density of the mass system also has a significance and governing effect on the thermal properties of pavement materials. Kersten (31) concluded for a constant moisture content the rate of increase in thermal conductivity varies from 1.2 to 4.4 per cent for each one pound per cubic foot of density increase in unfrozen soils.

For the frozen soils, the values varied from 1.6 to 4.6 per cent increase per additional pound in density. The relation between thermal conductivity  $K$ , and density is given by equation:

$$K = A(10)^B \cdot \text{Density} \quad (1.4.7)$$

$A$  and  $B$  are constant for a particular soil at a constant moisture content (31).

Kersten (31) found reliable empirical equations which express the thermal conductivity of a soil as a function of its water content for a given density. For unfrozen soils, he recommended the following equation:

$$K = A(\log_{10} \text{moisture content}) + B \quad (1.4.8)$$

where A is the difference in conductivity between the 1 per cent and 10 per cent moisture content, and B is the value of thermal conductivity at 1 per cent moisture content.

For frozen soils, Kersten (31) derived the following relationship:

$$K = A + B(\text{moisture content}) \quad (1.4.9)$$

where A and B are constants for the soil at a given density. Kersten (31) combined Equations (1.4.7), (1.4.8), and (1.4.9), to derive expressions defining thermal conductivity of soils in terms of soil type, moisture content, and dry density. For fine-grained soils the following equations relate:

$$\text{unfrozen } K = (0.9 \log_{10} \omega - 0.2) 10^{0.01} \gamma_d \quad (1.4.10)$$

$$\begin{aligned} \text{frozen } K = & 0.01(10)^{0.022} \gamma_d \\ & + 0.085(10)^{0.008} \gamma_d (\omega) \end{aligned} \quad (1.4.11)$$

For coarse-grained soils the resulting equations were as follows:

$$\text{unfrozen } K = (0.7 \log_{10} \omega + 0.4) 10^{0.01} \gamma_d \quad (1.4.12)$$

$$\begin{aligned} \text{frozen } K = & (0.076(10)^{0.013} \gamma_d \\ & + 0.032(10)^{0.0146} \gamma_d (\omega) \end{aligned} \quad (1.4.13)$$

The expressions for fine-grained soils are valid for moisture contents of 7 per cent or more, while Equation (1.4.12) and (1.4.13) are valid for moisture contents of 1 per cent or more. These equations are presented graphically in Figure 1.4.2.

Gemant (22) derived an equation to predict thermal conductivity of soils in terms of water content, thermal conductivity of water and solid components, and the dry density of the soil particles.

Makowski and Mochlinski (33) compared the basic equations of Kerten (31) and Gemant (22) and presented a nomograph (Fig. 1.4.3) for rapid solution of determining thermal conductivity and resistivity of sandy soils.

This nomograph is based on the following equations:

$$K = (a \log_{10} w + b) \times 10^{\gamma/100} \text{ watts/cm}^2 - c/\text{cm}$$

$$w = \text{moisture content} \quad (1.4.14)$$

$$\gamma = \text{dry density}$$

The values of  $a$  and  $b$  are defined differently for Kersten (31) and Germant (22) equation as following:

For the Kersten (31) equation:

$$a \text{ for sand} = 1.03; (\text{clay} = 1.29)$$

$$b \text{ for sand} = 0.565; (\text{clay} = -0.283)$$

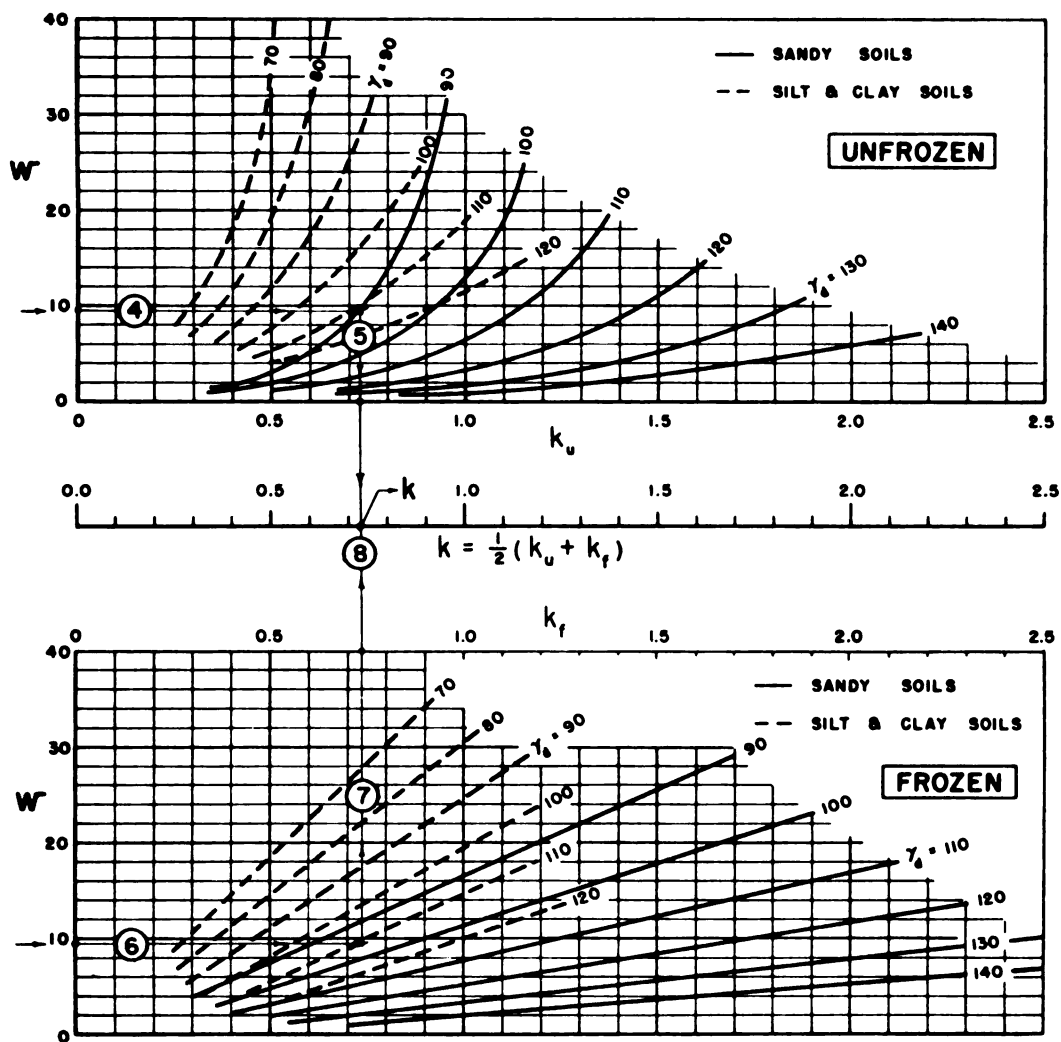


Figure 1.4.2 Thermal conductivity of soils after Kersten (31)

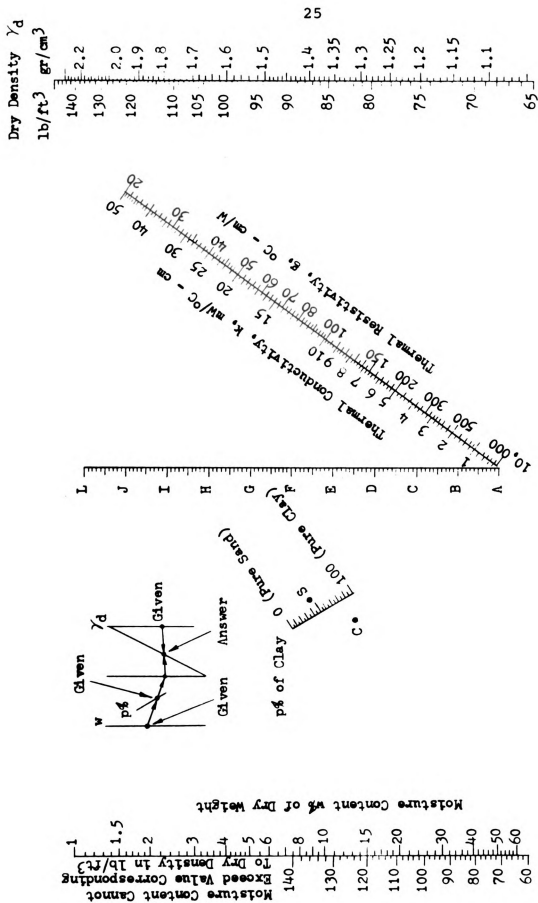


Figure 1.4.3 Thermal properties of sandy soils after Makowski and Mochlinski (33)

For the Gemant (22) equation:

$$a = 1.424 - 0.00465 P$$

$$b = 0.419 - 0.00313 P \text{ and}$$

$P$  = percentage of clay in the soil

In the nomograph points C and S correspond to the Kersten (31) data for clay and sand respectively.

Heat capacity and latent heat of fusion:

The volumetric heat capacity of soils may be expressed as follows: (16)

$$\text{For dry soil} \quad C = C\gamma_d \quad (1.4.15)$$

$$\text{For moist, unfrozen soils} \quad C_u = \gamma_d \left( C + 1.0 \frac{w}{100} \right) \quad (1.4.16)$$

$$\text{For moist, frozen soils} \quad C_f = \gamma_d \left( C + 0.5 \frac{w}{100} \right) \quad (1.4.17)$$

$$\text{The average value for moist soils} \quad C_{avg} = \gamma_d \left( C + 0.75 \frac{w}{100} \right) \quad (1.4.18)$$

where

$c$  = specific heat of the dry soil

$\gamma_d$  = dry unit weight

$w$  = moisture content of the soil in the percentage of dry weight.

The value of  $c$  equal to 0.17 BTU/lb °F has been recommended by most of the investigators including Kersten (31) and Aldrich (2).

The latent heat of fusion of water is assumed to be 144 BTU/lb; and it follows that the latent heat of fusion of a soil,  $L$ , may be given by the following expression (16):

$$L = 144 \gamma_d \frac{w}{100} \quad (1.4.19)$$

#### 1.4.2 Thermal Properties of Asphaltic Concrete

The thermal properties of soils have been the subject of numerous laboratory and field studies, while little effort has been directed at evaluating the thermal properties of bituminous concretes. Although relatively little information is available in the literature with respect to the thermal properties of bituminous concrete mixtures, it appears that there is less variation in magnitude of the thermal properties of asphalt concrete than for soils (20). The purpose of this section is to introduce and describe the various factors which have the strongest influence on the thermal properties of asphaltic concrete, and finally a review of literature and research will be presented which has been conducted both in the laboratory and field in the study of thermal properties of asphaltic concrete.

#### 1.4.2-1 Factors Influencing Thermal Properties of Asphaltic Concrete

Bituminous concrete may be defined as a system composed of the solid, semi-solid or liquid, and gaseous phases, with a temperature dependent thermal properties. The solid phase is the mineral material consisting of sand, gravel, crushed stone, slag, and mineral filler.

The semi-solid phase is the visco-elastic asphaltic material produced from petroleum (or bitumen) in a variety of types and grades ranging from hard brittle solid to almost water-thin liquids. The gaseous phase is the air which fills the voids.

The mineral materials are surrounded and bound together by asphaltic material.

Thermal properties of bituminous concrete mixtures vary depending upon the temperature, types of aggregates, asphalt content, density, porosity, and the presence of moisture in the voids available in the mixture.

Moisture: Water in either vapor or liquid phase, enter the bituminous concrete through the voids available in the mixture. The presence of accessible pores, crevices, and capillary forces results in the penetration of water into the pores. Bituminous aggregate coatings are believed to have very small pin holes through which water may penetrate. In high void ratio mixes, such as most base course material, water may freely circulate through the voids. Well compacted hot-rolled asphalt mix,



has a very low permeability to water, while in open-graded mixtures water penetrates easily into the asphalt concrete.

The results of studies by Heley (24) showed that high moisture content associated with relatively open-graded bituminous concrete mixed used on many highways in West Virginia have been responsible for obtaining higher thermal conductivity of pavement materials.

Aggregates: An increase in thermal conductivity may be expected depending upon the types of aggregates. Most of the rock-forming minerals exhibit the conductivity-temperature behavior which is characteristic of dielectric solids at high temperature; that is, the thermal conductivity follows roughly the law  $K = (AT + B)$ , where  $K$  is thermal conductivity,  $T$  is temperature, and  $A$  and  $B$  are constants (10). Thermal property of the rocks is affected by the type rock-forming minerals, porosity, and the direction of heat flow. Quartz has the highest conductivity in the direction parallel to its optic axis, while mica has the lowest value in the direction perpendicular to the cleavage (10). Thermal properties of aggregates depend on their parent materials and the state of the pore spaces inside the aggregate. Thermal conductivity of aggregates is estimated by Saal (44) and a value of  $K = 0.7$  to  $1.4 \text{ BUT Ft/ft}^2, \cdot\text{F, hr}$  has been suggested for most aggregates.

Little reliable information is available concerning specific heat-capacity of aggregates. Hogbin (59) conducted experiments on five common road aggregates, and a filler, from sources in Great Britain. A value of  $C = 0.2 \text{ BTU/lb } ^\circ\text{F}$  is suggested by Hogbin (59) for most aggregates.

#### 1.4.2-2 Changes in Volume and Density Due to Temperature

A material like asphaltic concrete undergoes volume change with change in temperature. This volume change has a significant effect on the thermal property of asphaltic concrete. A dry mixture of asphaltic concrete may be assumed as a three-phase system composed of mineral, asphaltic, and gaseous matter. For a given temperature, gaseous matter expands more than asphaltic material and asphaltic material expands more than the mineral materials. The cubical coefficient of expansion gives a change in volume of material over a particular temperature range and can be defined by:

$$\beta = \frac{\Delta V}{V_o \Delta t} \quad (1.4.20)$$

in which

$V_o$  = volume at the same reference temperature, and

$\Delta V$  = change in volume due to temperature change,  
 $\Delta t$ , from reference temperature.

This coefficient for a variety of asphalts is given in tabulated form by Saal (44) and Abraham (1) with an average volume change of  $\beta = 1.08 \times 10^{-3}$  per °F.

Thermal expansion of asphalts and other forms of bituminous matter may be calculated from the equation (1):

$$V_T = V_{60} [1 + A(T - 60) + B(T - 60)^2] \quad (1.4.21)$$

where

$$A = 3.41 \times 10^{-4}$$

$$B = 1.0 \times 10^{-7}$$

$V_{60}$  and  $V_T$  are the volumes of asphalt at 60°F and at a temperature of T°F, respectively. The values of  $V_{60}/V_T$  are given in a tabulated form for various temperature ranges. Abraham (1) established a value of  $\beta = (0.4 - 0.43) \times 10^{-4}$  per °F for asphaltic material.

For aggregates, the average values of the linear coefficient of expansion given by Troxell and Davis (47) and Mitchell (36) is  $\beta = 0.135 \times 10^{-4}$  per °F. Comparing the values of thermal expansion for aggregates with those of asphalts, it can be seen that there is at least an order of magnitude difference in the expansion characteristics of these materials.

The cubical coefficient of expansion of asphaltic mixture may be obtained by including the effect of aggregate type, asphalt hardness, and asphalt content.

Disregarding the volume of air voids in a volume of asphaltic concrete, we may write,

$$\Delta V_{\text{mix}} = \Delta V_{\text{asph}} + \Delta V_{\text{agg}} \quad (1.4.22)$$

where

$$\Delta V_{\text{mix}} = \Delta V_{\text{mix}} \beta_{\text{mix}} \Delta T \quad (1.4.23)$$

Let  $n$  be the percentage of asphalt content by volume of aggregate, then from Equation (1.4.23), the expansion coefficient of asphaltic mixture will be obtained equal to:

$$\beta_{\text{mix}} = [n \beta_{\text{asph}} + (100 - n) \beta_{\text{agg}}] \quad (1.4.24)$$

The coefficient of linear and cubical expansion of asphaltic concrete has been investigated also by Hook (26) and Goetz (26). They suggested an average value of  $\beta_{\text{mix}} = 1.26 \times 10^{-4}$  per °F for the cubical coefficient of expansion. The small value of cubical coefficient of expansion indicates that the density of asphaltic concrete is much more insensitive to temperature change than either thermal conductivity or specific heat; it is thus assumed to be constant in this study.

#### 1.4.2-3 Thermal Conductivity of Asphaltic Mixture

Thermal conductivity of soils have been the subject of numerous laboratory and field studies while little

effort has been directed at evaluating the thermal conductivity of asphaltic concrete. The United States Army Corps of Engineers reference gave a thermal conductivity value of 0.82 BTU/hr ft °F for dry asphaltic concrete. Aldrich (2) used a value of 0.84 BTU/hr ft °F in calculation of frost penetration and Barber (5) has suggested a value of 0.7 BTU/hr ft °F in computation of pavement temperature.

The significance of asphalt content within the mixture was evaluated by Saal (44) in his empirical equation for thermal conductivity of the mix:

$$\log K_{\text{mix}} = x \log K_{\text{asph}} + (1 - x) \log K_{\text{aggr}} \quad (1.4.25)$$

where

- $K_{\text{mix}}$  = thermal conductivity of the mixture
- $K_{\text{asph}}$  = thermal conductivity of the asphalt
- $K_{\text{aggr}}$  = thermal conductivity of the aggregate, and
- $x$  = fraction by volume of asphalt.

The thermal conductivity of various asphalt is obtained by Saal (44). A value of 0.09 BTU/ft °F hr is suggested for most asphalts. In general, the thermal conductivity of asphalts decreases as the temperature increases and varies linearly in the range of 0 to 110 °F (32).

$$K = K_0 (1 - C_2 \Delta T) \quad (1.4.26)$$

where  $C_2$  is constant for a particular asphalt, and  $K$  and  $K_0$  are thermal conductivity of asphalt at particular temperatures and reference temperature, respectively.

A comparison between obtained values of,  $K$ , for rock and aggregate by Saal (44) and Birch et al (10) indicates that the conductivity of aggregate is approximately one order of magnitude larger than that of the asphalt.

In deriving Equation (1.4.25), Saal (44) assumed a value of asphalt content equal to 5 per cent by weight of mixture. The bituminous concrete is assumed to be dry and the thermal conductivities of aggregates and bitumen are assumed to be equal to 1.50 and 0.44, respectively.

The calculation of thermal conductivity of bituminous concrete, using Equation (1.4.25), have a value of 1.29 BTU/hr ft °F, which is substantially higher than commonly accepted values.

O'Blenis (40) and Heley (24) attempted to utilize field temperature data to compute the thermal conductivity of highway pavement materials. Values of conductivity obtained by O'Blenis (40) varied from 0.49 to 1.34 BTU/hr ft °F. Heley (24) used field data to calculate the conductivity of bituminous concrete for various seasons and concluded that thermal conductivity varied considerably with the season, with the highest values occurring during the freezing period.

#### 1.4.2-4 Specific Heat Capacity of Asphaltic Mixture

The specific heat capacity of asphaltic mixtures, like other engineering materials, is not a constant but is a function of temperature. The literature contains few references to the specific heat of bituminous concrete mixture. Abraham (1) has suggested the following relationship:

$$C_{\text{mix}} = 0.01[(100 - x) C_{\text{asph}} + x C_{\text{aggr}}] \quad (1.4.27)$$

in which  $x$  = per cent by weight of aggregate; and  $C_{\text{mix}}$ ,  $C_{\text{asph}}$ , and  $C_{\text{aggr}}$  represent the specific heat capacity of asphaltic mixture, asphalt, and aggregates, respectively.

Values for  $C_{\text{asph}}$  for a series of asphalts over the temperature range 32 to 570°F were obtained by Saal (44). These values indicate that the specific heat increases linearly with temperature by the following equation suggested by Mack (32):

$$C = C_o + C_1 \Delta T \quad (1.4.28)$$

where

$C$  = specific heat at a particular temperature,

$C_o$  = specific heat at reference temperature (e.g., 32°F), and

$C_1$  = constant for a particular asphalt.

Abraham (1) suggested the following relationship for specific heat capacity of asphalt:

$$C_{\text{asph}} = \frac{1}{\sqrt{d}} (0.388 + 0.00045 T) \text{ BTU/lb } ^\circ\text{F} \quad (1.4.29)$$

where

$d$  = specific gravity of asphalt, and

$T$  = temperature in  $^\circ\text{F}$ .

A value of 0.4 BTU/lb  $^\circ\text{F}$  is suggested for most asphalts.

In cases where asphalt is mixed with various amounts of solids such as sand, crushed rock, etc., the following equation is suggested by Abraham (1) for specific heat of the mixture:

$$C_n = 0.01[(100 - x)C_a + x C_s] \quad (1.4.30)$$

where  $x$  = percentage by weight of solids, and the subscripts  $n$ ,  $a$ , and  $s$  refer to mixture, asphalt, and solid, respectively.

Hogbin (25) employed a method based on Equation (1.3.27) to obtain the specific heat capacity of a series of course materials. An average specific heat value of  $C = 0.2$  BTU/lb  $^\circ\text{F}$  was obtained for wearing and base courses with various compositions.



### 1.5 Estimated Thermal Properties of Pavement Materials Based on Field Temperature Measurement

Field temperature measurement in conjunction with classical periodic wave analysis (13) has been used to evaluate thermal properties of soils and pavement materials. Jumikis (28) introduced a method to calculate temperature distribution at various depths below the ground surface. The analysis is based on periodic surface temperature variation. He assumed that surface temperatures vary diurnally and annually about a mean temperature in a manner which approximates a sine wave. It is further assumed that the soil beneath the surface has a constant thermal property and follows the same temperature function as the surface, but is reduced in amplitude and delayed in time. In a given cycle the temperature amplitude at two different depths,  $x_1$ , and  $x_2$ , are given by the two equations:

$$T_1 = T_o \cdot e^{-x_1 \sqrt{\frac{\pi}{\alpha \cdot P}}} \quad (1.5.1)$$

$$T_2 = T_o \cdot e^{-x_2 \sqrt{\frac{\pi}{\alpha \cdot P}}} \quad (1.5.2)$$

where  $\alpha$  is the thermal diffusivity of the material under consideration in BTU/hr ft °F and P is the period of the temperature wave in hour. Solving these two equations simultaneously for  $\alpha$  gives:

$$\alpha = \frac{\pi}{P} \left[ \frac{x_1 - x_2}{\frac{1}{n} T_1 / T_2} \right]^2 \quad (1.5.3)$$

The general wave equation may also be solved in terms of time which yields:

$$\alpha = \frac{\pi (x_2 - x_1)^2}{P (\theta_2 - \theta_1)^2} \quad (1.5.4)$$

where  $(\theta_2 - \theta_1)$  is the phase difference between the two temperature curves at the two depths. If  $t_1$  and  $t_2$  are the time of temperature maximum at depth  $x_1$  and  $x_2$  in hour, Equation (1.5.4) may be written in the following form:

$$\alpha = \frac{P}{4\pi} \frac{(x_2 - x_1)^2}{(t_2 - t_1)^2} \quad (1.5.5)$$

Equations 1.5.3 and 1.5.5 may be used with either the diurnal or annual temperature cycle to calculate theoretically thermal properties of the pavement materials. [Most investigators agree, however, that the annual cycle could lead to errors in conclusions, because of the wide range of weather phenomena experienced during an entire year.] O'Brien (40) used the recorded temperature data obtained at twelve locations in the state of West Virginia to calculate thermal properties of pavement materials. He found out that the thermal property obtained by Equations (1.5.3) and (1.5.5) could be equal if the comparative

variation between the depths follows a true sinusoidal pattern. He selected those days which most closely follow a sine wave temperature variation. Assuming a sinusoidal temperature variation at any two depths  $d_1$ , and  $d_2$ , the Equation 1.5.3 and 1.5.5, for a period of twenty-four hours is written in the following form:

$$\alpha = \frac{\pi}{24} \left[ \frac{d_1 - d_2}{\ln T_1/T_2} \right]^2 \quad (1.5.6)$$

$$\alpha = \frac{24}{4\pi} \frac{(d_1 - d_2)^2}{(t_1 - t_2)^2} \quad (1.5.7)$$

O'Blenis (40) equates these two equations with the resultant expression:

$$T_1/T_2 = e^{0.262(t_1 - t_2)} \quad (1.5.8)$$

which is the relationship between the amplitude ratio and time lag for any two depths. Since Equation (1.5.8) represented the conditions resulting from a sinusoidal variation, O'Blenis (40) selected days on which the amplitude ratio and time lag satisfies this equation, and then used Equations (1.5.6) and (1.5.7) to calculate thermal diffusivity.

Voluminous primary data was processed to determine a few days which approximate a sine wave and satisfies the criterion given by Equation (1.5.8). Since the daily

heating cycle is normally other than the simple sine function, Carson (14) proposed higher harmonics and the Fourier analysis for daily temperature wave. He recommended a second or third harmonic for a daily temperature cycle and a single harmonic for the annual temperature cycle.

Heley (24) programmed the O'Brien (40) method and reduced the manual calculation to a great extent. O'Brien (40) and Heley (24) concluded that the magnitude of the daily temperature wave becomes inappreciable at depths below 18 inches and the application of this method to layers below the 18-inch depth produces extremely large values of thermal conductivity. It was concluded that either the assumptions of the method did not satisfy the natural conditions or that the method itself was in error. Chudnovski (15) introduced a method which eliminates the assumption of sinusoidal surface temperature, but requires a linear temperature distribution with depth. This method, denoted as "generalized wave method" offered a definite advantage over the periodic method employed by O'Brien (40) and Heley (24).

The analysis of Chudnovski (15) is based on the solution of the general heat equation in a semi-infinite body with a time variable surface temperature and constant thermal properties which is given by Duhamel's integral (15):

$$T(x,t) = \frac{x}{2\sqrt{\pi 2}} \int_0^t T(0,\lambda) \frac{e^{-x^2/4\alpha(t-\lambda)}}{(t-\lambda)^{3/2}} d\lambda + T_i(x) \quad (1.5.9)$$

Where  $\lambda$  is a dummy time variable of integration, and initial temperature  $T_i$  is assumed to be uniform at  $t = 0$ . Thermal diffusivity may be obtained by using this equation for a given temperature variation at a certain depth. However, it is not practical to determine  $\alpha$  directly from this equation.

Chudnovski (15) transformed this equation by multiplying by  $dx$  and integrating between the limits  $x = 0$  and  $x = \infty$ . The result may be written:

$$\alpha = \frac{\pi \int_0^\infty (T(x,t) - T(x,0)) dx}{\int_0^t \frac{T(0,\lambda) - T(0,0)}{t - \lambda} d\lambda} \quad (1.5.10)$$

The numerator of Equation 1.5.10 represents the area between the temperature-depth curve at the instant  $(t)$ , and the initial time  $t = 0$  which is determined with a planimeter. To evaluate the integral in the denominator, the integral is divided into sub-intervals in each of these  $T(0,\lambda) - T(0,0)$  can be regarded as linear.

Finally the value of diffusivity is determined by the following expression:

$$\alpha = \frac{\pi \int_0^{\infty} (T(x,t) - T(x,0)) dx}{2\sqrt{t}[a_1 s_1 + \dots + b_n t(2/3 - \sigma_{n-1})]} \quad (1.5.11)$$

Where  $a_i$  and  $b_i$  are the initial temperature ordinates and the slope of each time-temperature curve in the sub-interval, respectively.

The values of  $s_i$  and  $\sigma_i$  are computed for various values of dummy time variable (15). The generalized wave method is utilized to calculate thermal diffusivity of pavement material subjected to any surface heat pulse.

The requirement for initial condition is met by selecting the time period to begin just as the daily heat pulse reaches the upper interface of the layer under consideration and is continued until the temperature at the lower interface begins to rise. This process provides a linear initial temperature profile. O'Blemis (40) and Heley (24) employed this method to calculate thermal properties of pavement materials from field temperature data. They indicated that the generalized wave method is best used on those layers having little or no moisture present and to those layers which are waterproof, such as the wearing course and waterproof base. The finite difference method also was employed by Heley (24) to evaluate thermal conductivity of deeper layers and subgrade soils in West Virginia. Of all the methods presented, the numerical method required the least time, but most precise

raw data. In this method the one dimensional heat equation approximated by finite difference method and finally was solved directly for the thermal conductivity K.

$$K = \frac{T_{i,j+1} - T_{i,j-1}}{2\Delta t} \cdot \frac{\Delta x^2}{T_{i+1,j} - 2T_{i,j} + T_{i-1,j}} \cdot C \quad (1.5.12)$$

where i and j represent location and time, respectively. It is observed that when the temperature in the data point location were such as to have the sum of the upper and lower values equal to two times the center value, the denominator of second term in Equation (1.5.12) becomes zero and the corresponding value of K approached infinity.

Despite the simplicity of the entire procedure the limited applicability and sensitivity of the method to the form of data has made it impractical. The thermal properties obtained by this method are questionable.

#### 1.6 Temperature and Rheological Characteristics of Asphaltic Concrete

Temperature has a significant influence on the mechanical and rheological characteristics of asphaltic concrete. A great deal of laboratory work has been accomplished concerning temperature dependent properties of asphalt concrete pavement. These properties include deflection, stresses and strains, stiffness, and viscosity.

The load-carrying capacity and stiffness of the asphaltic mixtures are much lower during the summer months than the winter months. There is a possibility of the pavement rutting under the heavy loads during the summer months. On the other hand, during the winter months the pavement does not deflect under heavy loads and cold temperatures may cause cracking in the asphaltic concrete. Stress-strain characteristics of asphaltic material are defined by various coefficients such as dynamic modulus  $E^*$ , relaxation modulus, and relation modulus  $E(t)$ .

The dynamic modulus  $E^*$ , in compression, tension, and tension-compression can be determined by (20),

$$|E^*| = \frac{\sigma_o}{\epsilon_o}$$

where  $\sigma_o$  is the applied stress and  $\epsilon_o$  is the resultant strain. The dynamic tension-compression modulus of asphaltic concrete may be obtained through the application of a sinusoidal loading to a specimen. If the material is viscoelastic, the deformation resulting from the load will have the same sinusoidal variation with time but will lag behind the stress by a time represented by (20)

$$\phi = \frac{t_i}{\omega} (360^\circ)$$

where  $t_i$  is the time lag between the sinusoidal cycle of



stress and strain in second, and  $\omega$  is the frequency of loading per second.

The absolute value of the dynamic modulus  $|E^*|$  and phase lag  $\phi$  for the wearing course, binder course, and hot mix asphaltic base course similar to the existing asphaltic concrete pavement at Bishop Airport in Flint, Michigan, are given in Table 1.6.1.

The absolute values of the dynamic modulus and phase lag over a range in frequencies and various temperatures of 10°, 40°, 70°, and 100°F indicate the visco-elastic response of the asphaltic concrete.

Table 1.6.1 Dynamic Modulus  $E^*$  and Phase Lag  $\phi$  for Bishop Airport Asphalt Concrete Wearing and Binder Courses, and Hot-Mix Asphalt Base Course, after The Asphalt Institute Laboratory.

Pavement Course	Temperature (F°)	LOADING FREQUENCY					
		1 cps		4 cps		16 cps	
		E* (psi x 10 <sup>5</sup> ) (deg.)	φ	E* (psi x 10 <sup>5</sup> ) (deg.)	φ	E* (psi x 10 <sup>5</sup> ) (deg.)	φ
Asphalt Concrete Wearing Course	10	25.2	3	28.2	5	30.4	1
	40	10.2	22	13.2	21	15.9	18
	70	1.54	43	2.88	41	4.42	37
	100	0.32	28	0.49	32	0.80	48
Asphalt Concrete Binder Course	10	31.6	3	34.6	0	36.1	0
	40	13.7	22	17.8	18	20.4	17
	70	2.58	39	4.30	37	6.35	36
	100	0.40	26	0.58	35	1.04	41
Hot-Mix Asphalt Base Course	10	29.5	2	32.3	3	34.1	2
	40	12.9	21	16.4	17	19.4	19
	70	3.20	39	5.23	35	7.30	32
	100	0.59	37	1.00	42	1.83	48

## CHAPTER II

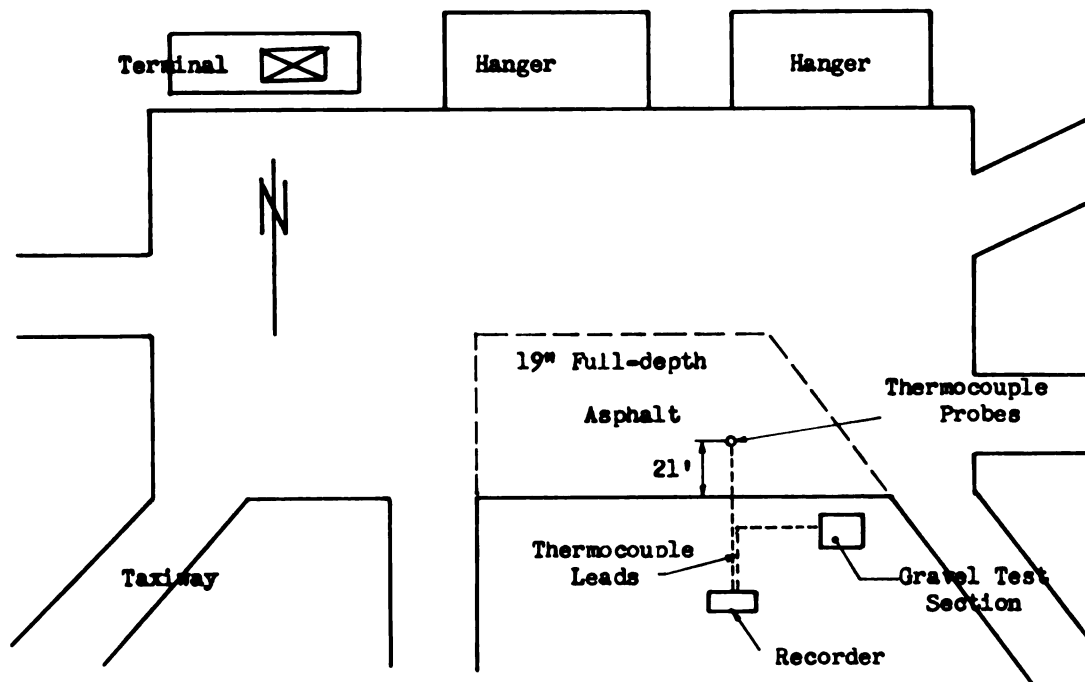
### DATA COLLECTION

#### 2.1 Site Location and Climate

A portion of the actual apron pavement of the Bishop Airport, Flint, Michigan, has been selected for this study (see Fig. 2.1.1). Flint, with a central Michigan climate, is located in the Flint River Valley with a latitude of  $42^{\circ} 58' N$ , longitude of  $83^{\circ} 44' W$ , and an elevation of 771 feet. The Great Lakes influence the climate in this area to a large extent. Temperatures of  $100^{\circ}F$  or higher are rare and cold periods of  $0^{\circ}F$  are less severe than in adjoining states. During the winter months, snow showers occur with strong north-westerly winds. The cold periods are tempered by Lake Michigan, lying 120 miles to the west. Considerable cloudiness and rather high relative humidity characterize the winter months.

#### 2.2 A Comparison Between the Recorded and the Long-Term Average Temperature

Collected temperature data and obtained results are more useful if it is possible to indicate how representative the pavement temperature data are for an



Installation-Plan View

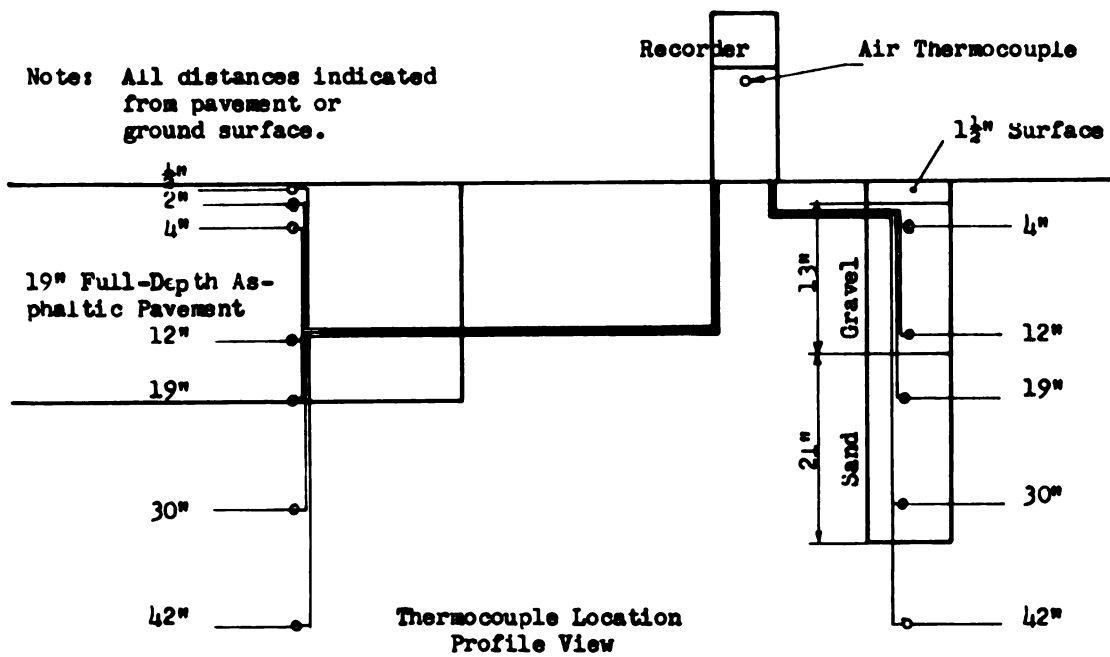


Figure 2.1.1 Bishop Airport Temperature Study

average year in the central Michigan climate. For this reason, climatic data for the past thirty years was studied for the Flint, Michigan area.

Table 2.2.1 lists the average annual temperature from 1943 through 1969, plus the maximum and minimum temperature for the coldest and warmest months, January and July.

Total annual precipitation rates for these years are also included. A comparison has been made between the average monthly temperature during the period of this study and the mean average monthly temperature of the last twenty-seven years, as is shown in Figure 2.2.1.

Figure 2.2.1 indicates that the summers of 1969 and 1970 were representative of summers in the area of Flint, while the winter of 1970 was the coldest recorded in the past twenty-seven years. The fall of 1969 was cooler than usual, but spring of 1970 was warmer than average. The conclusion is that the summers of 1969 and 1970 were representative of the average for the area of study, while the winter of 1970 was not.

### 2.3 Observation Period and Auxiliary Data

The recording of temperature data began January 1, 1969, and continued through September, 1970. The period of study was considered necessary to develop sufficient information regarding daily, as well as annual, variations of temperature in the asphaltic pavement and

Table 2.2.1 Annual climatological data of Flint, Michigan

Year	Avg. Annual Temperature (°F)	Avg. Monthly Temp. (°F)		Total Annual Precipitation Water Equiv. (in)	Air Freezing Index
		Coldest	Warmest		
1943	46.4	18.4	72.8	32.01	-
1944	47.8	20.6	72.2	24.38	-
1945	46.3	15.6	68.8	39.44	-
1946	48.9	22.6	72.4	25.78	-
1947	46.5	19.8	76.0	41.99	-
1948	47.2	17.0	71.5	29.45	-
1949	49.3	27.5	74.5	36.99	-
1950	46.0	22.4	68.3	44.74	1284
1951	46.6	24.7	70.2	33.91	1224
1952	48.3	26.9	73.7	30.13	1171
1953	49.3	26.7	71.6	24.25	1304
1954	47.5	22.3	69.7	30.36	1271
1955	48.9	23.2	75.5	23.27	1322
1956	46.7	22.1	68.7	35.54	1453
1957	46.5	17.6	69.9	35.54	1283
1958	45.5	17.8	69.5	20.08	1243
1959	46.6	15.9	73.3	37.82	1208
1960	45.6	21.7	68.2	22.43	1302
1961	47.0	19.2	69.7	30.54	1159
1962	45.6	17.8	68.0	23.29	1276
1963	45.6	15.0	70.4	18.08	1336
1964	47.9	25.8	71.7	24.59	1315
1965	47.3	22.1	68.4	25.79	1404
1966	45.6	18.5	70.5	20.54	1191
1967	45.5	18.3	68.5	30.29	1306
1968	46.7	20.8	68.9	33.90	1263
1969	46.2	22.6	70.1	28.58	-

Mean Temperature of  
Last 27 Years  
Avg. Monthly Temp.  
(1969-1970)

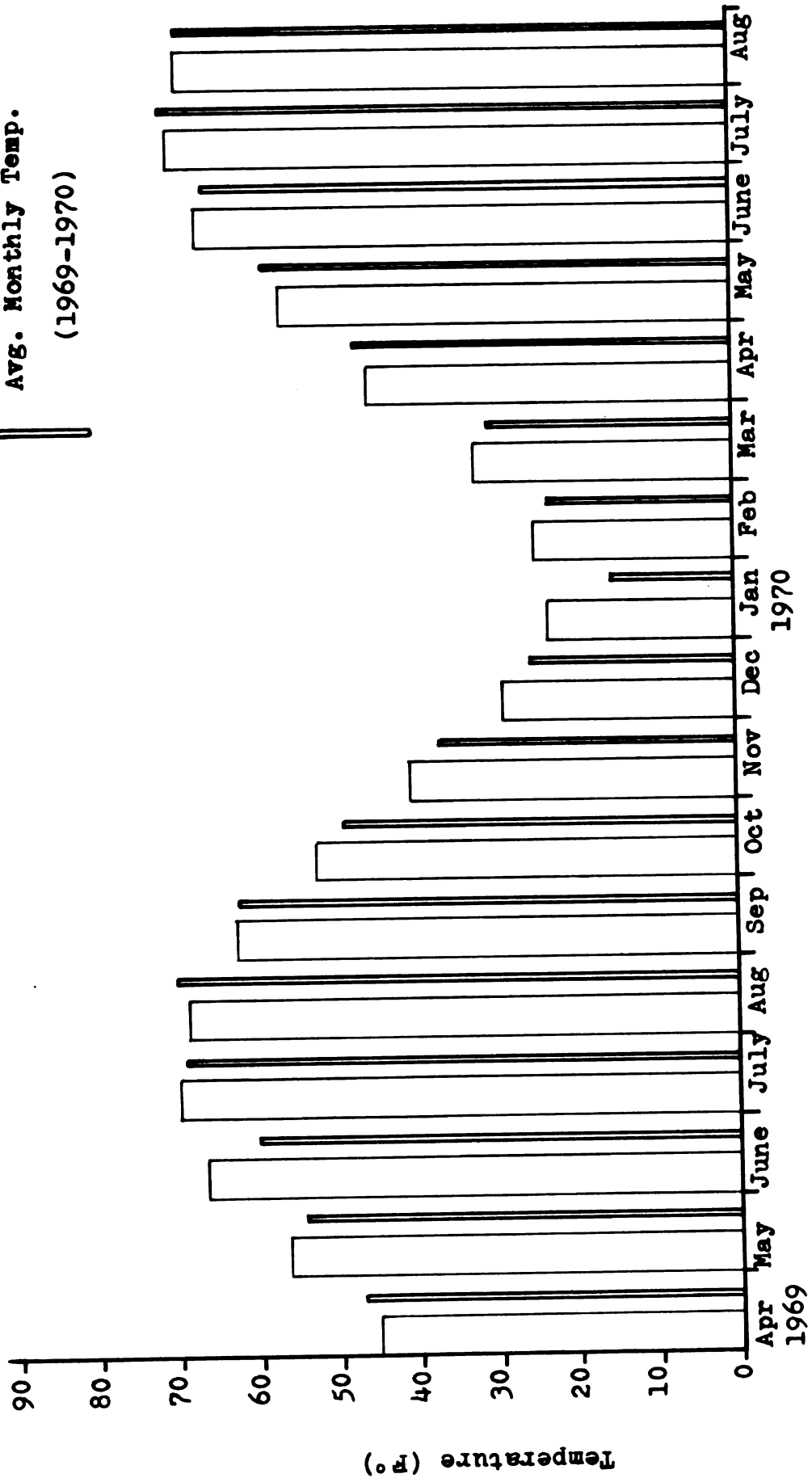


Figure 2.2.1 Average monthly temperatures during 1969-1970 compared with mean temperatures of 1942-1969.

underlying subgrade. During winter months, results obtained from the recorder were confused and nearly indistinguishable. For this reason, it was felt necessary to compare these data with previously studied temperature data. The data used for comparison was concerned with temperature variation in a 7-inch thick asphalt pavement in Alger Road, Gratiot County, Michigan, which was conducted and reported by Glenn P. Manz (34).

#### 2.4 Installation

The facilities utilized for recording temperature data consisted of two basic components: (1) a recorder and supporting equipment, and (2) the thermocouples and connecting leads.

A Minneapolis Honeywell-Brown 12-channel temperature recorder was utilized to compile the data. The recorder was furnished by Leonard Refineries, of Alma, Michigan. The recorder was capable of recording twelve thermocouples, one each thirty seconds, hence, the same thermocouple once every six minutes.

The temperature range of the recorder was 0°F to 160°F with an accuracy of plus or minus one-half degree F. An ice bath was utilized for checking the recorder for accuracy during the testing period. One of the probes attached to the automatic recorder was an ambient air temperature probe, and was located in the shade of the recorder. A glass, mercury-filled, air thermometer



was placed beside this probe to check the air temperature thermocouple. A time synchronized check was made periodically.

## 2.5 Thermocouples

Temperature probes were placed at various critical depths in the pavement and subgrade to record the necessary data. Probes were also placed in an untreated base and subgrade section outside the paved area. All probes were 20 gauge iron-constantan thermocouple probes.

## 2.6 Data Analysis

The data compiled by the multi-point recorder indicated a temperature reading for each probe every six minutes. This collection procedure resulted in a voluminous amount of temperature data which was later selectively reduced, to represent hourly temperature values. These hourly values were extracted from the recorder chart and transferred to data sheets.

The high and low temperatures for each pavement probe and subgrade probe were recorded to establish the extreme temperatures for a given twenty-four period (see Figures 2.7.1 through 2.7.7). From the twenty-four hour period cycles of data an average temperature for each period was also calculated for each depth (see Tables 2.8.1 and 2.8.2).

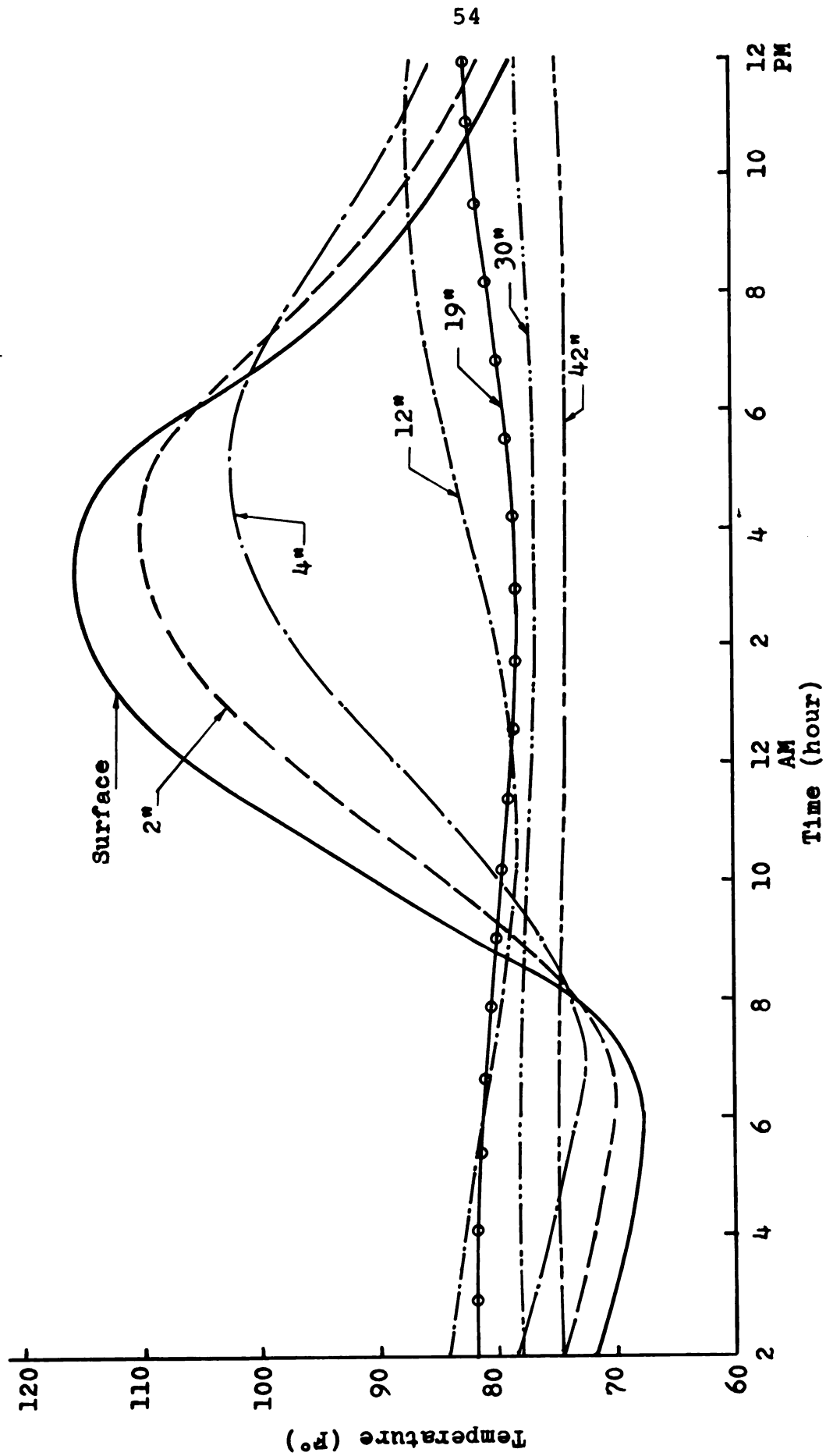


Figure 2.7.1 Full-depth asphaltic pavement temperature during a summer day (sunny).

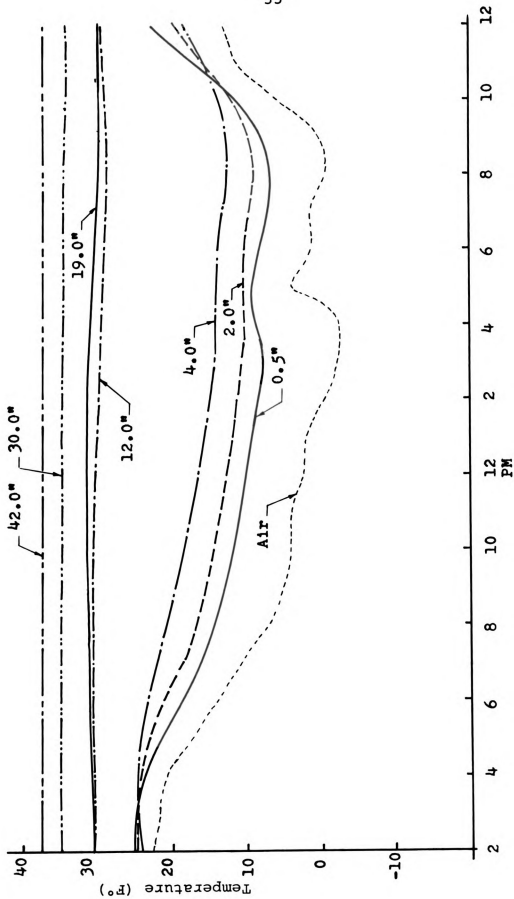


Figure 2.7.2 Pavement temperature during a winter day (1/5/70).

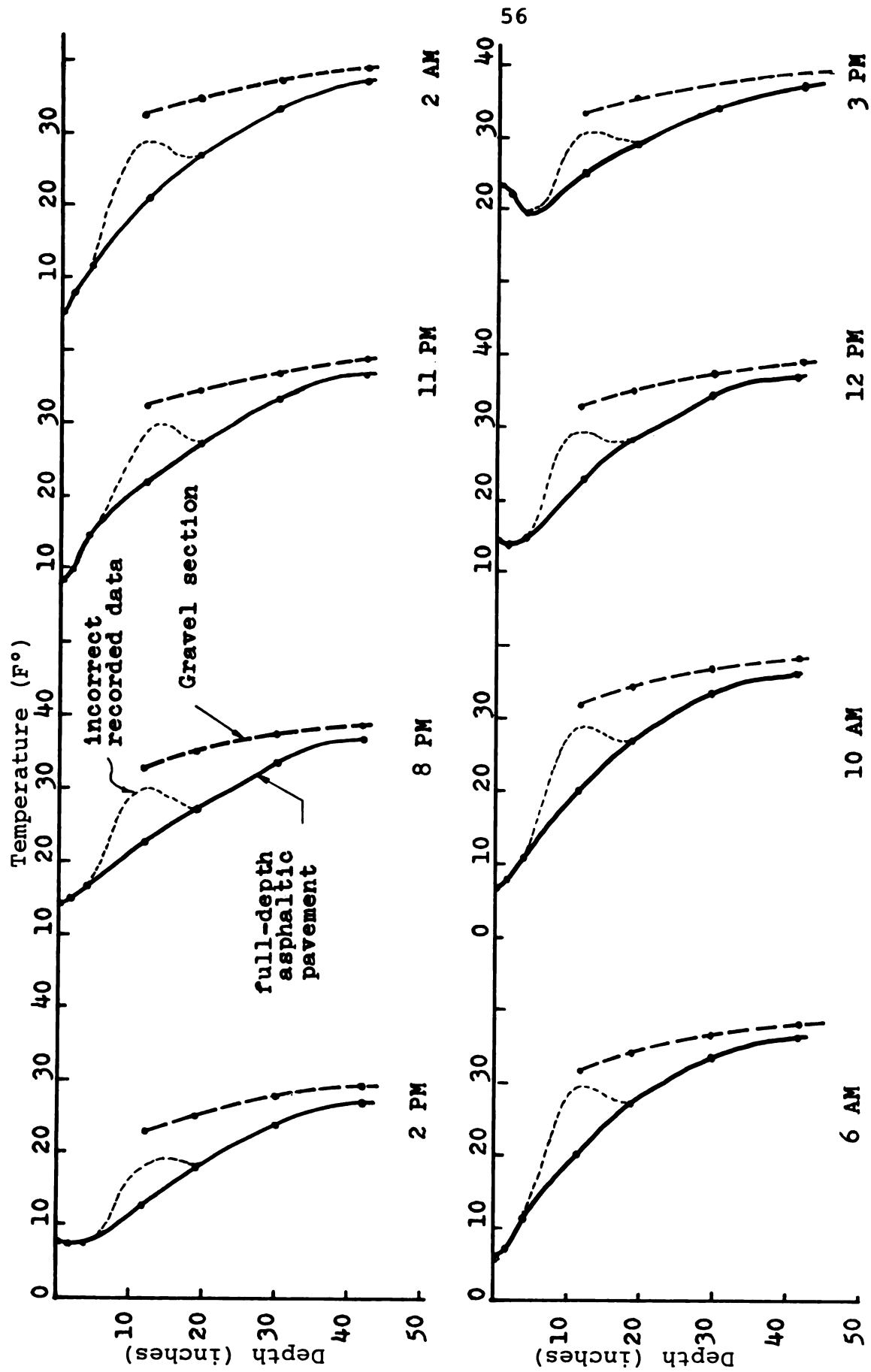


Figure 2.7.3 Temperature distribution in 19" full-depth asphaltic pavement and a gravel section at selected times during a winter day.

To facilitate this study some data relative to solar radiation of the Flint area was desired. Upon searching for such data, it was found that none was available for the Flint area, however, similar data for the East Lansing, Michigan area was available. Knowing the climatological data of the Flint and East Lansing areas, a correlation of the solar radiation for the Flint area could be obtained provided the amount of cloud cover and temperatures were considered equal.

## 2.7 Daily Temperature Distribution

Daily temperature distribution graphs were plotted based on hourly data collected from recorder charts. During a continuous sunshiny day in summer the temperature cycles generally would be represented as is given in Figures 2.7.1 and 2.7.7. The air and surface temperature curves are regular with only one peak, occurring during the middle of the afternoon. Cloud cover will, however, effect the surface temperature resulting in several peaks and irregular air and surface temperature curves. During the cloudy and the rainy days the temperature within the pavement was uniform and nearly equal at all depths, consequently, distinguishment between the various thermocouple records was difficult.

Analysis of such collected field data required a comprehensive information concerning the local climatological data, which provided necessary information

concerning cloud cover, wind velocity, and precipitation. The above information was obtained from the National Weather Service which is located less than a mile from the study site location. All readings of cloud cover were recorded by physical observation.

Additional information such as hourly precipitation in the form of rain and snow, direction and intensity of wind speed may be obtained from the local climatological data sheets.

Temperature distribution in a 19-inch Bishop Airport asphalt concrete pavement and the underlying soil during a summer day is shown in Figure 2.7.1. Variation of temperature at different depths, down to 42 inches below the surface of the full-depth asphaltic pavement for a winter day are shown in Figures 2.7.2 and 2.7.3. A similar curve for a spring day is plotted in Figure 2.7.4.

Daily temperature profile in a 7-inch asphalt concrete pavement and subgrade on Alger Road, Gratiot, Michigan, during a winter day are shown in Figure 2.7.5. The temperature distribution curves shown in Figure 2.7.6 illustrate variation of temperature in the Alger Road pavement and subgrade during a few days in winter. Figure 2.7.7 shows temperature distribution for a few summer days in a 7-inch pavement layer.

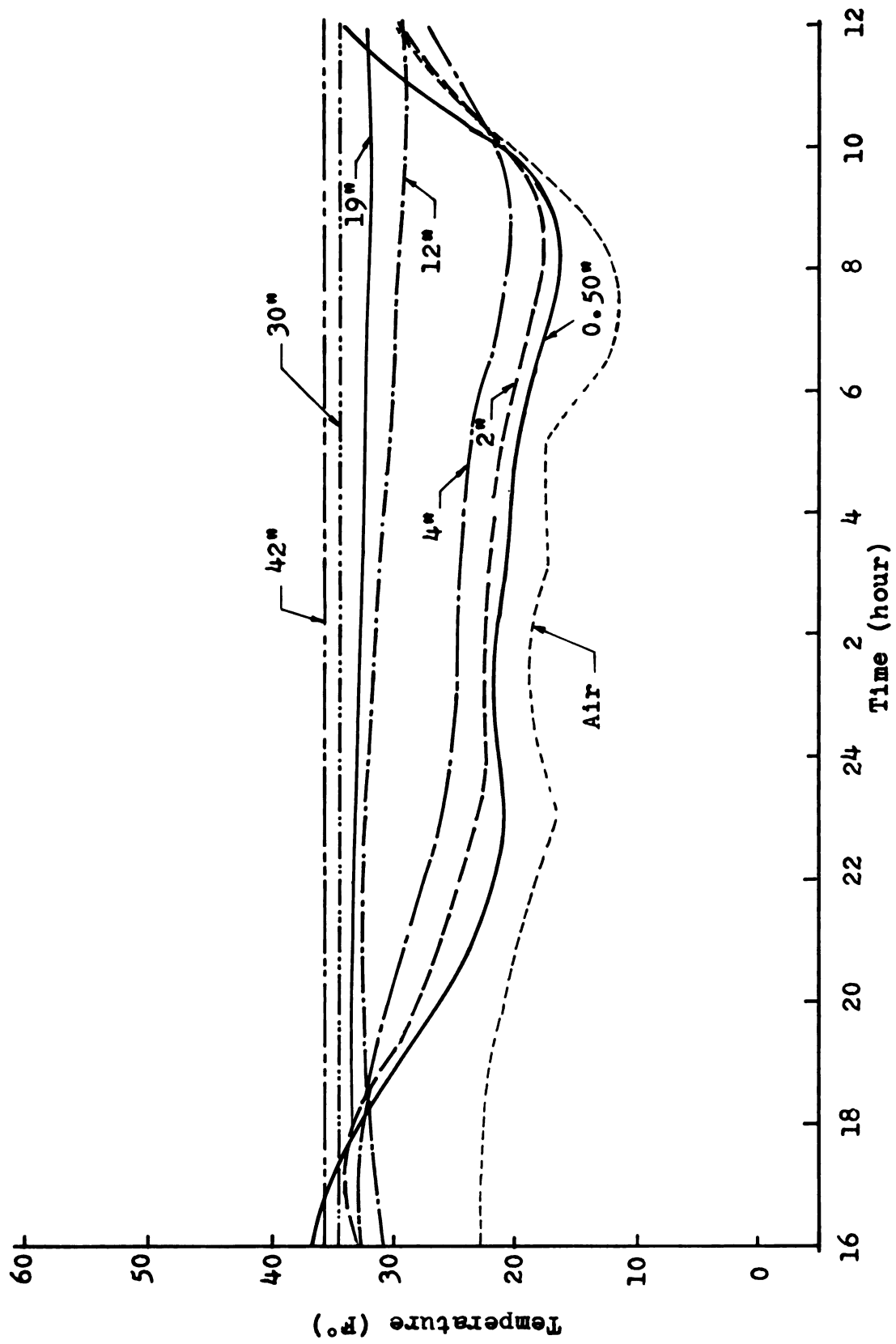


Figure 2.7.4 Pavement temperature during a spring day

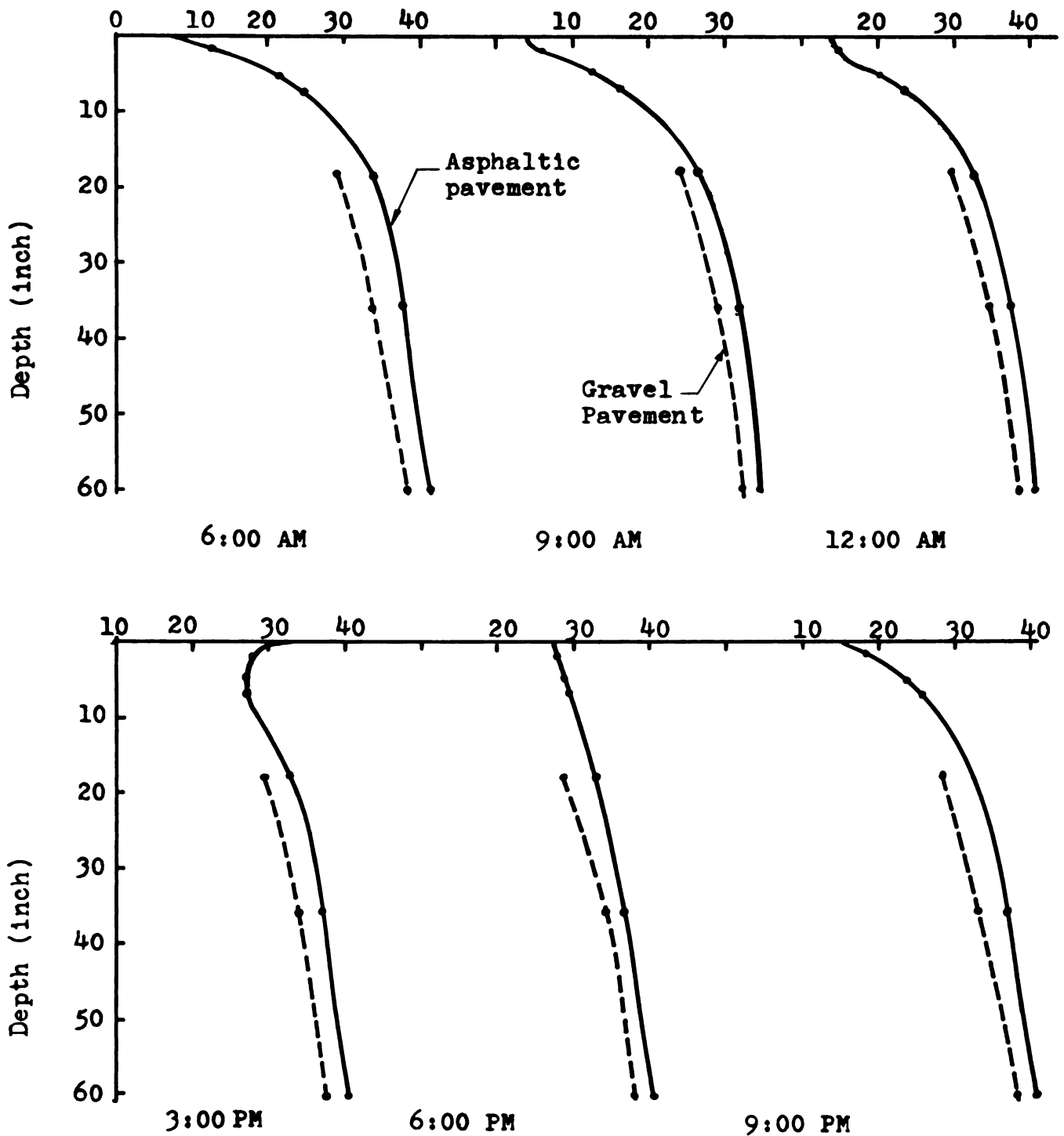


Figure 2.7.5 Temperature distribution in a 7" asphaltic pavement and a gravel pavement during a winter day (1/13/65)



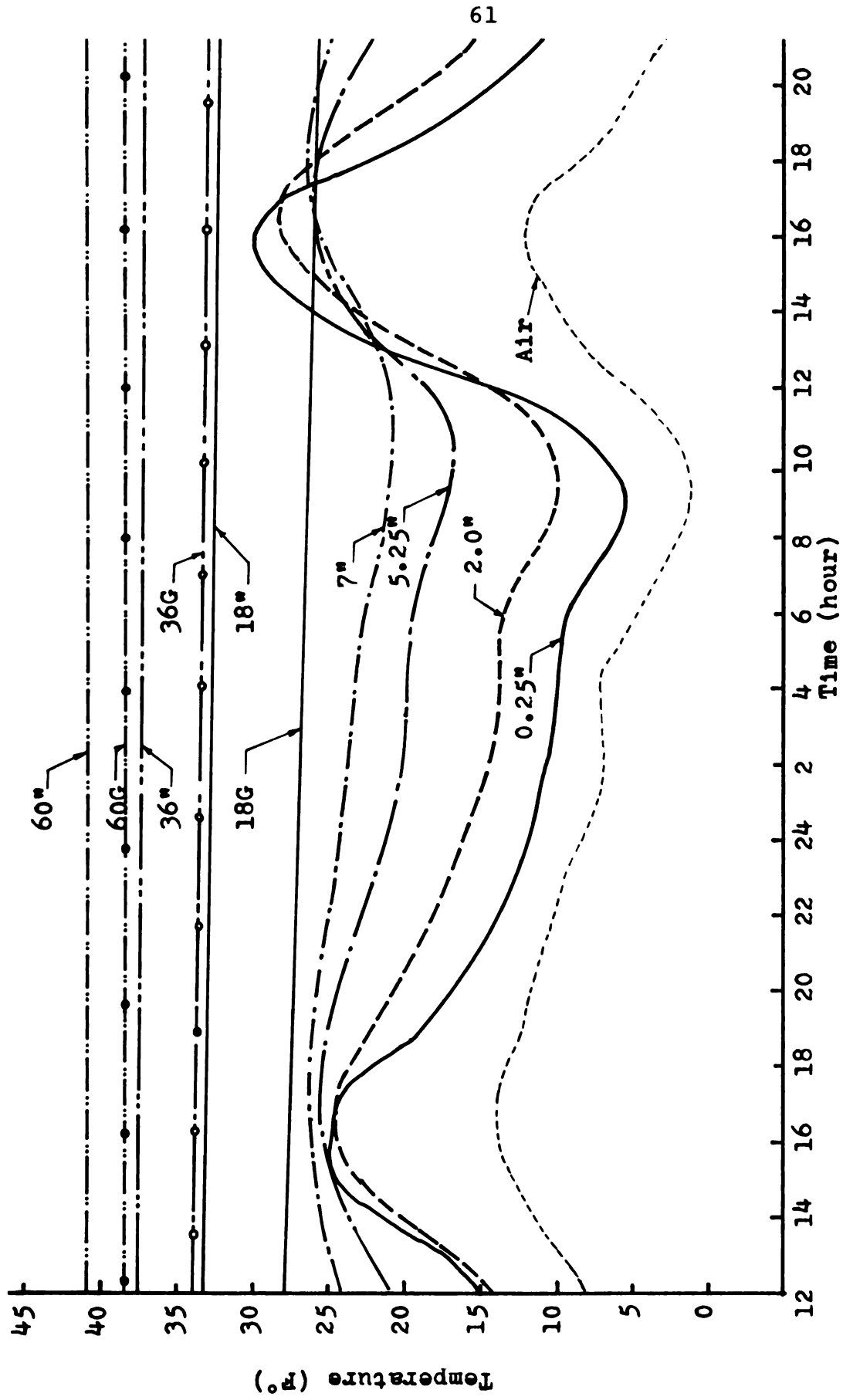


Figure 2.7.6 Pavement temperature during a winter day.

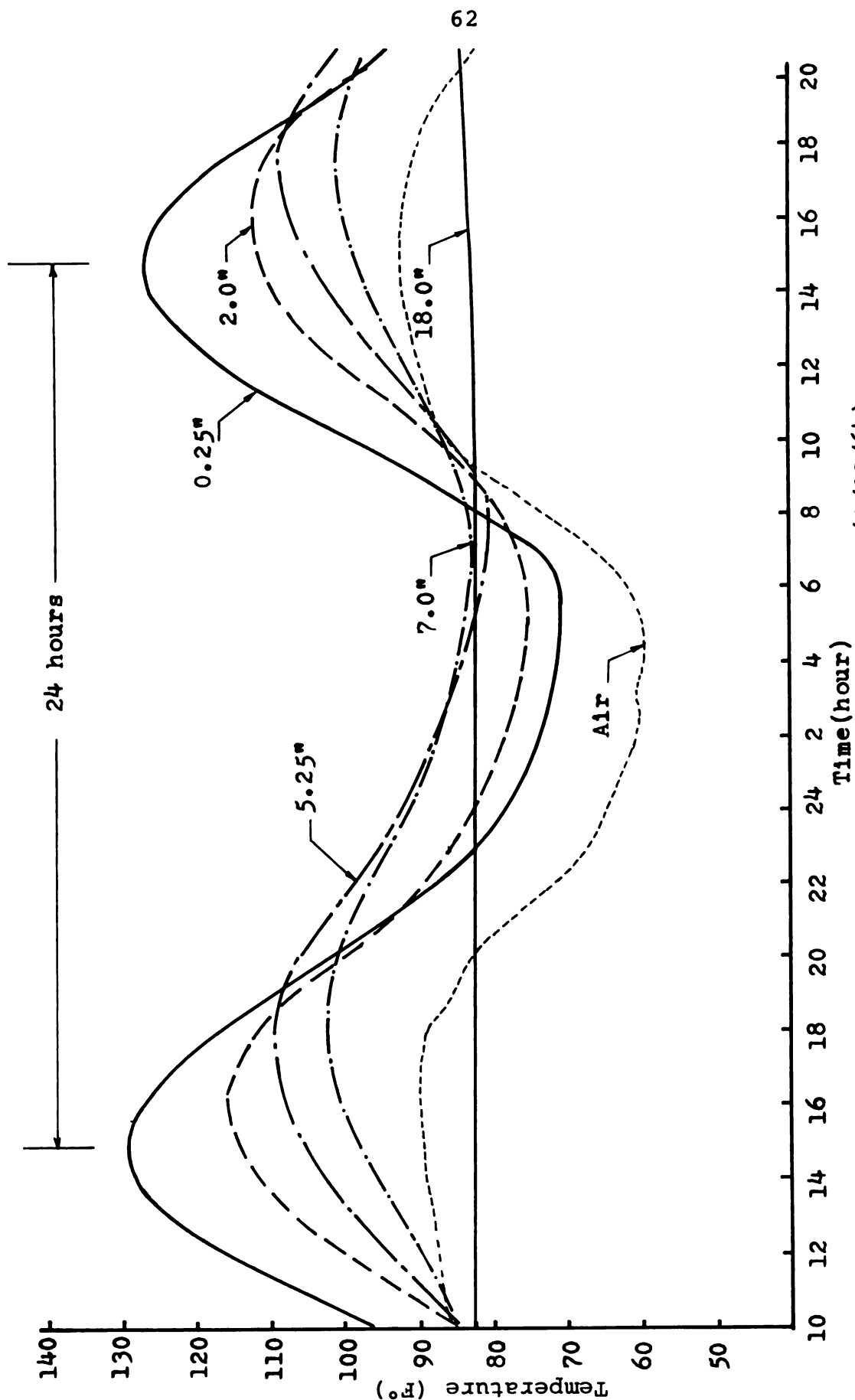


Figure 2.7.7 Pavement Temperature during a summer day (7/27/64)

## 2.8 Monthly Temperature Distribution

Monthly temperature distribution graphs were plotted based on hourly data collected from each depth (1/2-, 2-, 4-, 12-, 19-, 30-, and 42-inch) in the airport pavement and subgrade. Figure 2.8.1 shows the temperature distribution of wearing, binder, and mix base course of a 19-inch asphalt concrete pavement and soils beneath the pavement during the summer of 1969. Minimum daily temperature of the subgrade beneath the 19-inch full-depth asphaltic pavement and a gravel test section during February, 1970 are shown in Figure 2.8.2. Average daily temperatures of air and pavement surface are given in Figure 2.10.1. Discontinuous curves of temperature distributions, are resultant of incomplete temperature data during these periods.

During the summer, variations of temperature in top layers of asphalt concrete were of primary interest, while during the winter months the subgrade temperature was more relevant. Duration of a given temperature as well as maximum, minimum, and average temperature was useful in a long-term study of pavement performance. Trott (46) introduced an apparatus for recording the duration of various temperatures in roads. Determination of the percentage of time that a depth remained at an individual temperature during a specific interval was deemed important.

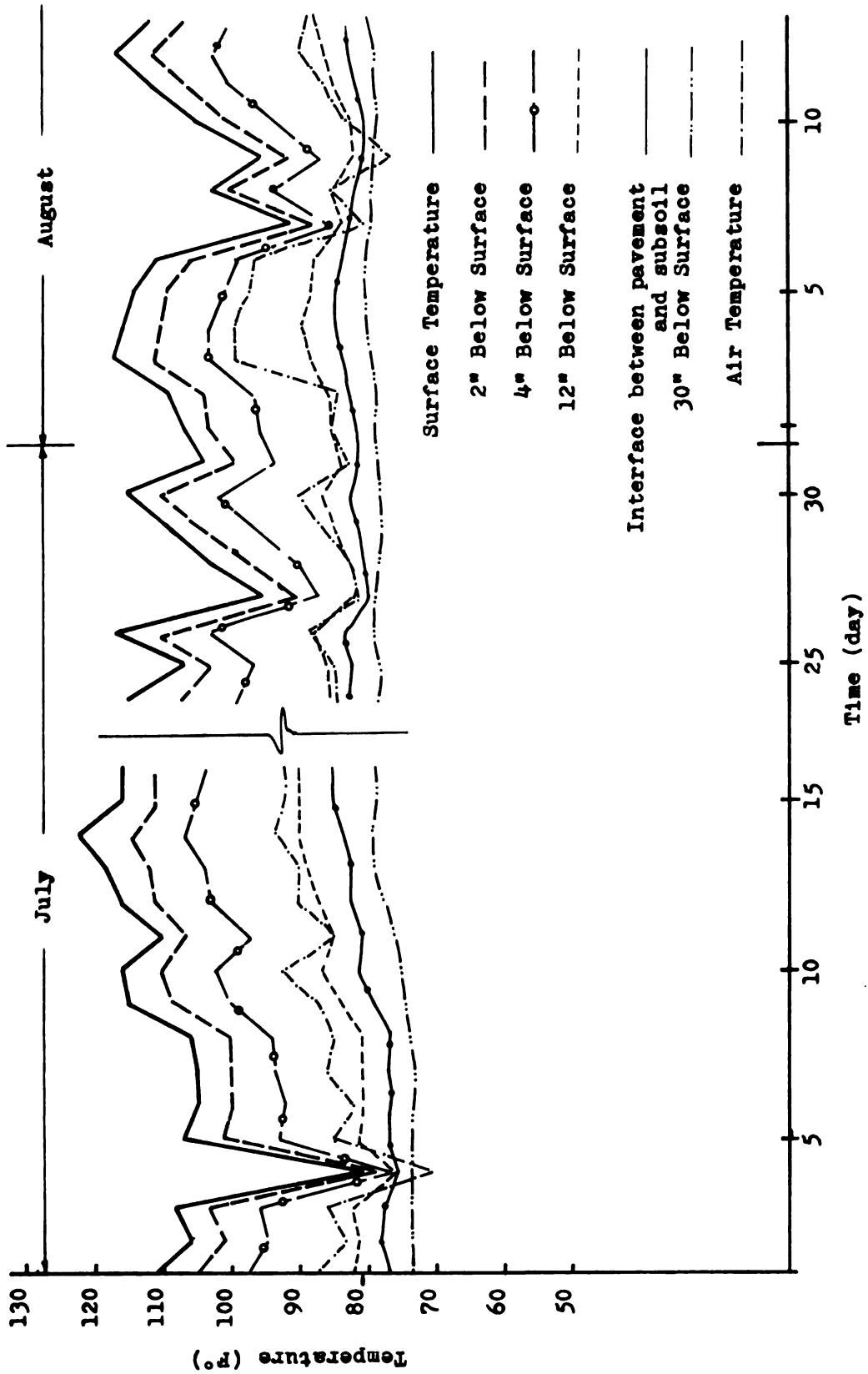


Figure 2.8.1 Full-depth asphaltic pavement temperature during the July and August of 1969

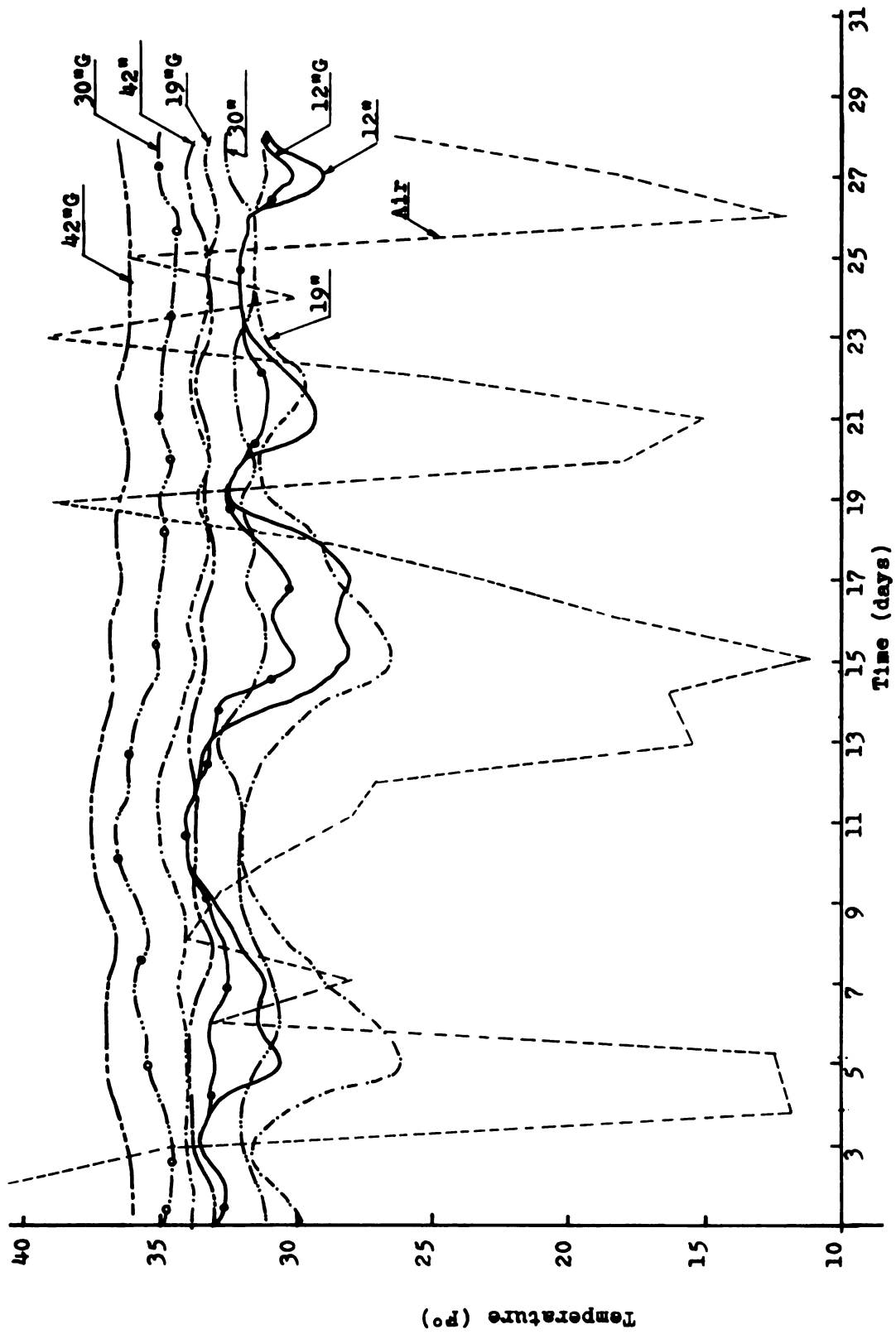


Figure 2.8.2 Subgrade temperatures beneath the 19" full-depth asphaltic pavement and a gravel section (February 1970)

The percentage of time may be determined for a period of one day, one month, or one year. Due to incomplete and discontinuous annual data, only daily and monthly duration of temperature are possible to calculate.

A 10°F increment of temperature was utilized as a standard for temperature retention in the pavement. This made best use of the available field data. The result of the above calculations, which are the duration of temperature levels at various depths of 19-inch asphalt concrete during the summer of 1969 and the winter of 1970, are tabulated in Tables 2.8.1 and 2.8.2.

Temperatures ranging between 130°F and 140°F at the pavement surface occurred only 1 per cent of the time during the summer months. During these periods, temperatures at 4 inches depth beneath the pavement surface did not exceed 107°F and at a depth of 12 inches beneath the pavement surface temperatures reached a maximum of 90°F. Similar results were obtained by B. K. Kallas (29) in studying variation of temperature in an asphalt concrete pavement in College Park, Maryland.

The duration temperature data given in Table 2.8.1 and the results of previous field studies, support the commonly accepted standard of 140°F for paving mixture stability, and for asphalt consistency testing. The data in Table 2.8.1 indicates that laboratory testing temperatures below 110°F should be considered in designing paving mixtures for the lower courses of the pavement.

Table 2.8.1 Duration of warmest temperature levels at various depths for a 19-inch asphalt concrete pavement during the summer of 1969.

Percent of the period during which the temperature (°F) was between										
	50 & 59	60 & 69	70 & 79	80 & 89	90 & 99	100 & 109	110 & 119	120 & 129	130 & 139	140 & 149
Air	-	1	9	65	25	-	-	-	-	-
1"	-	-	2	2	8	39	45	3	1	-
2"	-	-	5	5	10	55	25	-	-	-
4"	-	-	2	13	48	37	-	-	-	-
12"	-	-	20	80	-	-	-	-	-	-
19"	-	-	22	78	-	-	-	-	-	-

Table 2.8.2 Duration of coldest temperature levels at various depths of a 19-inch asphalt concrete pavement during the winter of 1969-70.

Percent of the period during which the temperature (°F) was between									
	0 & 9	10 & 19	20 & 29	30 & 39	40 & 49	50 & 59	60 & 69		
Air	32	23	23	17	3	2	-		
½"	10	25	40	15	10	-	-		
2"	-	-	14	86	-	-	-		
19"	-	-	32	68	-	-	-		
30"	-	-	-	84	16	-	-		
42"	-	-	-	75	25	-	-		



Duration of temperature, as well as temperature variation in wearing course, binder course, and hot mix asphalt base should be considered in the selection of dynamic modulus,  $E^*$ , and phase lag  $\phi$  in design procedures.

The dynamic modulus,  $E^*$ , and phase lag,  $\phi$ , for temperatures of 40°, 70°, and 100°F and different loading cycles are given in Table 1.6.1.

## 2.9 The Effect of Snow

A comparison between the temperature distribution at various depths of the gravel test section and the actual pavement at Bishop Airport pointed out that during the winter months the temperature at various depths of the gravel section is generally higher than those of the actual pavement. The opposite was observed from the Alger Road data. Figures 2.7.3 and 2.7.6 show the temperature distribution at various depths of the Bishop Airport test section and the Alger Road pavement respectively.

The observation of temperature distribution during the winter pointed out that even when the air temperature dropped below 10°F, the temperature at various depths of the gravel section did not fall below 30°F. The higher temperature beneath the gravel sections was mainly due to the insulation effect of the covering layer of snow and ice that had not been removed from the surface of the gravel section.

According to Beskaw (9), the effect of the layer of snow covering the surface may be taken as an equivalent increase in the thickness ( $S_f$ ) of the frozen soil.

$$S_f = S_s \frac{k_f}{k_s}$$

where  $S_s$  = thickness of snow,  $k_f$  and  $k_s$  = thermal conductivity of frozen soil and snow respectively.

Since the thermal conductivity of the snow,  $k_s$ , is about 10 to 15 per cent of that of ordinary pavement material (Beskaw [9]), the thermal resistance of snow is equivalent to a soil layer approximately seven to ten times thicker than the thickness of the snow cover. The result is that the insulating effect of this equivalent layer has protected the lower layers of the gravel section from freezing.

## 2.10 Freezing Indices

The depth of frost penetration beneath the pavement is influenced by many factors, such as: thermal properties of pavement material, pavement structure, and surface conditions. The depth to which freezing penetrates is principally dependent upon the amount of water available within the subgrade soils and the magnitude and duration of below freezing temperature. The freezing index is used as a measure of combined duration and magnitude of below freezing temperature. Freezing index is defined as the number of degree-days between the highest and lowest

point on a curve of cumulative degree-days versus time for one freezing season (16).

The degree-days for any one day equals the difference between the average daily air temperature and 32°F ( $T_{avg} - 32$ ). Degree-days are negative when the average daily temperature is below 32°F and positive when above (see Figure 2.10.1). These are referred to as freezing degree-days and thawing degree-days, respectively.

The freezing index may also be calculated by determining the area between the 32°F line and the curve of the average monthly temperature and time (16). The air freezing index may be calculated on a daily or a monthly basis from either the monthly or annual summary of the climatological data published by the National Weather Service. Monthly climatological data includes maximum, minimum, and average daily temperature while the annual summary includes the average monthly air temperature.

Freezing index isograms are available for the continental United States. However, it is preferable to compute the local freezing index from the recorded daily temperature data. This is because freezing conditions may vary widely over short distances due to the differences in elevations, topographic position, bodies of water or other sources of heat. This fact has been observed from the calculated freezing index for the Midland and Tri-City airports, Michigan, which are located less than fifty

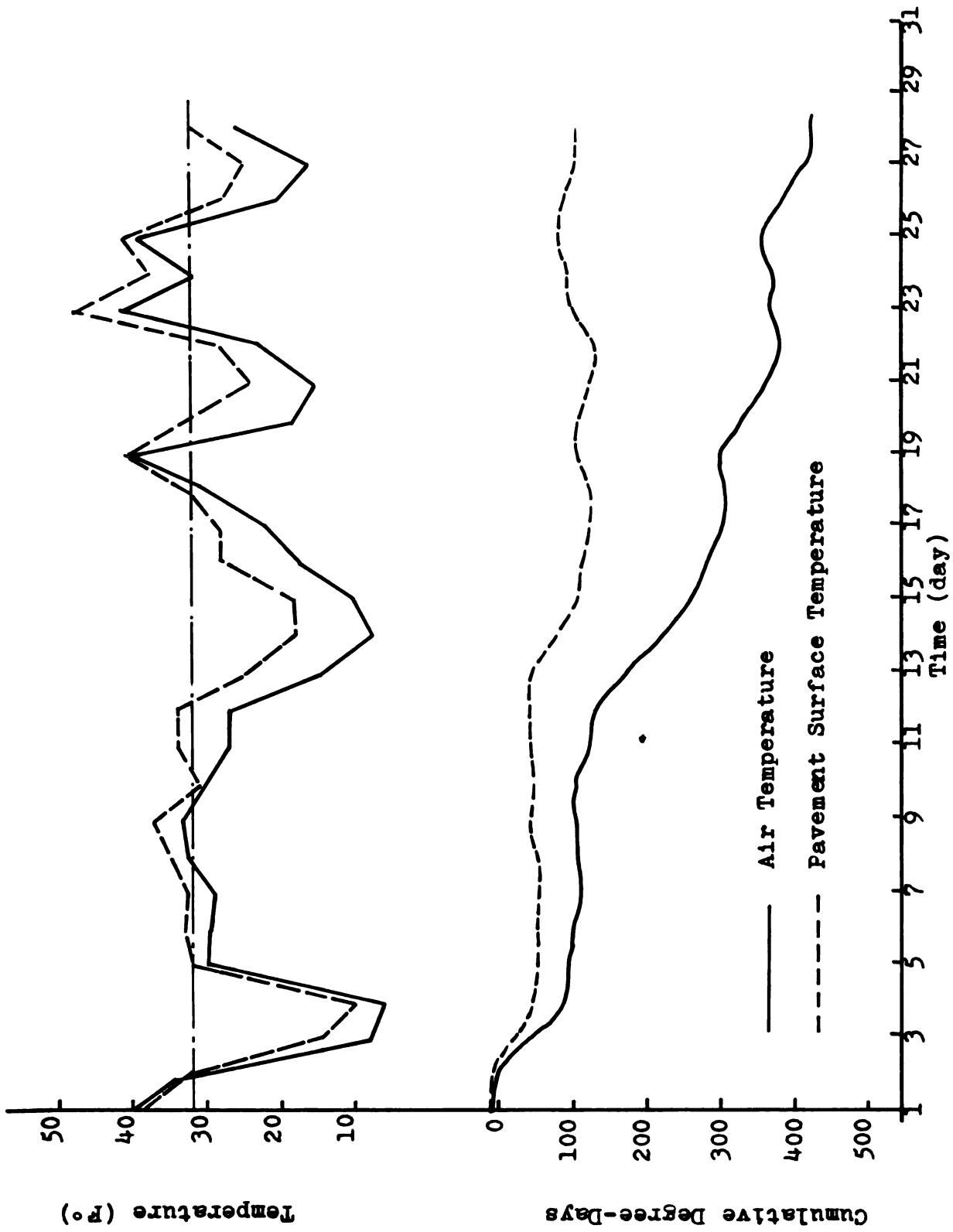


Figure 2.10.1 Average daily temperature and cumulative degree days (February 1970)

miles from the study site location. A difference of 360 degree-days has been observed between the freezing indices of these two locations, probably due to the influence of the Tittabawassee River which moderates the temperature of the Midland area (41).

Figure 2.10.2 shows the cumulative degree-day curves obtained from the recorded temperature data at Bishop Airport during the winter of 1969-1970. The average daily temperature, based on hourly temperature, would be slightly more accurate, but such precision is not usually warranted. The air freezing index, as well as the surface freezing index, are given in Figure 2.10.2. The air freezing indices obtained from the annual climatological data since 1950 at Flint, Michigan, are given in Table 2.2.1. An average air freezing index of the three coldest winters since 1950 must be used for design purposes (41).

#### 2.11 Correlation Factor "n"

The existing method of calculating pavement temperature and predicting the depth of frost penetration requires a correlation between the air and surface indices. The ratio of the surface index to the air index is designed as the "n-factor" for the purpose of correlation (38). Most designers still employ the empirical correlation factor,  $n$ , to convert the air freezing index to the surface freezing index.

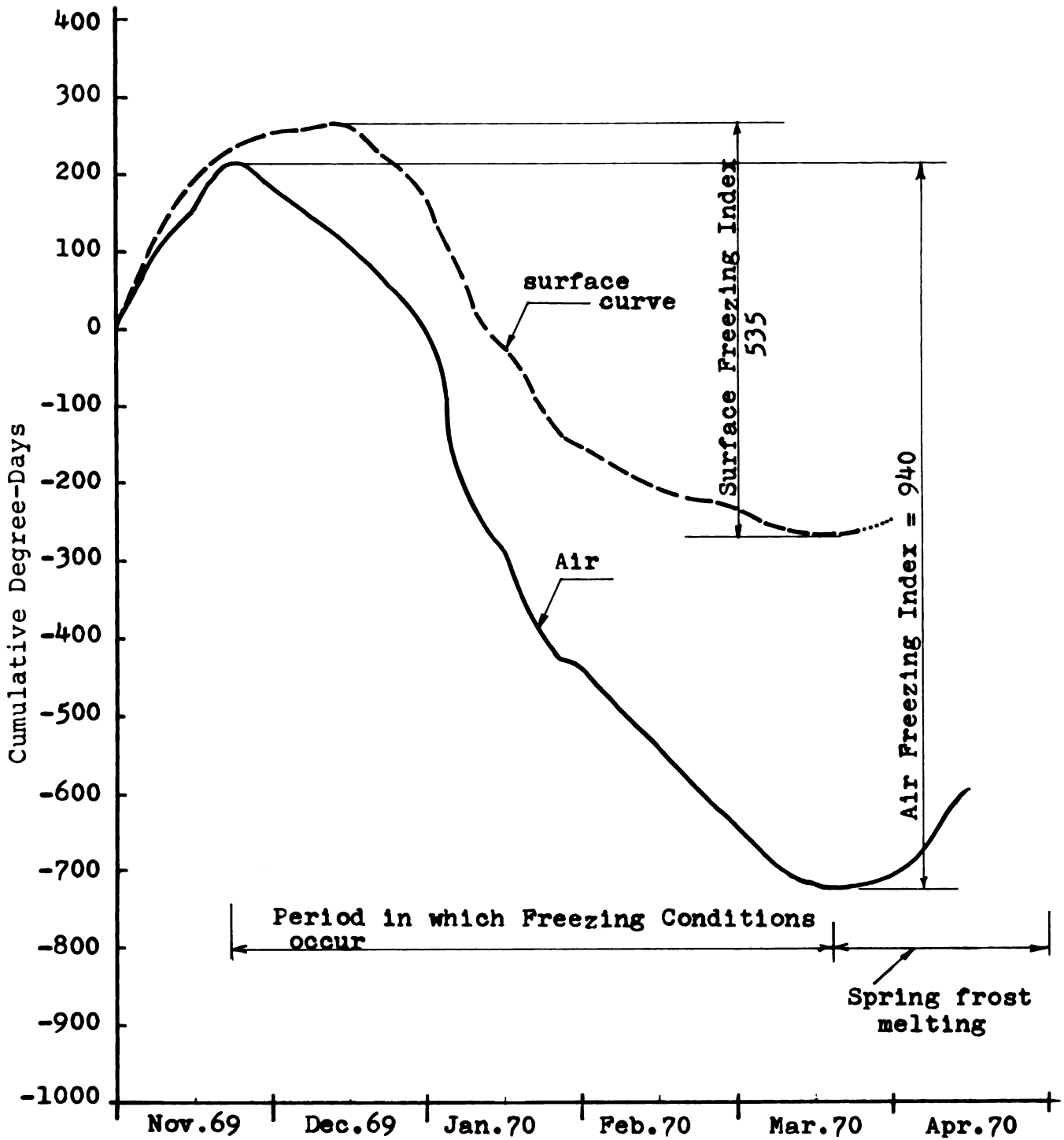


Figure 2.10.2 Cumulative degree-days above and below 32°F at Bishop Airport, Flint, Michigan

A correlation factor,  $n$ , of 0.51 is obtained from the freezing indices shown in Figure 2.10.2. An accurate value of  $n$ -factor requires concurrent observation of air and surface temperature throughout a number of complete freezing and thawing seasons. However, the temperature data at Bishop Airport is recorded discontinuously during one freezing period. Consequently, the obtained value of the correlation factor is questionable.

#### 2.12. Air and Surface Temperature

As indicated in the literature review, a number of mathematical relationships between the air and pavement surface temperature have been developed. However, there has not been any significant progress in the application of these methods to the determination of cumulative pavement surface cold quantities from basic meteorological data. Usually air temperature is available, but surface temperature is not. In order to obtain a correlation between the air temperature and surface temperature, the combined effects of radiative, convective, and conductive exchange at the surface must be considered. The difference between the air and surface temperature at any specific time is influenced by the latitude, cloud cover, time of year, time of day, surface characteristic, and finally, the thermal properties of pavement materials and the heat transfer coefficient. Surface temperature is also

influenced by ambient conditions such as wind velocity, temperature level, and precipitation (45).

Realistic values of the pavement thermal property are necessary in order to obtain a correlation between air and surface temperature. A major portion of this thesis is devoted to the estimation of thermal property of paving material with particular regard to asphaltic concrete, in recognition of this need. A method of calculating the coefficient of air-heat transfer from the thermal conductivity of pavement is given in Chapter V.



## CHAPTER III

### EXPERIMENTATION

#### 3.1 Purpose of the Experiment

The purpose for obtaining experimental data is to provide a means of comparison of thermal properties obtained from available field pavement studies to those obtained by simulated laboratory model tests under controlled conditions.

For determining thermal conductivity and specific heat of asphalt concrete, the knowledge of the combination of temperature and heat flux histories is necessary. In the field pavement data, no information concerning the heat flux was available. Hence, a simulated model was prepared in the laboratory in order to obtain required data for evaluation of both thermal properties. The experimentation consisted of: (1) measuring temperature as a function of time and at several locations of the specimen, and (2) calculating heat flux from measured temperatures of the calorimeter.

Table 3.2.1 Composition and density of dynamic modulus test specimens (Bishop Airport asphalt concrete wearing and binder courses, and hot-mix asphalt base course) after The Asphalt Institute Laboratory, July, 1970.

Pavement Course	AGGREGATE GRADING-PERCENT PASSING											Asphalt Content%	Average Density Lbs/Ft <sup>3</sup>
	1 in. 3/4 in.	3/8 in.	1/2 in.	3/4 in.	#4	#8	#16	#30	#50	#100	#200		
Asphalt Concrete Wearing Course			100	81	62	52	39	21	7	4.4		6.0	140.9
Asphalt Concrete Binder Course	100	95	59	44	38	33	27	19	8	1	0.4	4.5	145.8
Hot-Mix Asphalt Base Course	100	92	84	69	57	48	37	28	17	9	5.7	4.0	143.0

### 3.2 Preparation of Test Specimen

A mixture of asphalt concrete similar to an in-use field pavement was prepared in the laboratory. The composition and density of the samples were that of a wearing course, binder course, and hot mix asphalt base course for the existing asphaltic concrete pavement at Bishop Airport in Flint, Michigan, which is given in Table 3.2.1. Samples of asphaltic concrete representing various courses of the pavement were prepared having a diameter of 3 inches and a thickness or height of 1.5 to 2.0 inches.

Iron-constantan thermocouples 30 gauge were placed at various depths of the specimen by drilling round holes into the cylindrical surface of the specimen. The hole was 1/2-inch deep into which thermocouples were carefully affixed using asphaltic cement. Due to the non-homogeneity of asphalt concrete, considerable difficulties were encountered in locating each set of four thermocouples in the various horizontal planes at varied heights of the specimen.

Figure 3.2.1 indicates the location of the thermocouples in the specimen. Four thermocouples were located at each of the depths of 0.25, 0.50, 1.0, and 1.25 inches measured from the top surface of the specimen. The thermocouples were connected two by two at each depth, with a resultant of two average temperature readings obtained for each sample's level. At each depth two

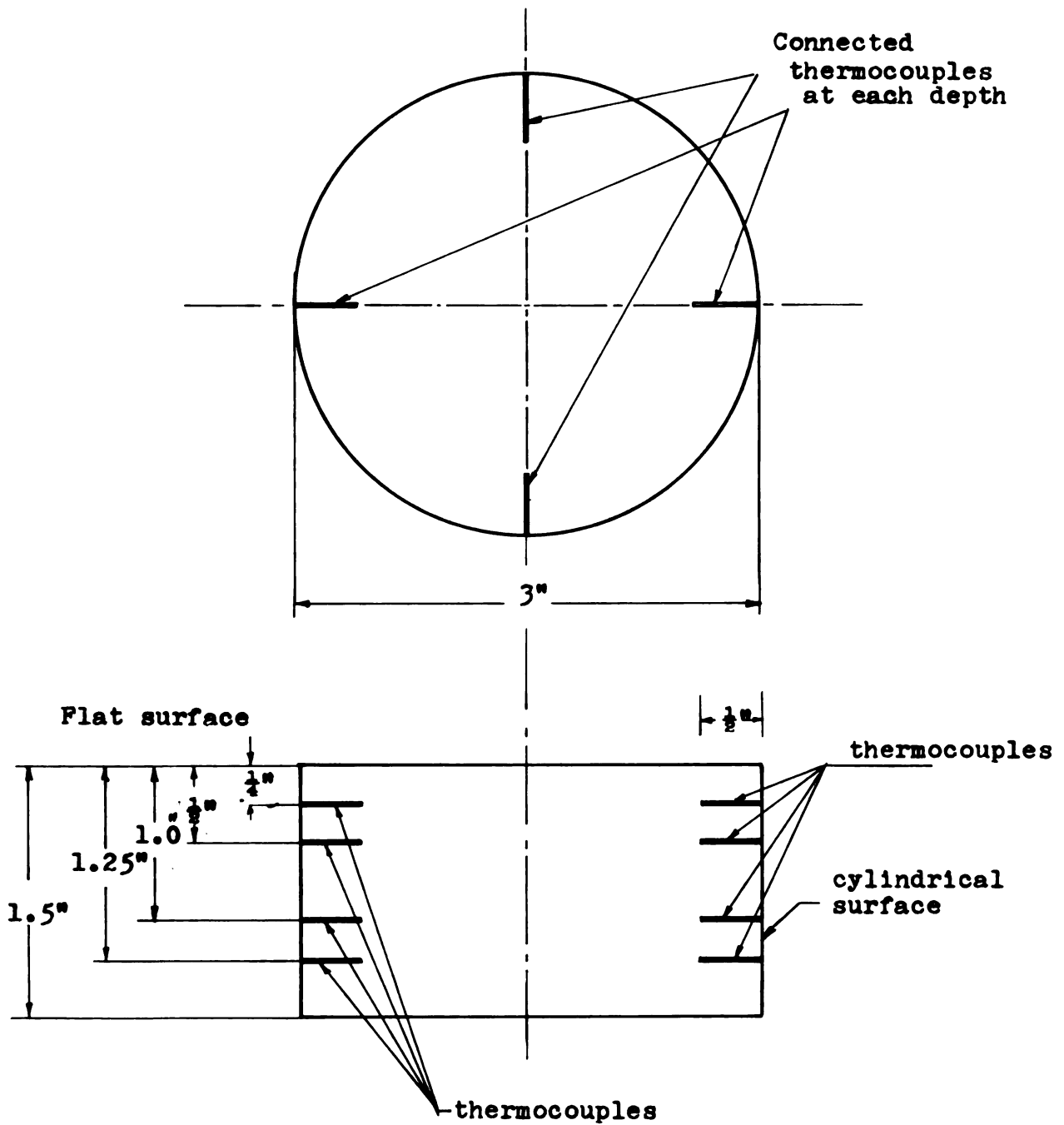


Figure 3.2.1 Location of thermocouples in the asphaltic sample

thermocouples were connected to produce an average of these; hence, eight temperature histories were measured, two at each of the four depths.

### 3.3 Facilities and Equipment

The facilities used in this experiment may be grouped as following:

1. Hardware and data acquisition equipment.
2. Data analysis facilities.

Hardware and data acquisition facilities consist of the heat transfer frame, hydraulic system, controls, signal amplifiers, and an IBM 1800 to digitize the data. The heat transfer frame retains the specimen and a standard plate calorimeter in two separately insulated containers.

In this experiment, sixteen thermocouples at four levels and at varied distances from the surface of the specimen were utilized. One thermocouple near the heated surface of the calorimeter was utilized to measure the surface temperature during the test.

Temperatures were obtained in terms of voltage by the quadratic equation (6)  $T = A_i V^2 + B_i V + C_i$ , where  $i = 1$  to 10, and  $T$  is temperature in degrees Fahrenheit, and  $V$  is voltage in volt. Coefficients  $A_i$ ,  $B_i$ , and  $C_i$ , are found by a least-square fit. The temperature rises in the experiments produced voltage changes on the order of several millivolts.

The IBM 1800 was used to digitize the analog signals produced by the thermocouples. It can take analog inputs between  $\pm 10$  volts; therefore, the amplifiers were utilized to raise the millivolt thermocouple signals to the order of several volts (for the details, see reference [6]).

The temperature data were recorded by the IBM 1800. There are two programs for printing and punching the data. One is the off-line which stores the data until the test is completed, and the other is a non-line program which prints and punches during the test. In this experiment, the off-line program was employed. For analyzing data, a high speed digital computer, such as the CDC 3600 or 6500 is used. The properties were calculated by the "Property Program" which will be described in the next chapter.

The facilities utilized in this experiment are capable of simultaneously measuring thermal conductivity, specific heat, thermal diffusivity, and a number of properties not used in this study. The method may be used to measure thermal properties of metals, porous materials, and most of the materials which change in composition when heated. Organic material and soils which are a multiphase-system composed of solids, liquids, and air are also included in this group.

### 3.4 Procedure

For one-dimensional heat flow, the specimen should be insulated on all surfaces except the interface with the calorimeter. The interface of the specimen and the calorimeter should be as smooth as possible and should provide intimate thermal contact. The opposite surfaces acquire an insulation condition by attaching the calorimeter and the specimen to insulating solids. For high thermal conducting materials, it was easy to approximate an insulation condition by attaching the specimen to a low conductivity material, while for very low thermal conductivity materials, such as asphaltic concrete, the specimen in effect, insulates itself.

The specimen was made thick enough (1 1/2 inches in this case) so that the temperature does not rise significantly at the "insultated" surface during the test; the specimen is then said to be effectively semi-infinite in thickness. The cylindrical surfaces of the calorimeter and specimen were insulated using fiberglass.

The required duration of the test, as well as side heat losses, can be reduced by decreasing the thickness of the specimen and the calorimeter. The thickness of the calorimeter was 1-inch and the asphalt sample had a thickness of 1.5 inches. Both the specimen and the calorimeter were 3 inches in diameter. There are a variety of methods which may be utilized to heat the

calorimeter, including an electric heater which was used in this test. The sample of asphaltic concrete was deformed at a temperature beyond 150°F. Hence, the 150°F temperature was utilized as the limit in heating the specimen. In one test, the temperature of the sample was decreased to -30°F by employing dry ice (CO<sub>2</sub>). The copper calorimeter with accurately known specific heat and high thermal conductivity, was heated to a uniform temperature of about 120°F and then brought suddenly into contact with the specimen which was at another uniform initial temperature (-30°F in one test).

A series of tests at several initial temperature levels of the specimen were performed. The initial temperatures represented various seasonal temperatures with the laboratory tests to simulate the natural conditions. In the tests described above, each successive test was started with a higher uniform initial temperature and the specimen was heated. In another series of tests, the specimen was at a relatively high initial temperature (about 120°F) and the calorimeter cooled.

The specimen and the initial temperature of the specimen decreased from test to test. In order to evaluate the effect of moisture on thermal properties of asphaltic concrete, tests were performed on a sample before and after it was soaked in water and the obtained temperature data were compared. Before initiating the



series of tests, the thermocouples were calibrated. (For the details and further information, see reference 6.)

### 3.5 Heat Flux Calculation

One of the main objectives of the experimentation was to compensate for the lack of information on heat flux in field data. In order to obtain the values of thermal conductivity,  $K$ , and specific heat,  $C_p$ , the heat flux as well as temperature data must be known (8). (Also see Figure 6.4.1 and related heat transfer equation.)

Experimentally measured temperature at the surface of the calorimeter may be employed to calculate the heat flux at the interface of the calorimeter and the specimen. There is usually a significant resistance to heat flow at the interface due to an imperfect contact. Regardless of the magnitude of the resistance, the same heat flow leaving the calorimeter at the common interface must enter the specimen.

The heat flux  $q(t)$  may be calculated by employing the first law of thermodynamics for the calorimeter to obtain:

$$q(t) = \rho C_p L \frac{dT}{dt} \quad (3.5.1)$$

where  $\frac{dT}{dt}$  is the gradient of temperature/time curve over time interval  $dt$  at the surface and  $\rho C_p$  and  $L$  are the volumic specific heat and thickness of standard, respectively.

This equation is valid if:

1. There is a negligible temperature difference across the calorimeter at any time, and
2. All surfaces are insulated except the common interface.

Experimentally measured temperatures at the surface of the standard are given as the function of time in Figure 3.5.1.

Curves of temperature versus time, similar to the one shown in Figure 3.5.1 are plotted for each test. The most sensitive part of the evaluation process is determining the temperature gradient  $\frac{dT}{dt}$ .

Since the temperature gradient is not constant over the entire time period, it was determined by taking the differences of temperature at different time intervals. The heat flux has been calculated by utilizing the obtained temperature gradient for different time intervals in Equation 3.5.1. The calculated heat flux will be used as a boundary condition in the mathematical model, used while estimating the thermal conductivity and specific heat of asphalt concrete.

### 3.6 Results

The experimentally measured temperature at various depths of a sample of asphaltic concrete as the function of time are shown in Figure 3.5.1. Two sets of temperatures were measured for each level of the specimen. It

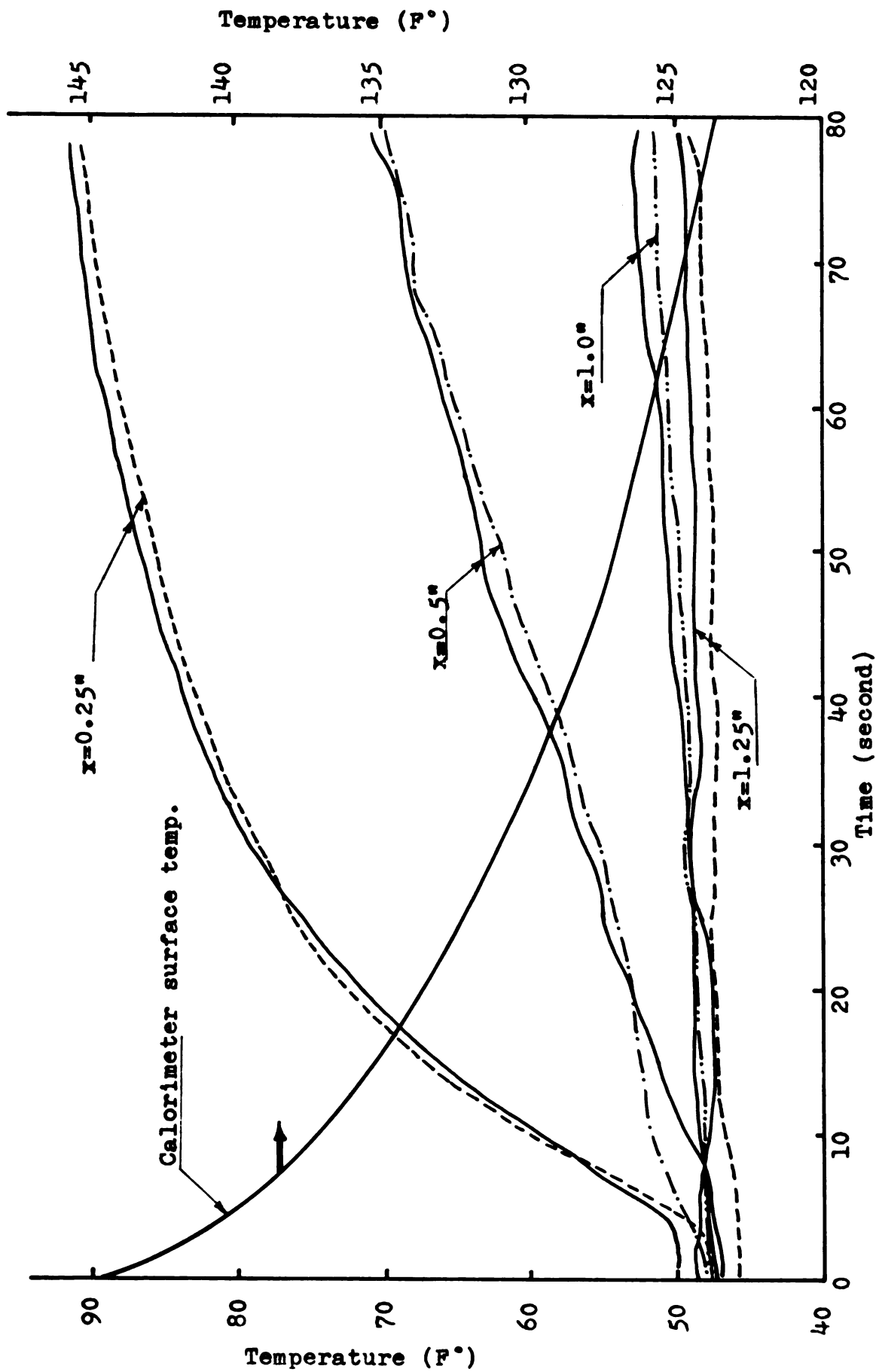


Figure 3.5.1 Experimentally measured temperature at the calorimeter surface and various depths of the asphaltic sample (solid and dashed lines refer to first and second thermocouple sets)

was observed that error in measuring temperatures at various levels was mainly a systematic error rather than an independent random variable. This may be verified by comparing each two columns of temperature data or by the curves of temperature versus time, similar to the one shown in Figure 3.5.1.

Systematic error in measuring temperature was due mainly to the error in measuring the location of the thermocouples, bad contact between the thermocouples and the specimen, as well as error due to the presence of the thermocouples themselves.

The observed systematic error in measuring temperature could also have been due to the inhomogeneity of the asphaltic concrete.

In calculating thermal properties by the nonlinear estimation method from these transient temperature data, the correction for the biased error caused by the systematic errors should be made if possible. The average measured temperature as well as a separate set of data at various depths of the specimen was utilized to calculate thermal conductivity and volumetric specific heat of the asphaltic concrete specimens. The obtained values of thermal properties are given in Tables 3.6.1, 3.6.2, and 5.8.4. The results indicated that the average of the thermal properties obtained by using each set of data separately was equal to the result obtained when

Table 3.6.1 Calculated thermal diffusivity of asphaltic concrete from laboratory data (nonlinear estimation method)

Case	Condition	Sample Temp (F°)		Root-Mean-Square	Thermal Diffusivity (ft <sup>2</sup> /hr)
		Max	Min		
1.1	dry	146	118	1.76	0.040
1.2	"	146	118	0.79	0.041
1.3	"	146	118	0.93	0.042
1.4	"	146	118	1.17	0.041
2	"	130	97	1.72	0.045
3	"	124	80	2.82	0.043
4	"	117	75	2.99	0.049
5.1	"	80	5	1.33	0.047
5.2	wet	75	2	2.91	0.061
5.3	dry	85	-1	3.12	0.055
6.1	dry	26	-27	2.57	0.052
6.2	wet	25	-25	0.91	0.067
6.3	dry	32	-15	0.78	0.058

Table 3.6.2 Calculated thermal conductivity and specific heat of asphaltic concrete from experimental data (nonlinear estimation method)

Case	Condition	Sample Temp (F°)		Root-Mean-Square	Thermal conductivity (Btu/hr ft·F)	Volumetric Specific heat (Btu/cuft/F°)
		Max	Min			
1.1	dry	146	118	3.62	1.20	29.36
1.2	"	146	118	2.66	1.28	29.30
1.3	"	146	118	3.98	1.25	29.05
1.4	"	146	118	3.02	1.22	28.90
2	"	130	97	2.12	1.29	28.32
3	"	124	80	3.98	1.35	29.05
4	"	117	75	2.72	1.45	29.15
5.1	"	80	5	1.06	1.40	29.36
5.2	wet	75	2	2.32	2.14	30.62
5.3	dry	85	-1	2.95	1.62	29.00
6.1	dry	26	-27	1.68	1.50	30.01
6.2	wet	25	-25	1.72	2.08	31.13
6.3	dry	32	-15	0.98	1.76	30.54

employing the average of the temperature for each depth (see cases 1.1 through 1.4 in tables).

The data obtained on the moist specimen differed from that of the dry ones due to the existence of liquids in the pore space and the fact that thermal conductivity of water is approximately twenty times that of air (11) (see cases 7 and 8 in Tables 3.6.1 and 5.8.4). Thermal diffusivity of the wet samples were approximately 10 per cent higher than the dry samples. Although in this study only a few tests were conducted, their results pointed out the effect of moisture on thermal properties of asphaltic concrete.

In order to see if the two sets of measured temperature data agree reasonably with each other, a case was considered as the representative of all the cases, and the analysis of variance was performed for each set of data. Since there are two sets of thermocouples at each depth of the specimen, with a resultant of two average temperatures for each sample level, the sample variance is obtained as (48):

$$s^2 = \frac{1}{N-1} \sum_{t=1}^n \frac{1}{2} (T_{i1} - T_{i2})^2$$

where subscript "i" refers to the time and  $T_{i1}$  and  $T_{i2}$  are the average temperatures measured by each set of thermocouples at the same depth of the specimen. The

calculated values of the variance are given in Table 3.6.3A. The low values of the variance which were a measure of variation or the spread of the measured temperature near the mean indicates a good agreement between the two sets of data.

The adequacy of the model which was utilized in calculating thermal properties was confirmed by comparing the calculated average values of variance from the data alone with the values of root-mean-square (RMS) obtained in the process of iteration in estimating thermal properties by the nonlinear estimation method. The calculated values of RMS for the representative case are given in Table 3.6.3B.

An accepted procedure for determining the adequacy of the model is to calculate the ratio of the calculated variances and root-mean-squares to determine whether or not the values of RMS are significantly greater than the calculated variance. Average values of 0.94 and 1.16 were obtained for calculated values of variance and the value of RMS for the representative case, respectively. It is observed that the calculated values of variance are in good agreement with the values of root-mean-squares and there is not a significant difference between these values. With this rational, there appears to be no reason to doubt the adequacy of the model.



Table 3.6.3-A Analysis of the variance for the representative case

Thermocouple level (inch)	Calculated Variance (F ) <sup>2</sup>	Standard Deviation (F )
0.25	0.70	0.84
0.50	0.70	0.84
1.00	1.35	1.16
1.25	1.00	1.00

Table 3.6.3-B Calculated values of root-mean-square and thermal diffusivity for the representative case

Case	Root-mean-square (RMS)	Thermocouples	Calculated Thermal Diffusivity ft <sup>2</sup> /hr
1.1	0.93	1,3,5,7	0.0424
1.2	1.76	2,4,6,8	0.0397
1.3 (avg)	0.79	(1&2),(3&4), (5&6),(7&8)	0.0412

The close agreement of the calculated variances and root-mean-squares leads to the conclusion that the model has fully described the relevant physical process and there is a reasonable agreement between the measured and calculated temperatures at various depths of the specimen.

Even though the model has been found adequate, as a standard procedure in regression analysis, the residuals are plotted in Figure 3.6.1. Several ways of examining the residuals in order to check the model are given in reference (48). Discussion concerning examination of residuals is beyond the scope of this study.

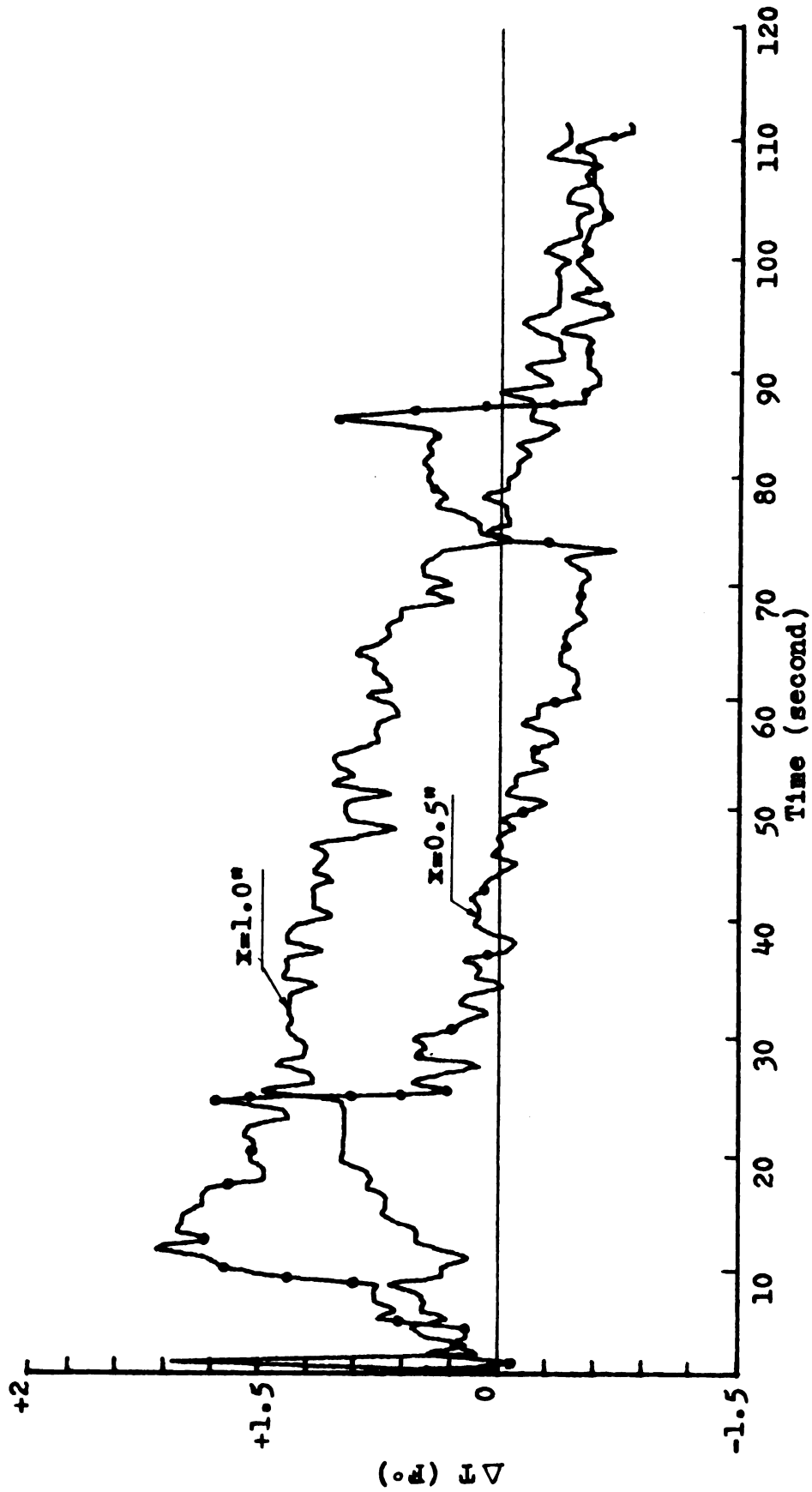


Figure 3.6.1 Difference between calculated and measured temperature (residuals) at 1/2-inch and 1-inch below the surface of the specimen (representative case)

## CHAPTER IV

### NONLINEAR ESTIMATION METHOD

#### 4.1 Nonlinear Estimation Method of Measuring Thermal Properties

The conventional methods of thermal property measurement determine the properties utilizing a simple mathematical model for a simple geometric and simplified experimental conditions. Each of these methods have some restrictions and generally are capable of measuring a single thermal property (i.e., a guarded hot-plate has been used frequently to measure thermal conductivity). The guarded hot-plate method requires the existence of a steady-state and a controlled constant temperature-boundary condition for obtaining accurate values of the thermal conductivity. In estimating thermal properties by classical periodic wave analysis, it is assumed that surface temperature varies about a mean temperature in a manner which approximates a sine wave (28).

Recent procedures using the nonlinear estimation method to measure thermal properties is not subjected to any of the above mentioned restrictions. The digital computer has made it possible to model a complex physical system accurately.

The models may describe numerous phenomena which are difficult to separate when designing experiments to measure individual properties. The models in this dissertation are not extremely complex, but nonlinear estimation must be used.

#### 4.2 Nonlinear Estimation Procedure

A mathematical procedure referred to as nonlinear regression, nonlinear least-square, or nonlinear estimation, has been known for a century before the high-speed digital computer made it practical to use routinely. Beck (8) developed this method to determine the thermal properties of solids. One of his interests has been to design analytically an optimum experiment for the simultaneous determination of thermal conductivity and specific heat.

The use of this method for determining the value of thermal diffusivity requires minimizing the sum-of-square function

$$F(\alpha) = \sum_{i=1}^n \sum_{j=1}^n W_i^j \left[ T_{(\text{cal})_i}^j(\alpha) - T_{(\text{exp})_i}^j \right]^2 \quad (4.2.1)$$

with respect to thermal diffusivity,  $\alpha$ . The expression  $T_{(\text{cal})_i}^j$  represents the calculated temperature at position  $x_i$  and  $t_j$ .  $T_{(\text{exp})_i}^j$  is the experimental temperature at  $x_i$  and  $t_j$ . The weighting factor  $W_i^j$  is used to give greater weight for accurate measurement and less for

inaccurate ones. However, in most of this work  $W_i^j$  was set equal to a constant.

In this procedure, the best value of the thermal diffusivity is the one which minimizes the difference in a least-square sense between theory and experiment for all of the available data. In other words, by varying  $\alpha$ ,  $T_{(cal)}^j$  is made to agree in a least-square sense with the measured temperature  $T_{(exp)}^j$  for  $n$  thermocouples and  $m$  discrete times. The summation is over all the thermocouple measurements except the first that serves as a boundary condition (see Figure 6.4.2). The limits of  $m$  depend on the time interval for which  $\alpha$  is to be found and on the time step chosen.

Minimizing the sum-of-square function  $F(\alpha)$  with respect to thermal diffusivity ( $\alpha$ ) implies differentiation and setting the resultant equal to zero; or

$$\frac{\partial F(\alpha)}{\partial \alpha} = \sum_{i=1}^n \sum_{j=1}^m W_i^j \left( T_{(cal)}^j - T_{(exp)}^j \right) \frac{\partial T_{(cal)}^j}{\partial \alpha} = 0 \quad (4.2.2)$$

At each iteration step, the calculated temperature is approximated by the Taylor series as follows:

$$T_{cal}(\alpha)_{\ell+1} = T_{cal}(\alpha)_{\ell} + \left. \frac{\partial T(\alpha)}{\partial \alpha} \right|_{(\alpha)_{\ell}} (\Delta \alpha)_{\ell} + \dots \quad (4.2.3)$$

where

$$(\Delta\alpha)_\ell = (\alpha)_{\ell+1} - (\alpha)_\ell$$

The derivative is approximated by:

$$\left. \frac{\partial T}{\partial \alpha} \right|_\ell \approx \frac{T(\alpha)_{\ell+1} - T(\alpha)_\ell}{(\Delta\alpha)_\rho} \quad (4.2.4)$$

$\frac{\partial T}{\partial \alpha}$  is called the "sensitivity coefficient."

The T's on the right-hand side of Equation 4.2.4 are calculated using a finite-difference method (see Chapter VI). The initial value of diffusivity  $\alpha_0$  is estimated, and the iterative procedure begins with an estimated value for  $\alpha_0$ . The value of thermal diffusivity  $(\alpha)$  at the  $\ell$ th iteration would be equal to:

$$(\alpha)_\ell = (\alpha)_{\ell-1} + (\Delta\alpha)_{\ell-1} \quad (4.2.5)$$

Substituting (4.2.3) into (4.2.2) gives:

$$(\Delta\alpha)_\ell = (\alpha)_\ell - (\alpha)_{\ell-1} = \frac{\sum_{i=1}^n \sum_{j=1}^m \left. \frac{\partial T}{\partial \alpha} \right|_{(\alpha)_\ell} [T_{\text{exp}} - T_{\text{cal}}(\alpha)_\ell]}{\sum_{i=1}^n \sum_{j=1}^m \left( \left. \frac{\partial T}{\partial \alpha} \right|_{(\alpha)_\ell} \right)^2} \quad (4.2.6)$$

and Equation (4.2.5) becomes:

$$\alpha_{\text{new}} = \alpha_{\text{old}} + \frac{\sum_{i=1}^n \sum_{j=1}^m [T_{\text{exp}} - T_{\text{cal}}(\alpha)_\ell] \left. \frac{\partial T}{\partial \alpha} \right|_{(\alpha)_\ell}}{\sum_{i=1}^n \sum_{j=1}^m \left( \left. \frac{\partial T}{\partial \alpha} \right|_{(\alpha)_\ell} \right)^2} \quad (4.2.7)$$

The iteration procedure continues until all the  $(\alpha)_\ell - (\alpha)_{\ell-1}$  satisfy some predetermined criterion such as:

$$\frac{(\alpha)_\ell - (\alpha)_{\ell-1}}{(\alpha)_{\ell-1}} \leq 0.001 \quad (4.2.8)$$

With this process, the original thermal diffusivity would be replaced by that determined by Equation 4.2.5.

In the analysis of the data, it was found that the thermal diffusivity,  $\alpha$ , converged to the correct value without significant oscillation. The number of iterations depended on the estimated value of thermal diffusivity. For a well-designed experiment and with the initial estimation of  $\alpha$  about 10 per cent in error, only a few iterations are usually necessary to satisfy Equation 4.2.8.

#### 4.3 Computer Program

The nonlinear estimation method is well adapted for use with the digital computer. A basic computer program for estimation of thermal properties has been developed by J. V. Beck (7). This program, referred to as "Property Program," is on magnetic tape in the Computer Center at Michigan State University and may be called into use as needed. This program has been utilized to calculate thermal properties of asphalt concrete, as well as to predict the temperature at various depths of pavement and underlying soils. A finite difference method is employed



for the solution temperature as the boundary condition to the model and calculated the temperature at desired locations in the pavement. The properties are found by making the calculated temperature match the measured temperature in a least-square sense. (See the descriptions following Equation 4.2.1.)

#### 4.3.1 Data Input

In order to determine the thermal properties by "Property Program," some of the variables or environmental conditions that effect the transfer of thermal energy in asphalt pavement may be used directly as data input. Measured temperature and heat flux are two basic inputs which serve as the boundary conditions for the model. In the following paragraphs, these boundary conditions are briefly described.

#### 4.3.2 Temperature Boundary Conditions

In order to determine thermal diffusivity only the measured temperatures are necessary. This is evident from Figure 6.4.1 and the describing equations. The property program uses this temperature as a boundary condition to the model and calculates the properties. Variation of temperature, taken at the surface and at various depths of both a 7-inch and a 19-inch asphalt pavement have been used as the temperature boundary condition to calculate thermal diffusivity of asphalt concrete. In order to get

some estimate of the thermal properties at different seasonal temperatures, measured temperatures during winter, spring, fall, and summer have been utilized. These data provide an extensive range of temperature which is necessary in determining temperature-dependent thermal properties of the asphalt concrete.

Similar temperature data obtained in the laboratory from the sample of asphalt concrete has also been used as the temperature boundary condition to determine the thermal properties under the controlled condition in comparison to the field condition.

#### 4.3.3 Heat Flux Boundary Condition

To determine the values of thermal conductivity ( $K$ ), and specific heat ( $C_p$ ), heat flux and temperature must be known. Here the program uses the heat flux and an insulation condition as the boundary conditions to the model and calculates the properties (see Figure 6.4.1).

Since there was no information relative to the heat flux in the field data, it was necessary to perform laboratory experiments and employ the results to calculate thermal conductivity and specific heat of asphalt concrete. (The details of this experimentation was discussed in Chapter III.)

#### 4.3.4 Other Variable Input

Other variable input included length of regions, the number of nodes in each region, the number of regions, and the time for given data.

The pavement is broken into a number of regions (see Figure 6.4.2) and in turn, each region is divided into equal thicknesses which are equal to  $\Delta n = \frac{L}{n}$ . Where  $L$  is the length of the region and specified by the distance between two consecutive thermocouples and  $n$  is the number of subdivisions in the region. Each one of these subdivisions represents a finite control volume which may be denoted as a nodal point at the center of the volume. It is conceptually advantageous to imagine that the nodes are located at the center of the volume. The interface of each two regions is at the location of a thermocouple.

The first and the last nodes are used as the boundary condition, while the internal nodes are located between the thermocouples to improve the finite difference approximation.

#### 4.4 Output and Results

The program outputs the time step, the calculated temperature "CAL TEMP," measured temperature "ETEMP," and their differences denoted as residual "DTETC." As a standard procedure in regression analysis, the temperature differences (residuals) for various positions are plotted versus time in Figure 3.6.1. Printed output also

includes the sum of square of residuals "RMS," and sensitivity coefficients symbolized by "BDB." The various output quantities for a representative case are plotted in Figures 4.4.1 through 4.4.3.

The values of root-mean-square, which is a direct measure of agreement between the model and the experiment, are given in Tables 4.4.1 and 4.4.2. For perfect agreement between the calculated and the measured temperature, the value of "RMS," (i.e., root-mean-square), approaches zero. However, "RMS" will never reach zero since there is never perfect agreement between calculated and measured temperatures. The sources of the errors may be ascribed to experimental measurement error, imperfect model and finite difference calculation using the numerical model.

The sum-of-square function  $F(\alpha)$  is related directly to the root-mean-square. The program seeks out a minimum in the sum-of-square of the residual by using an iterative search procedure. Since the procedure is iterative, the initial estimate of the thermal diffusivity is very important. In many cases, solution of the problem occurs even for poor initial estimates of the parameters. In difficult cases, however, the convergence is strongly dependent on the use of good estimates of the thermal properties.

In performing the regression analysis, it is assumed that the error is independent, has a zero mean, a constant variance, and follows the normal distribution.

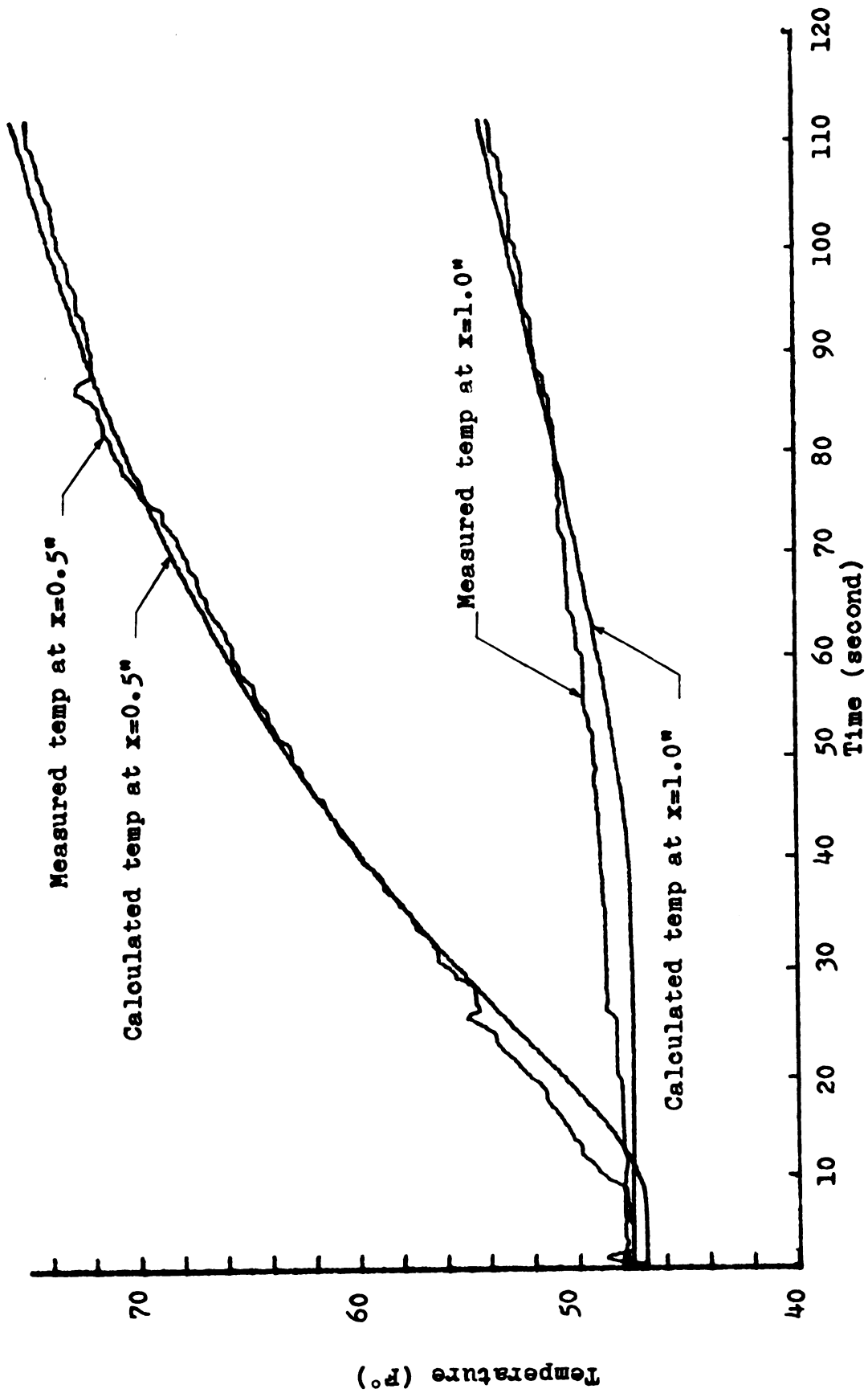


Figure 4.4.1 A comparison between calculated and measured temperature at 1/2-inch and 1-inch below the surface of the specimen (representative case)

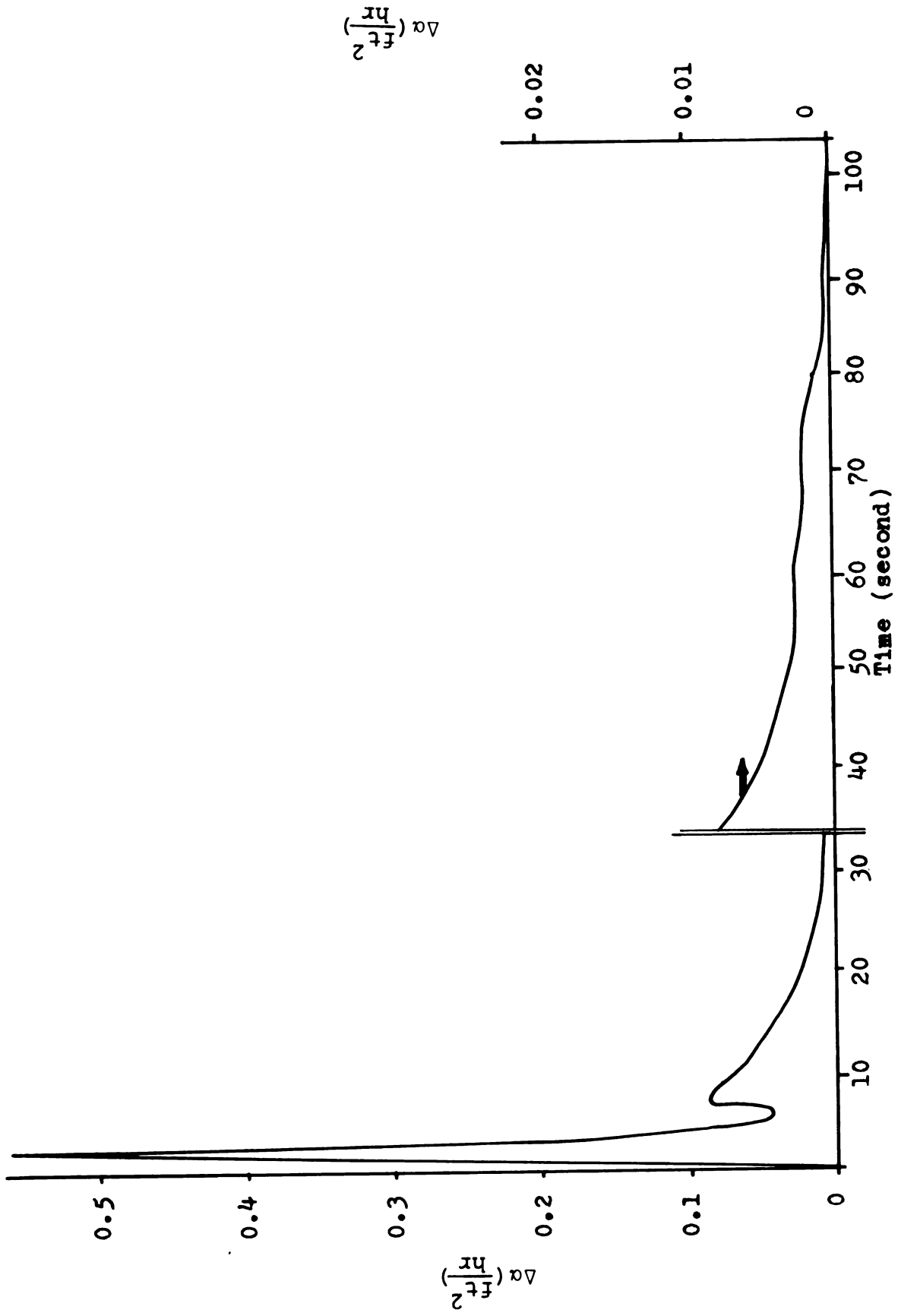


Figure 4.4.2 Variation of thermal diffusivity during one iteration process (representative case)

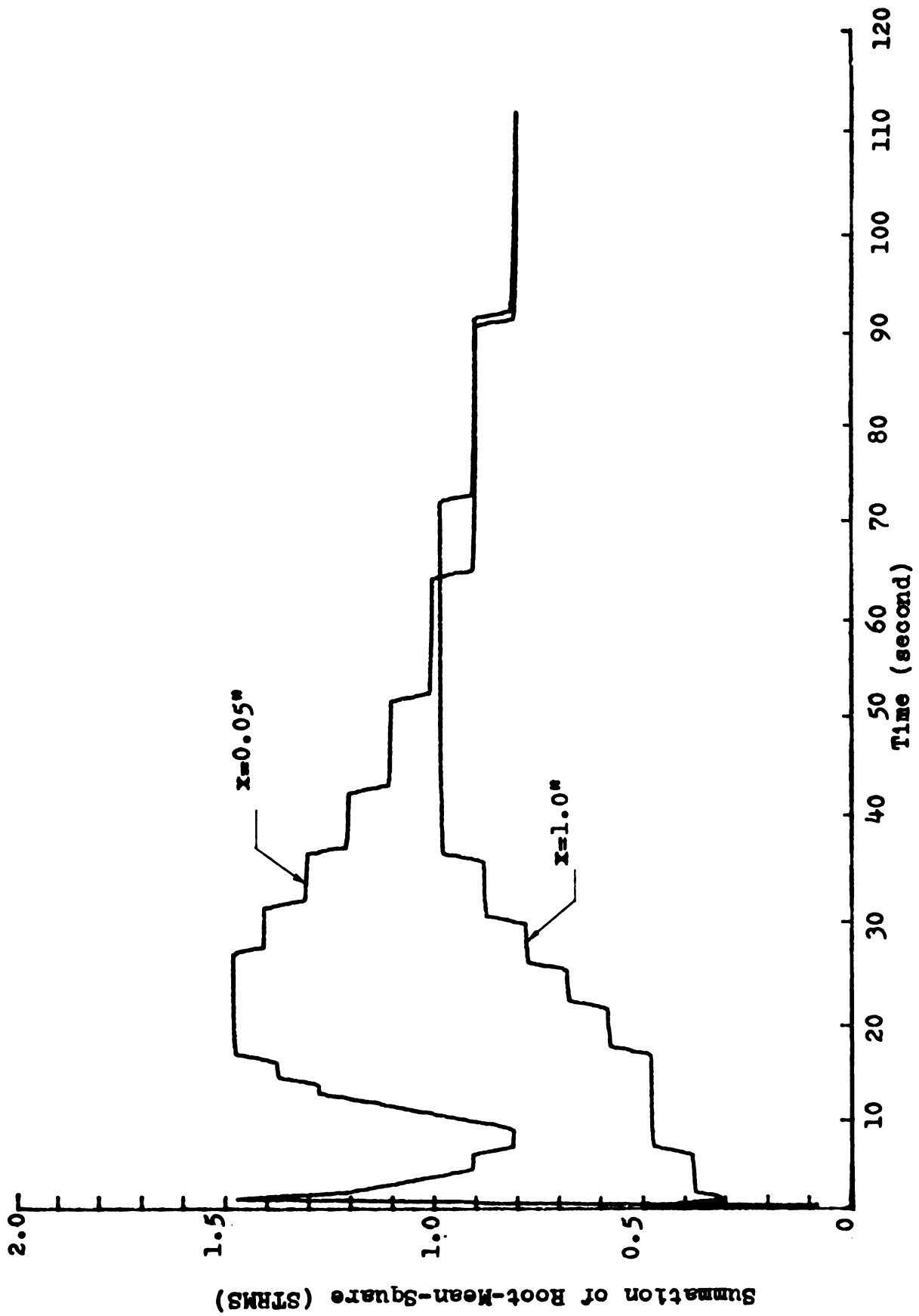


Figure 4.4.3 Summation of root-mean-square for the representative case

The residuals should exhibit tendencies to confirm these assumptions, or at least, should not exhibit a denial of them. To a limited extent, the residuals appear to be random. The nonlinear estimation method yields smaller errors in the calculated property when the errors are random. For the case of systematic errors, corrections for biased errors may be made.

Figure 4.4.2 illustrates the change in thermal diffusivity ( $\alpha$ ) as the function of time steps during one iteration process for the given case. These values are given in the list of the output. The change in  $\alpha$  at the  $\ell$ th iteration  $[(\Delta\alpha)_{\ell} = (\alpha)_{\ell} - (\alpha)_{\ell-1}]$  is an iteration variable for which an optimum value is sought. The value of  $\Delta\alpha$  continuously varies with time during each iteration process. The current estimates of the thermal properties including the number of iterations, are printed at the end of each iteration. When convergence occurs, or if the maximum number of iterations has been exceeded, the final values of the calculated thermal properties are printed.

The analysis of field data, as well as laboratory experiments, has been accomplished with as few as two iterations for convergence. On the average, the number of iterations was equal to three.

Calculated thermal diffusivity of asphaltic concrete for various seasons and under different ambient



conditions are given in Tables 4.4.1 and 4.4.2. The calculated thermal diffusivity of asphaltic concrete from experimental temperature data are given in Table 3.6.1. The values of thermal conductivity and volumetric specific heat of bituminous concrete calculated from experimental data are given in Table 3.6.2.

Table 4.4.1 Calculated thermal diffusivity of asphaltic concrete  
(entire pavement) from recorded temperature data  
(nonlinear estimation method)

Case	Date	Ambient Condition	Surface Temp (°F)		t <sub>max</sub> (hr)	Root Mean Square (RMS)	Thermal Diffusivity ft <sup>2</sup> /hr
			Max	Min			
1	7.69	Sunny	127	65	120	2.62	0.038
2	8.69	"	115	64	21	2.39	0.047
3	6.69	"	120	60	16	1.42	0.037
4	4.69	"	112	41	16	1.94	0.051
5	3.69	"	56	37	70	0.97	0.057
6	1.70	"	34	5	16	1.18	0.058
7	1.70	"	28	-2	118	1.92	0.054
8	8.69	Cloudy	135	70	16	1.39	0.048
9	4.69	"	116	68	35	2.08	0.051
10	1.70	"	28	-3	16	1.09	0.051
11	1.70	"	36	10	118	273	0.055
12	7.69	Rainy	118	73	16	2.10	0.049
13	3.69	"	33	20	16	2.29	0.058
14	7.65	Sunny	131	68	70	0.97	0.041
15	7.65	(Alger Road)	123	69	68	1.69	0.046
16	1.65	"	29	6	96	2.34	0.053
17	1.64	"	40	-5	62	1.88	0.057

Table 4.4.2 Calculated thermal diffusivity of wearing and binder courses from recorded temperature data (nonlinear estimation method)

Case	Date	Ambient Condition	Surface Temp (F°)		t <sub>max</sub> (hr)	Root-Mean-Square	Thermal Diffusivity (ft <sup>2</sup> /hr)
			Max	Min			
1	7.69	sunny	127	65	120	2.43	0.049
2	8.69	"	115	64	21	3.00	0.046
3	6.69	"	120	60	16	1.13	0.040
4	4.69	"	112	41	16	0.63	0.058
5	3.69	"	56	37	70	0.95	0.053
6	1.70	"	34	5	16	1.30	0.050
7	1.70	"	28	-2	118	2.33	0.057
8	8.69	cloudy	135	70	16	1.08	0.051
9	4.69	"	116	68	35	0.93	0.054
10	1.70	"	28	-3	16	0.96	0.059
11	1.70	"	36	10	118	3.10	0.065
12	7.69	rainy	118	73	16	1.02	0.064
13	3.69	"	33	20	16	0.89	0.060
14	7.65	sunny (Alger)	131	68	70	0.68	0.052
15	7.65	"	123	69	68	1.49	0.053
16	1.65	"	29	6	96	1.25	0.052
17	1.64	"	40	-5	62	1.76	0.061

## CHAPTER V

### SIMPLIFIED METHOD

#### 5.1 Simplified Analysis for Estimation of Thermal Diffusivity Using the Laplace Transform

The traditional approach to property measurement is to create an experimental condition for which system behavior is approximated in the laboratory. The obtained thermal properties under the controlled conditions of the laboratory may not be capable of predicting accurate thermal behavior and temperature distribution in the pavement under the natural conditions.

Estimated thermal properties from the periodic heat analysis was based on the assumption that the surface temperature varies according to a sine wave. Since the daily heating-cycle is normally other than the simple sine function, higher harmonics and the Fourier analysis have been introduced for the daily temperature variation (14). The mathematical treatment for approximating such a natural boundary condition is usually time consuming and impractical.

The results of the analysis undertaken by O'Brien (40) and Heley (24) dealing with the periodic heat method concluded that either the periodic assumption of the surface temperature did not satisfy the natural conditions or that the method itself was in error.

The estimation of thermal properties by the nonlinear estimation method is an iterative search procedure which requires a considerable amount of computer time.

In comparison with the nonlinear estimation method, the simplified method described herein saves on computer time, since it is not an iterative procedure. For these reasons, a method of estimating thermal properties from natural recorded surface temperature is needed.

The method described in this chapter, eliminates the assumption of sinusoidal surface temperature. This method may be utilized to estimate thermal diffusivity of pavement materials subjected to any surface heat pulse.

## 5.2 Simplified Laplace Transform Method

Consider a semi-finite body to be initially at a constant uniform temperature and at the surface ( $x = 0$ ) the temperature varies with time in an arbitrary but known manner:

$$T(0,t) = T_0(t) \quad (5.2.1)$$

The partial differential equation describing one-dimensional heat conduction in such a system, assuming

constant properties and no internal heat generation may be written:

$$\frac{\partial T(x,t)}{\partial t} = \alpha \frac{\partial^2 T(x,t)}{\partial x^2} \quad (5.2.2)$$

where  $T$  is temperature,  $t$  is time, and  $\alpha$  is the thermal diffusivity of the conducting medium which is equal to  $K/\rho C_\rho$ .  $K$  is the thermal conductivity,  $\rho$  is density, and  $C_\rho$  is specific heat. The initial temperature is known and is

$$T(x,0) = T_{\text{initial}} \quad (5.2.3)$$

and the temperature  $x = \infty$  may be considered to be  $T(\infty, t)$  but with the assumption of uniform initial temperature, we may write:

$$T(\infty, t) = T_{\text{initial}} \quad (5.2.4)$$

Let  $T'(x, t)$  be defined as:

$$T'(x, t) = T(x, t) - T_{\text{initial}} \quad (5.2.5)$$

then the mathematical problem may be written as:

$$\frac{\partial T'(x, t)}{\partial t} = \alpha \frac{\partial^2 T'(x, t)}{\partial x^2} \quad (5.2.6)$$

$$T'(0, t) = [T(0, t) - T_{\text{initial}}] = T'_0 \quad (5.2.7a)$$

$$T'(x,0) = [T(x,0) - T_{\text{initial}}] = 0 \quad (5.2.7b)$$

$$T'(\infty,t) = [T(\infty,t) - T_{\text{initial}}] = 0 \quad (5.2.7c)$$

Taking the Laplace transform of Equation 5.2.6, gives:

$$\mathcal{L}\left[\alpha \frac{\partial^2 T'(x,t)}{\partial x^2}\right] = \mathcal{L}\left[\frac{\partial T'(x,t)}{\partial t}\right] \quad (5.2.8)$$

or

$$\alpha \frac{\partial^2 \mathcal{L}T'(x,t)}{\partial x^2} = s\mathcal{L}T'(x,t) \quad (5.2.9)$$

Similarly, by taking the Laplace transform of Equation 5.2.7, we get:

$$\mathcal{L}(T'(0,t)) = \mathcal{L}(T'_0) \quad (5.2.10)$$

$$\mathcal{L}(T'(\infty,t)) = 0 \quad (5.2.11)$$

Solving Equation 5.2.9 gives:

$$\mathcal{L}(T'(x)) = C_1 e^{\sqrt{\frac{s}{\alpha}} x} + C_2 e^{-\sqrt{\frac{s}{\alpha}} x} \quad (5.2.12)$$

To find  $C_1$  and  $C_2$  in Equation 5.2.12, we know that as  $x$  approaches infinity,  $\mathcal{L}(T'(x))$  approaches zero rather than infinity, therefore,  $C_2 = 0$ . From Equation 5.2.10,  $C_1$  is evaluated and equation 5.2.12 becomes:

$$\mathcal{L}(T'(x)) = \mathcal{L}(T'_0) e^{\sqrt{\frac{s}{\alpha}} x} \quad (5.2.13)$$

Solving 5.2.13 for  $\alpha$  gives:

$$\ln \left[ \frac{\mathcal{L}(T'(x))}{\mathcal{L}(T'_0)} \right] = -\sqrt{\frac{s}{\alpha}} x \quad (5.2.14)$$

and

$$\alpha = \frac{sx^2}{\ln^2 \left[ \frac{\mathcal{L}(T'(x))}{\mathcal{L}(T'_0)} \right]} \quad (5.2.15)$$

where  $s$  is the Laplace transform parameter,

$$\mathcal{L}(T(t)) = \int_0^{\infty} e^{-st} T(t) dt \quad (5.2.16)$$

$s$  has the units of reciprocal time, and it may have any real value between zero and infinity and may also be complex. We shall choose a number of real values of  $s$  and obtain a value of  $\alpha$  for each one. An averaging scheme is needed to determine the best value of  $\alpha$  in some sense.

Let us use weight least squares:

$$s(\alpha) = \sum_{j=1}^n \sum_{s=s_i}^s W_{ij} \left[ \alpha - s_i x_j^2 / \ln^2 \frac{\mathcal{L}_i(T'_j)}{\mathcal{L}_i(T'_0)} \right]^2 \quad (5.2.17)$$

where  $\alpha$  is the actual value of thermal diffusivity and the second term in the brackets is the estimated value of thermal diffusivity defined by Equation 5.2.15. The subscripts of  $i$  and  $j$  relate to the  $s$  parameter and depth  $x$  respectively.



The best value of  $\alpha$  in the least-squares sense is the one for which the sum of square function  $s(\alpha)$  for  $n$  values of  $s$  and  $m$  discrete depths is minimized with respect to  $\alpha$ . In other words, by varying the values of  $\alpha$  the estimated value of  $\alpha$  is made to agree in a least-squares sense with the actual thermal diffusivity. Mathematically minimizing  $s(\alpha)$  with respect to  $\alpha$  implies differentiation and setting the resultant equal to zero; we then obtain:

$$\alpha \frac{\sum_{j=1}^n \sum_{s=s_i}^m W_{ij}}{\sum_{j=1}^n \sum_{s=s_i}^m s_i x_j^2 W_{ij}} = \frac{\sum_{j=1}^n \sum_{s=s_i}^m s_i x_j^2 W_{ij}}{\sum_{j=1}^n \sum_{s=s_i}^m s_i x_j^2 W_{ij}} \ln^2 \frac{\mathcal{L}(T'_j)}{\mathcal{L}(T'_o)} \quad (5.2.18)$$

or the estimated value of  $\alpha$ , designated  $\hat{\alpha}$ , is:

$$\hat{\alpha} = \frac{\sum_{j=1}^n \sum_{s=s_i}^m s_i x_j^2 W_{ij} \ln^2 \frac{\mathcal{L}(T'_j)}{\mathcal{L}(T'_o)}}{\sum_{j=1}^n \sum_{s=s_i}^m W_{ij}} \quad (5.2.19)$$

As noted in the nonlinear estimation method, the process of making actual and estimated thermal diffusivity agree in the least-square sense, requires a number of iterations. There are no iterations involved in the above procedure because Equation 5.2.15 is linear in  $\alpha$ .

The criteria for optimum experiments, as well as the limitations in the Laplace transform, leads to some

conclusions regarding the best value of  $s$ , which will be discussed in the next section.

Assuming equal experimental conditions, equal uncertainties in measuring the temperature and uncorrelated errors, the weighting factor,  $W_{ij}$ , may be given the value of one. These assumptions are not always there, but are used herein to simplify the choice of  $W_{ij}$ .

### 5.3 Laplace Transform Criteria

The Laplace transform of function  $T'(x,t)$  is given by:

$$\mathcal{L}(T'(x,t)) = \int_0^{\infty} e^{-st} [T'(x,t)] dt \quad (5.3.1)$$

where  $T'(x,t)$  is given by:

$$T'(x,t) = T(x,t) - T_{\text{initial}}$$

Geometrically, the value of this integral represents the area bounded by the curve  $e^{-st} [T'(x,t)]$ , the  $t$  axis and ordinates at  $t = 0$  and  $t = \infty$  (see Figure 5.3.1C). The values of  $T'(x,t)$  are selected from the hourly temperature distribution curves such as shown in Figure 2.7.1. The function  $e^{-st}$  is plotted versus  $(st)$  in Figure 5.3.1A. Curves of  $e^{-st}$  versus  $t$  for various real, positive values of  $s$  are represented in Figure 5.3.1B.

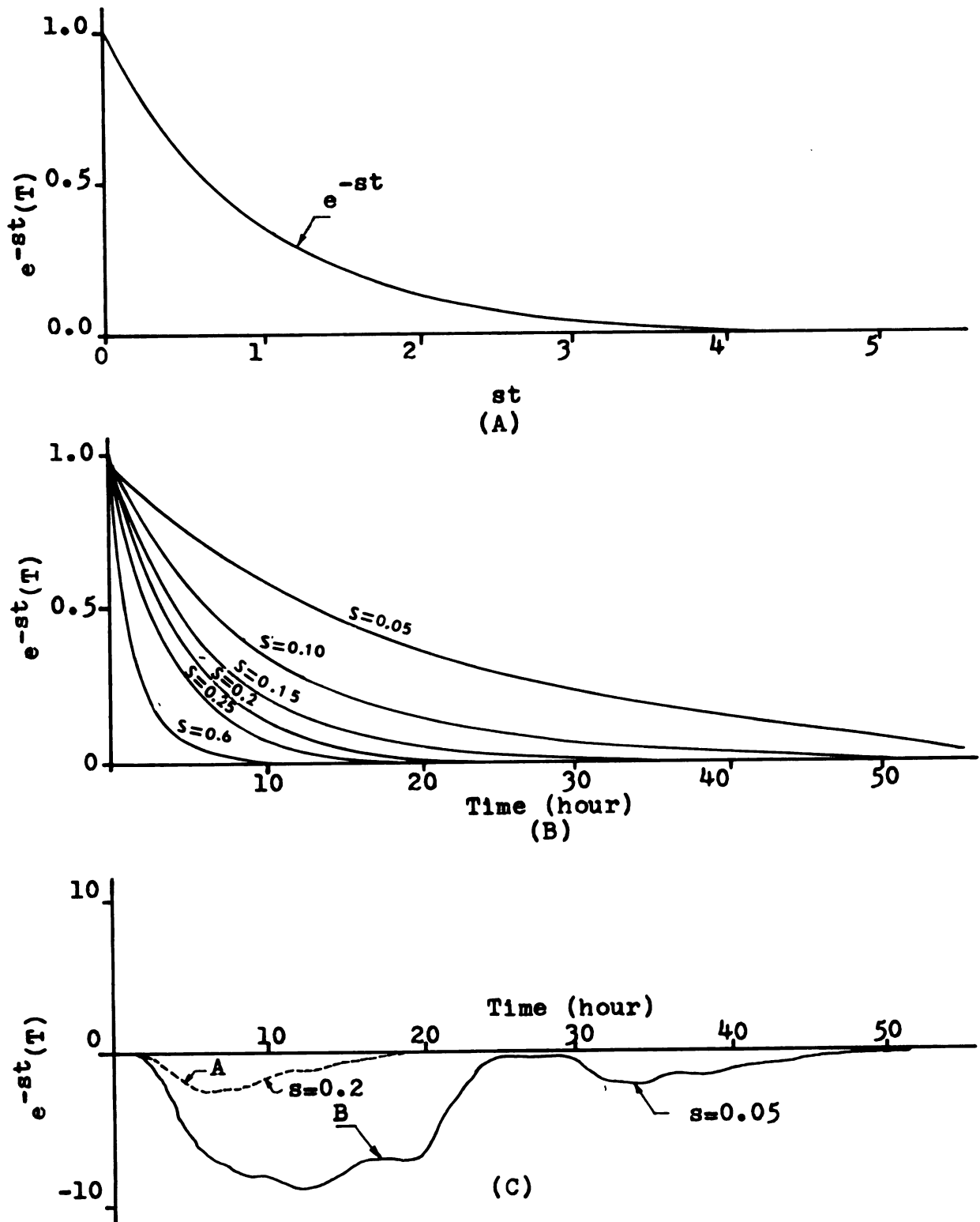


Figure 5.3.1 Laplace transform criteria

The calculated values of  $e^{-st}[T'(x,t)]$  for two values of  $s$  equal to 0.20 and 0.05 are shown by curves A and B in Figure 5.3.1C.

It may be observed that the magnitude of  $e^{-st}$  as well as  $e^{-st}[T'(x,t)]$  decreases with increasing the value of  $st$ , and for  $st \geq 4.6$ , the effect of  $T'(x,t)$  in Equation 5.2.19 is insignificant.

The above criterion may be used in estimating the parameter  $s$ . Therefore, real "s" values should be chosen such that:

$$s_i \geq \frac{4.6}{t_{\max}} \quad (5.3.2)$$

Complex values of "s" have not been investigated.

Let  $t_{\max} = N\Delta t$ , where  $N$  is equal to the number of time steps and  $\Delta t$  is the equally spaced time interval between the measurements. As  $t_{\max}$  becomes larger, a smaller value of  $s_i$  should be chosen. For a period of twenty-four hours,  $t_{\max} = 24$  hours and  $s_i = 1/6$  per hour. Possible  $s_i$  values might then be,  $s_i = 1/6, 1/3, 1/2, 3, \dots$ . However, the more temperature data effectively utilized in Equation 5.2.19, that is for the smaller  $s_i$  values, the more accurately thermal diffusivity would be obtained.

Equation 5.3.1 represents the area bounded by any curves such as A and B and  $t$  axis, Figure 5.3.1C, which are employed in estimating the thermal diffusivity from Equation 5.2.19. The calculated value of  $\alpha$  corresponding

to curve B usually would be more accurate than that of curve A because more temperature data is used for curve A.

As more equal time intervals are used in the program, the smaller the value of  $s$  might be. In order to obtain an accurate value for  $\alpha$ , the number of time steps should exceed some minimum number. Since  $t_{\max} = N\Delta t$ , then the combined values of  $N$  and  $\Delta t$  define a time interval for which  $\alpha$  is to be found. The optimum period of the experiment as well as the number of time steps will be discussed in the next section.

It is assumed that the value of  $e^{-st}$  after one time step drops no smaller than about 0.95. Hence, for  $e^{-s(\Delta t)} = 0.95$  this leads to another limit for the parameter  $s$ , such as:

$$s(\Delta t) \leq 0.051 \quad (5.3.3)$$

hence:

$$s \leq \frac{0.051}{\Delta t} = \frac{0.051N}{N\Delta t} = \frac{0.051N}{t_{\max}} \quad (5.3.4)$$

If " $s$ " is made equal to  $4.6/t_{\max}$  and  $N \approx 100$  (and thus  $t = t_{\max}/100$ ) both conditions on " $s$ " (Equations 5.3.2 and 5.3.4) are simultaneously made the equalities rather than inequalities. (These conditions have proven to be good ones.)

#### 5.4 The Optimum Experiment

To determine the optimum experiment, a criterion must be developed to obtain the optimum value of  $x$ , i.e., the location of a thermocouple, and the optimum value of the Laplace transform parameter  $s$ . The optimum location of  $x$  and the parameter  $s$  are found when the Laplace transform of an interior temperature contains the maximum information regarding  $\alpha$ . This occurs when the quantity  $\bar{\theta}(x, \alpha, s)$  defined by:

$$\bar{\theta}(x, \alpha, s) = \int_0^{\infty} e^{-st} [T(x, t, \alpha) - T_{\text{initial}}] dt \quad (5.4.1)$$

is most sensitive to changes in  $\alpha$ . Now from Equation 5.2.13

$$\bar{\theta}(x, \alpha, s) = \bar{\theta}(0, s) e^{-\sqrt{\frac{s}{\alpha}} x} \quad (5.4.2)$$

where

$$\bar{\theta}(x, \alpha, s) = \mathcal{L}\{T'(x, \alpha, t)\} \quad (5.4.3)$$

$$\bar{\theta}(0, s) = \mathcal{L}\{T'(0, t)\} \quad (5.4.4)$$

Note that the temperature at  $x = 0$  is a prescribed function and may have arbitrary time-dependence which is completely independent of the property  $\alpha$ . Given an interior location  $x$  and some arbitrary surface temperature history, the temperature at  $x$  is a function of  $\alpha$ . Both  $\bar{\theta}|_x$  and  $\bar{\theta}|_{x=0}$  are dependents upon  $s$ .

We can find how sensitive  $\bar{\theta}(x, \alpha, s)$  is with respect to  $\alpha$  by differentiating Equation 5.4.1 with respect to  $\alpha$  or

$$\alpha \frac{\partial \bar{\theta}(x, \alpha, s)}{\partial \alpha} = \bar{\theta}(0, s) \left( 1/2 \sqrt{\frac{s}{\alpha}} x e^{\sqrt{\frac{s}{\alpha}} x} \right) \quad (5.4.5)$$

where  $\partial \bar{\theta} / \partial \alpha$  is called the "sensitivity coefficient." The larger Equation 5.4.5 is in magnitude for a given surface temperature history with respect to  $x$  and  $s$ , the more accurately  $\alpha$  may be estimated.

### 5.5 Optimum Location (x)

The optimum thickness and location of thermocouples may be investigated by differentiating Equation 5.4.5 with respect to  $x$  and setting the resultant equal to zero.

$$\alpha \frac{\partial^2 \bar{\theta}}{\partial x \partial \alpha} = \bar{\theta}(0) \left[ \frac{1}{2} \sqrt{\frac{s}{\alpha}} e^{-\sqrt{\frac{s}{\alpha}} x} + \frac{1}{2} \sqrt{\frac{s}{\alpha}} x \left( -\sqrt{\frac{s}{\alpha}} \right) e^{-\sqrt{\frac{s}{\alpha}} x} \right] = 0 \quad (5.5.1)$$

or

$$\sqrt{\frac{s}{\alpha}} x_{\text{opt}} = 1 \quad (5.5.2a)$$

or

$$\boxed{x_{\text{opt}} = \sqrt{\frac{\alpha}{s}}} \quad (5.5.2b)$$

### 5.6 Optimum "s"

To determine the optimum value of  $s$ , we differentiate Equation 5.4.5 with respect to  $s$  while using the identity given by Equation 5.5.2a, or

$$\alpha \left. \frac{\partial^2 \bar{\theta}(x, \alpha, s)}{\partial s \partial \alpha} \right|_{x_{\text{opt}}} = \frac{1}{2} e^{-1} \frac{\partial \bar{\theta}(0, s)}{\partial s} \quad (5.6.1)$$

Equation 5.6.1 requires the knowledge of surface temperature  $\theta(0, t)$ . Two types of time variable surface temperatures will be discussed.

Consider first a step change in surface temperature or

$$\theta(0, t) = \theta_0 \quad (5.6.2)$$

then

$$\bar{\theta}(0, s) = \int_0^{\infty} e^{-st} \theta_0 dt = \theta_0 \left( -\frac{1}{s} \right) \Big|_0^{\infty} = \frac{\theta_0}{s} \quad (5.6.3)$$

For this case Equation 5.6.1 gives

$$\alpha \frac{\partial^2 \bar{\theta}(x_{\text{opt}}, \alpha, s)}{\partial s \partial \alpha} = \frac{1}{2} e^{-1} \frac{\theta_0}{-s^2} \quad (5.6.4)$$

Equation 5.6.4 approaches zero as  $s \rightarrow \infty$ . However,  $s = \infty$  corresponds to an infinitesimal duration of the experiment.



Substitution of Equation 5.6.3 into Equation 5.4.5 indicates that the values of  $\alpha \frac{\partial \bar{\theta}}{\partial \alpha}$  are positive, since the values of  $s$  should reside in  $[0, +\infty)$ . The values of the sensitivity coefficient given by Equation 5.4.5 approach zero as  $s \rightarrow \infty$ . Thus as  $s \rightarrow \infty$ , the sensitivity coefficient is not a maximum.

Equation 5.4.5 indicates that the maximum value of the sensitivity coefficient is obtained as  $s \rightarrow 0$ , for  $\bar{\theta}(0, s) = \frac{\theta_0}{s}$ . This corresponds to an infinite duration of the experiment. We now observe that given the restriction (5.3.2), the optimum value of  $s$  is then:

$$s_{\text{opt}} = \frac{4.6}{t_{\text{max}}} \quad (5.6.6)$$

We also observe from Equation 5.5.2b that the optimum location is

$$x_{\text{opt}} = \frac{1}{2} \sqrt{\alpha t_{\text{max}}} \quad (5.6.7)$$

which corresponds to

$$\alpha t_{\text{max}} / x_{\text{opt}}^2 = 4 \quad (5.6.8)$$

Consider next a periodic surface temperature as given by:

$$\theta(0, t) = \theta_0 \sin(\omega t) \quad (5.6.9)$$

for which

$$\bar{\theta}(0, s) = \int_0^{\infty} \theta(0, t) e^{-st} dt = \frac{\omega \theta_0}{s^2 + \omega^2} \quad (5.6.10)$$

Note that

$$\frac{\partial}{\partial s} \left( \frac{\omega \theta_o}{s^2 + \omega^2} \right) = - \frac{\omega \theta_o (2s)}{(s^2 + \omega^2)^2} \quad (5.6.11)$$

and then Equation 5.6.1 becomes:

$$\alpha \frac{\partial^2 \bar{\theta}(x_{opt}, \alpha, s)}{\partial s \partial \alpha} = - e^{-1} \theta_o \frac{\frac{1}{2} \left( \frac{s}{\omega} \right)}{\left( \left( \frac{s}{\omega} \right)^2 + 1 \right)^2} \quad (5.6.12)$$

which is equal to zero only when  $s/\omega = 0$ .

It is instructive to note the loss one must take for more realistic values of  $s$ .

Consider the "sensitivity coefficient " for the periodic surface temperature as given by:

$$\alpha \frac{\partial \bar{\theta}(x_{opt}, \alpha, s)}{\partial \alpha} = \theta_o e^{-1} \frac{1}{2} \frac{1}{\omega} \frac{1}{\left( \frac{s}{\omega} \right)^2 + 1} \quad (5.6.13)$$

Figure 5.6.1 shows values of  $\left[ \left( \frac{s}{\omega} \right)^2 + 1 \right]^{-1}$ . Depending upon the "loss" in effectiveness acceptable, a choice of several reasonable values of  $s/\omega$  may be made. A possible value is 0.2, hence,

$$\frac{s}{\omega} = 0.2 \quad \text{or} \quad s_{t_{max}} = 0.2 \omega t_{max} \quad (5.6.14)$$

Combining this result with Equation 5.5.2b, gives

$$x_{opt} = \sqrt{\frac{\alpha}{0.2\omega}} \quad (5.6.15a)$$

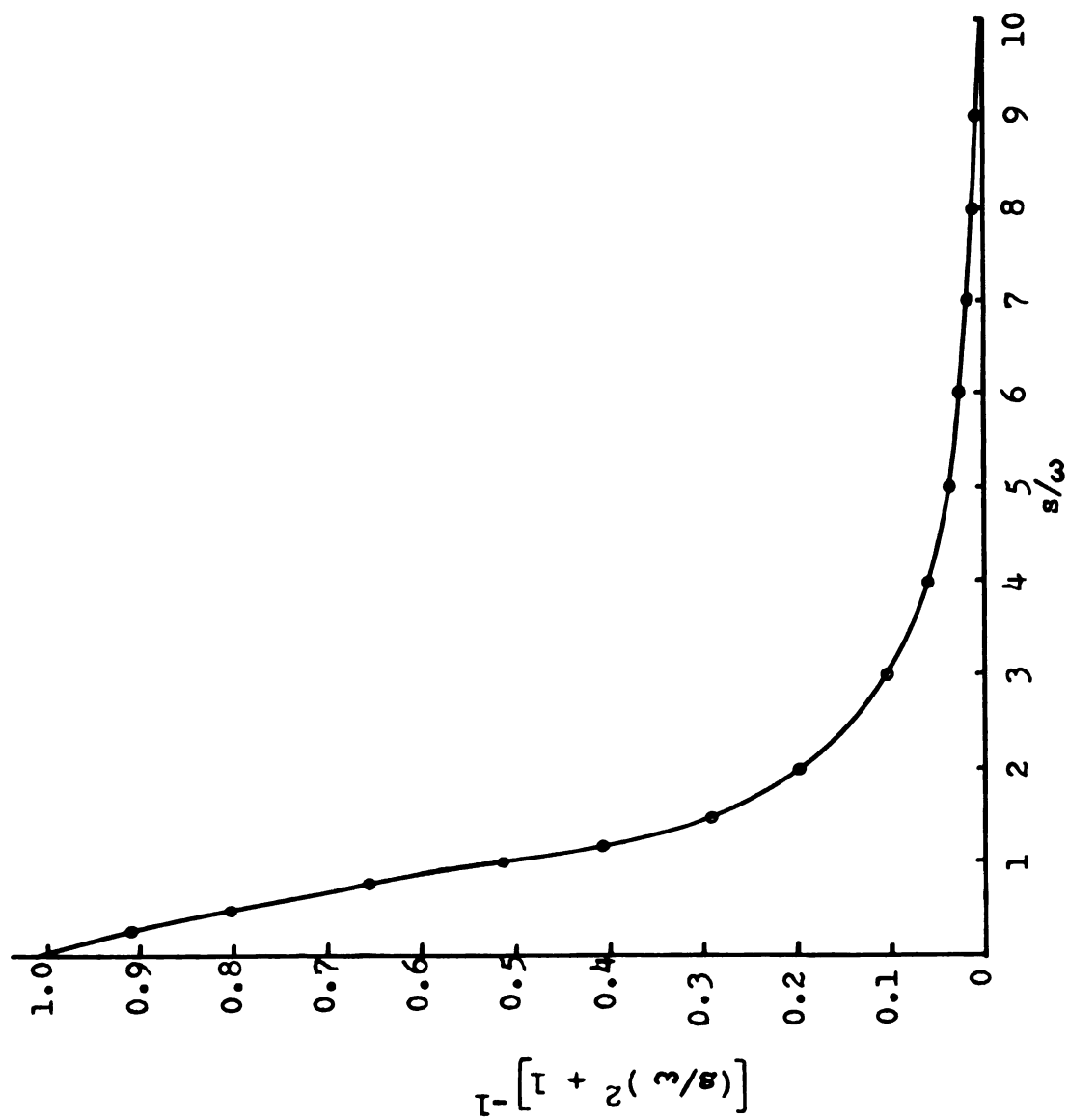


Figure 5.6.1 Calculated values of  $\left[\left(\frac{s}{\omega}\right)^2 + 1\right]^{-1}$

or

$$\frac{\alpha}{\omega x_{\text{opt}}^2} = 0.2 \quad (5.6.15b)$$

then

$$\frac{\alpha t_{\text{max}}}{x_{\text{opt}}^2} = 0.2 \quad \omega t_{\text{max}} = s t_{\text{max}} \quad (5.6.15c)$$

Note that with this choice of  $s$ , the sensitivity coefficient is reduced only 4 per cent compared to that for  $s \rightarrow 0$ .

For measurements in soils and pavements which are exposed to the daily ambient temperature

$$\omega = \frac{2\pi}{24} \frac{1}{\text{hr}} \quad (5.6.16)$$

and thus

$$s = 0.2 \frac{\pi}{12} \approx 0.0524 \text{ 1/hr} \quad (5.6.17)$$

Associated with this value is the optimum period of experiment,

$$t_{\text{max}} = \frac{4}{s} = 76.3 \text{ hr} \quad (5.6.18)$$

or approximately three days. Since  $t_{\text{max}} = N\Delta t$ , then the optimum number of time steps with a duration of one hour would be equal to  $N = 76$ .

The optimum distance corresponding to  $\alpha = 0.05 \text{ ft}^2/\text{hr}$  is:

$$x_{\text{opt}} = \sqrt{\frac{\alpha}{0.2\omega}} = \sqrt{\frac{\alpha t_{\text{max}}}{st_{\text{max}}}} = \sqrt{\frac{\alpha t_{\text{max}}}{4}} \approx 1.0 \text{ ft.} \quad (5.6.19)$$

Therefore, the optimum location of thermocouples in a semi-infinite body such as a pavement, is at  $x = 1.0 \text{ ft.}$

### 5.7 Heat Flux Condition

Assuming that the heat flux were known at  $x = 0$  as a function of time or

$$-K \left. \frac{\partial T}{\partial x} \right|_{x=0} = q(t) \quad (5.7.1)$$

Take the Laplace transform of Equation (5.7.1) to obtain

$$-K \left. \frac{\partial \bar{\theta}}{\partial x} \right|_{x=0} = \bar{q}(s) \quad (5.7.2)$$

The time dependence of  $q(t)$  need not be stored. All that is needed is  $\bar{q}$  which could be found sequentially, that is, all the detailed structure of  $q(t)$  need not be stored but only the current approximation to the integral,

$$\bar{q}(s) = \int_0^{\infty} e^{-st} q(t) dt \approx \sum_{i=1}^{\infty} e^{-st_i} q(t_i) \Delta t \quad (5.7.3)$$

From Equation 5.2.13

$$\theta(x, s, \alpha) = C_1 e^{-\sqrt{\frac{s}{\alpha}} x} \quad (5.7.4)$$

and also

$$\bar{q}(s) = -KC_1 \left( -\sqrt{\frac{s}{\alpha}} \right) \quad (5.7.5)$$

or

$$C_1 = \frac{\bar{q}(s)}{K \sqrt{\frac{s}{\alpha}}} \quad (5.7.6)$$

Note:

$$K \sqrt{\frac{1}{\alpha}} = K \sqrt{\frac{\rho C_\rho}{K}} = \sqrt{K \rho C_\rho} \quad (5.7.7)$$

$$\bar{\theta}(o, s, K \rho C_\rho) = \frac{\bar{q}(s)}{\sqrt{K \rho C_\rho s}} \quad (5.7.8)$$

Then

$$K \rho C_\rho = \left( \frac{\bar{q}(s)}{\bar{\theta}_o} \right)^2 \frac{1}{s} \quad (5.7.9)$$

where

$$\bar{\theta}_o = \bar{\theta}(o, s, K \rho C_\rho) \quad (5.7.10)$$

Thus, we have a means of calculating  $K \rho C_\rho$  and  $\alpha$  if there are means of calculating temperature and heat flow in a semi-infinite body. If  $\alpha$ , and  $K \rho C_\rho$  are measured we may obtain  $K$  and  $\rho C_\rho$  directly by:

$$K = \sqrt{K \rho C_{\rho} \alpha} \quad (5.7.11)$$

and

$$\rho C_{\rho} = \sqrt{\frac{K \rho C_{\rho}}{\alpha}} \quad (5.7.12)$$

### 5.8 Heat Transfer Coefficient

The value of the heat transfer coefficient,  $h_c$ , should be known in order to evaluate the quantity of heat flow between the air and the pavement surface. The value of  $h_c$  is required in the analysis of the air and pavement surface temperature. The pavement surface temperature may be determined from climatological data if a realistic value of the heat transfer coefficient,  $h_c$ , is available.

Scott (44) developed a procedure for estimating the heat transfer coefficient,  $h_c$ , between the air and ground surface. Scott's method is based on the ambient conditions such as wind velocity, atmospheric stability, and ground surface roughness. A lot of uncertainty and errors are involved in obtaining  $h_c$  from this method, since it depends on the ambient conditions which are random variables.

The heat transfer coefficient is also obtained by a "back computing" process to Equation 1.2.3. This procedure is also tedious and impractical. For these reasons, a method of estimating  $h_c$  from recorded surface

temperature is needed. The method introduced herein may be used to calculate  $h_c$  if the thermal properties of pavement material are known.

Assume the heated surface at  $x = 0$  is exposed to a medium which has no heat capacity, but possesses a conductance, or heat transfer coefficient,  $h_c$ , such as air. The temperature of air  $T_\infty(t)$  may be assumed to be known, but the temperature of the surface need not be known. The boundary condition would be

$$-K \left. \frac{\partial T}{\partial x} \right|_{x=0} = h_c [T_\infty(t) - T(0,t)] \quad (5.8.1)$$

Subtracting the initial temperature  $T_i$  from Equation 5.8.1 in the manner:

$$-K \frac{\partial (T(0,t) - T_i)}{\partial x} = h_c \left[ (T_\infty(t) - T_i) - (T(0,t) - T_i) \right] \quad (5.8.2)$$

Taking the Laplace transform of Equation 5.8.2 gives

$$-K \frac{\partial \bar{\theta}_0}{\partial x} = h_c [\bar{\theta}_\infty - \bar{\theta}_\alpha] \quad (5.8.3)$$

From Equation 5.2.13

$$\bar{\theta} = C_1 e^{-\sqrt{\frac{s}{\alpha}} x} \quad (5.8.4)$$



Assume the thermocouple nearest the heated surface is at  $x_1$ . Then, using Equation 5.8.4:

$$\bar{\theta}_1 = C_1 e^{-\sqrt{\frac{s}{\alpha}} x_1} \quad (5.8.5)$$

and hence:

$$C_1 = \bar{\theta}_1 e^{\sqrt{\frac{s}{\alpha}} x_1} \quad (5.8.6)$$

or

$$\bar{\theta} = \bar{\theta}_1 e^{\sqrt{\frac{s}{\alpha}} x_1} e^{-\sqrt{\frac{s}{\alpha}} x} \quad (5.8.7)$$

Introduce this result into Equation 5.8.3 to obtain:

$$\left(-\sqrt{\frac{s}{\alpha}}\right) \left(-K \bar{\theta}_1 e^{\sqrt{\frac{s}{\alpha}} x_1}\right) = h_c \left[\bar{\theta}_\infty - \bar{\theta}_1 e^{\sqrt{\frac{s}{\alpha}} x_1}\right] \quad (5.8.8)$$

Solving for  $h_c/K$  gives:

$$h_c/K = \frac{\bar{\theta}_1 e^{\sqrt{\frac{s}{\alpha}} x_1}}{-\bar{\theta}_1 e^{\sqrt{\frac{s}{\alpha}} x_1} + \bar{\theta}_\infty} \left(\sqrt{\frac{s}{\alpha}}\right) \quad (5.8.9)$$

or

$$h_c/K = \frac{1}{\frac{\bar{\theta}_\infty}{\bar{\theta}_1} e^{-\sqrt{\frac{s}{\alpha}} x_1} - 1} \left(\sqrt{\frac{s}{\alpha}}\right) \quad (5.8.10a)$$

or

$$h_c = \frac{\sqrt{sK\rho C_\rho}}{\frac{\bar{\theta}_\infty}{\bar{\theta}_1} e^{-\sqrt{\frac{s}{\alpha}} x_1} - 1} \quad (5.8.10b)$$

If in addition to the temperature at  $x_1$  and of the air,  $\alpha$  and  $K\rho C_\rho$  are known,  $h_c$  can be estimated from this equation. The surface thermocouple in the pavement was located at a depth of 1/2-inch from the surface of the pavement, and it is assumed that this thermocouple gives representative temperature for the surface of the pavement. Since the uppermost 1/2-inch of the pavement has a large temperature gradient, surface thermocouples should be located such that one side of the thermocouple be exposed to the air and the other sides be surrounded by asphaltic concrete.

In this case,  $x_1 = 0$  and Equation 5.8.10b becomes:

$$h_c = \frac{\sqrt{sK\rho C_\rho}}{\frac{\bar{\theta}_\infty}{\bar{\theta}_0} - 1} \quad (5.8.10c)$$

which is independent of thermal diffusivity unlike Equation 5.8.10b.

This method lends itself to computer solution and the value of  $h_c$  may be estimated directly for the thermal

conductivity installation sites. The ALPHA program (discussed in Section 5.10) may be expanded to calculate  $h_c$  from Equation 5.8.10c.

### 5.9 Correction for Initial Condition

One assumption in the simplified method for estimation of thermal diffusivity is that the initial temperature distribution is uniform throughout the semi-infinite body. In reality, this is not usually true for pavement under natural conditions. The temperature of the uppermost layer of the pavement is approximately uniform before sunrise. A uniform temperature may also be provided by placing an insulating blanket over the surface of the pavement. In this section, we seek an optimum initial condition and a method will be introduced for the correction of non-uniform initial conditions.

Examples of hourly temperature profiles of the pavement and underlying soil during winter, spring, and summer, are given in Figures 2.7.1, 5.9.1, and 5.9.2. Figure 5.9.1 shows a temperature profile which has been used as an initial condition during a winter day.

It is observed that the temperature is relatively uniform for the first few inches of pavement thickness, but as the depth increases, the temperature deviates further from the uniform temperature condition. Pavement at lower depths has a higher temperature than near the surface. Similar data for a summer day shows the reverse,

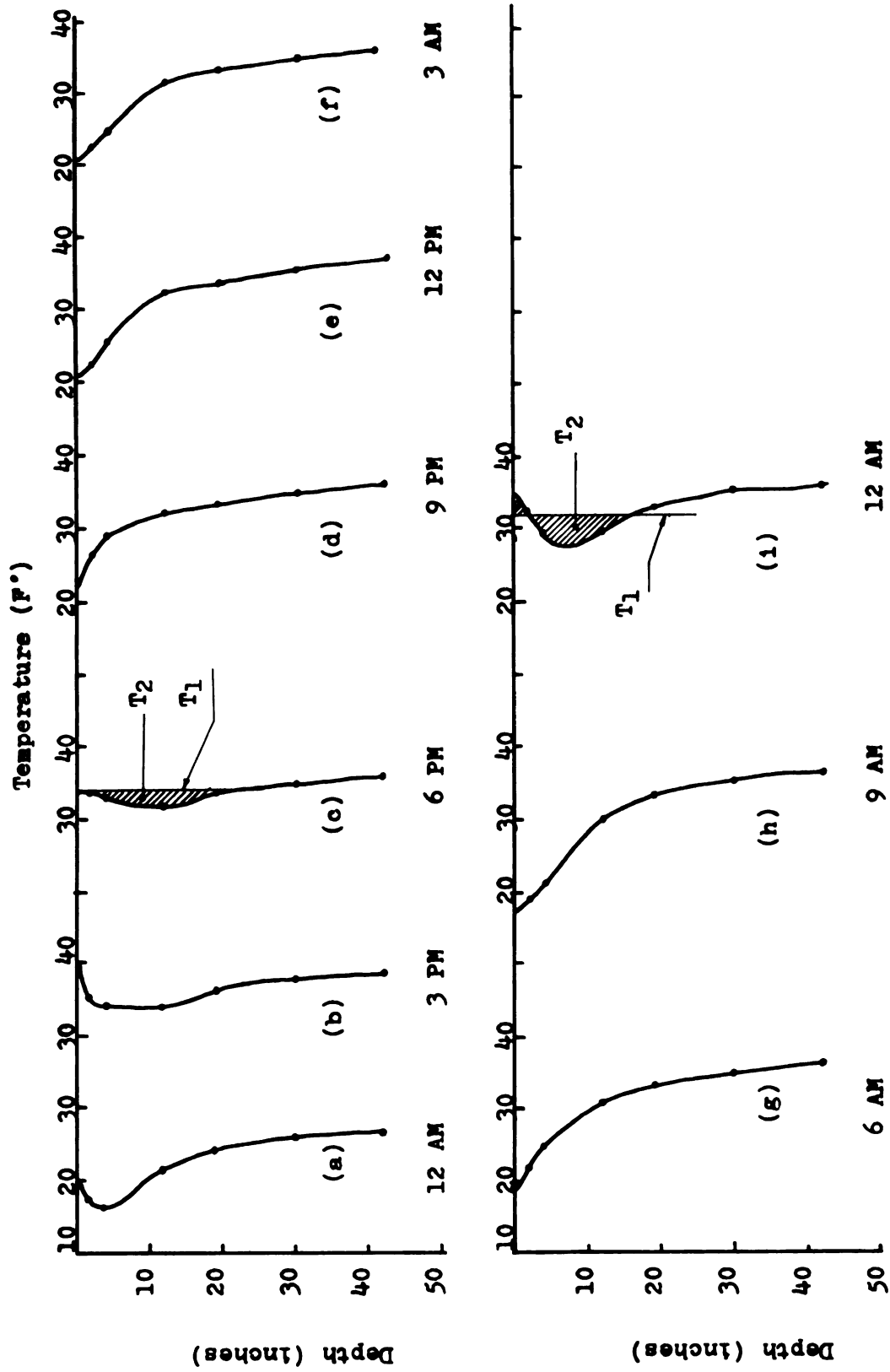


Figure 5.9.1 Temperature distribution in 19-inch full-depth asphaltic pavement at selected times during a winter day

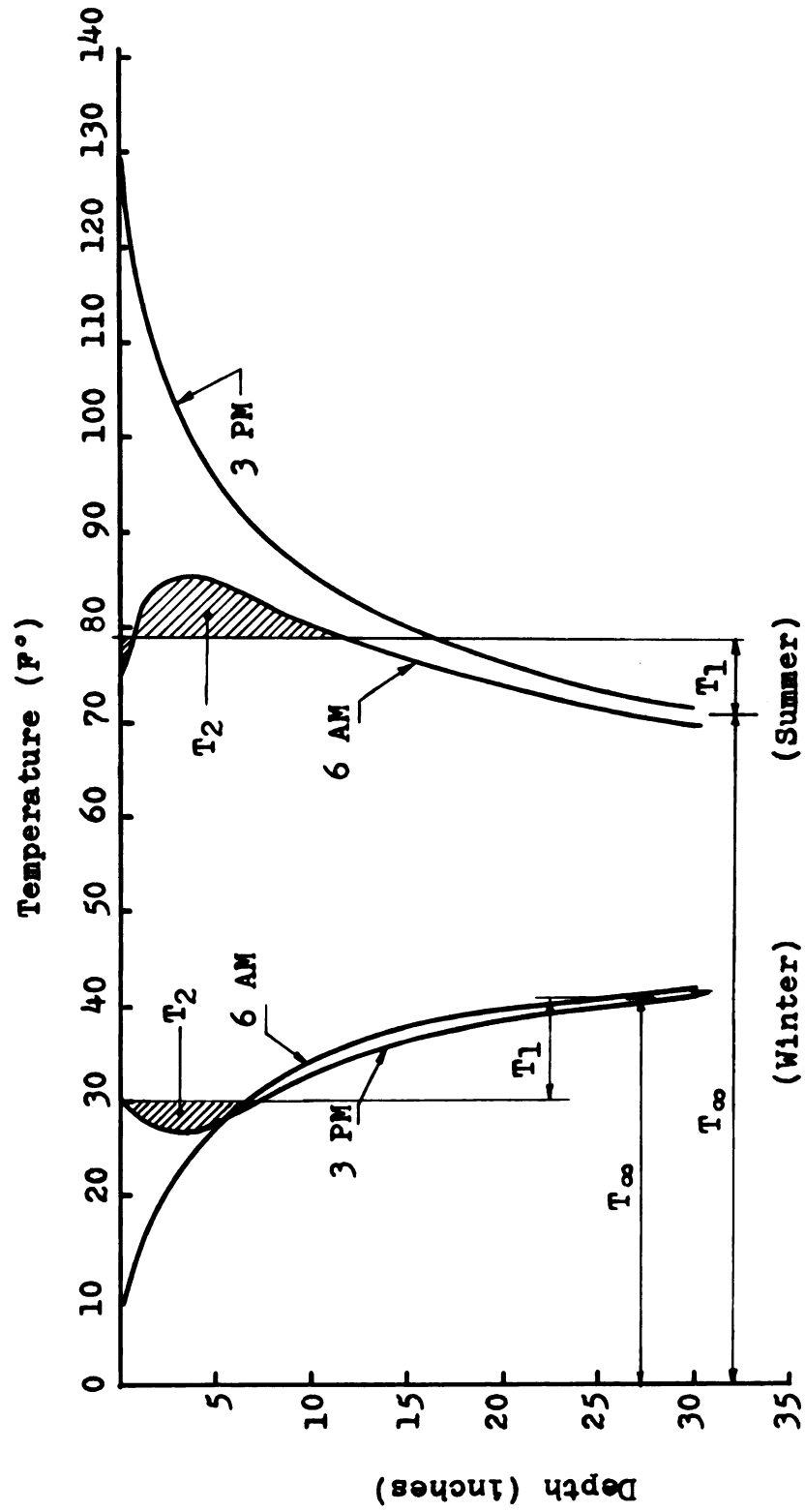


Figure 5.9.2 Temperature profile in a 19-inch full-depth asphaltic pavement during winter and summer

and the temperature is rarely uniform throughout the pavement at any one time.

Observation of temperature profiles at different seasons indicate that ground temperature profile is affected by the combined daily and seasonal changes, and the temperature at a point can be represented by:

$$T_{\text{meas}}(x,t) = T_{\infty} + T_1(x,t) + T_2(x,t) \quad (5.9.1)$$

where  $T_{\infty}$  is the temperature of underlying soils subjected to seasonal change as it is shown in Figure 5.9.2.

$T_1(x,t)$  is the difference between the average daily temperature of the top few feet and  $T_{\infty}$  (see Figure 5.9.2).

$T_2(x,t)$  is the difference between  $T_1(x,t)$  and the measured temperature at the initial time.

Since we are interested in evaluation of the thermal properties of asphalt concrete, only variations of  $T_1(x,t)$  and  $T_2(x,t)$  need be considered in the correction of the initial temperature. It is thus assumed that the measured temperature is composed of the two basic parts discussed next.

1. One part is a uniform temperature,  $T_1(x,t)$  equal to the average temperature of the top few feet of soil-pavement and with a time variable boundary condition at  $x = 0$ . For this uniform temperature, we have:

$$\alpha \frac{\partial^2 T_1(x,t)}{\partial x^2} = \frac{\partial T_1(x,t)}{\partial t} \quad (5.9.2)$$

and the boundary and initial conditions are:

$$T(0,t) = T_0(t) \quad \text{at } x = 0 \quad (5.9.3)$$

$$T_1(x,0) = T_i(x) = \text{constant} \quad t = 0 \quad (5.9.4)$$

2. The other part is the departure or deviation of the temperature at a given depth from the assumed uniform temperature at  $t = 0$ . This temperature deviation is called  $T_2(x,t)$  and the associated problem is mathematically given by:

$$\alpha \frac{\partial^2 T_2(x,t)}{\partial x^2} = \frac{\partial T_2(x,t)}{\partial t} \quad (5.9.5)$$

$$T_2(0,t) = T_2(0) = T_i(x) = \text{constant} \quad \text{at } x = 0 \quad (5.9.6)$$

$$T_2(\infty,t) \approx T_2(0) \quad \text{at } x \rightarrow \infty \quad (5.9.7)$$

$$T_2(x,0) = T_i(x) \quad t = 0 \quad (5.9.8)$$

Then, the measured field temperature is written in the form:

$$T_{\text{meas}}(x,t) = T_1(x,t) + T_2(x,t) \quad (5.9.9)$$

Mathematically,  $T_1(x,t)$  can be represented by:

$$T_1(x,t) = \frac{1}{tx} \int_0^t \int_0^x T(x,t), dx, dt \quad (5.9.10)$$

where  $t$  is the time during which the average temperature has been taken and  $x$  is the depth at which the effect of daily variations of temperature vanishes. This is represented graphically in Figure 5.9.2. Usually the initial time has been chosen to be a time between 6:00 and 9:00 A.M. Figure 5.9.1b shows the selected initial time as well as  $T_1(x,t)$  and  $T_2(x,t)$ .

Assuming an average value for  $T_1(x,t)$ , we can define  $T_2(x,t)$  as the deviation temperature from  $T_1(x,t)$  so that it has a value of zero at  $x = 0$  and a non-uniform initial temperature.  $T_2(x,t)$  can be approximated as the temperature in a region of which part is initially at constant temperatures  $T_a$ ,  $T_b$ ,  $T_c$ , etc. . . . and the remainder at zero. This approximation is illustrated in Figure 5.9.3A which shows that the area between curves of non-uniform temperature profiles is assumed to be composed of a number of rectangular-shaped temperature pulses,  $S_a$ ,  $S_b$ , and  $S_c$ . (Note that these pulses are the initial temperature distribution over position and not over time.)

Assigning to  $ST_2$  the area between these two curves, we can write for the case of three non-uniform initial temperature regions:

$$ST_2 = S_a + S_b + S_c \quad (5.9.11)$$



Each one of these temperature regions can be assumed to be an individual transient temperature problem. Thus, the transient temperature distribution as the function of time and depth should be used as the transient temperature distribution of  $ST_2$ .

Consider a heat pulse similar to each sub-area of  $ST_2$  such as shown in Figure 5.9.3B, where the region  $-a < x < a$  is initially at a constant temperature  $T_{\max}$  and the region  $|x| > a$  is initially at zero. The transient temperature distribution in an infinitely thick plate such as pavement at time  $t$ , due to this heat source, can be obtained by Carslaw and Jaeger (13):

$$\frac{T - T_1}{T_{\max} - T_1} = \frac{1}{2} \left[ \operatorname{erf} \frac{|a - x|}{2\sqrt{\alpha t}} + \operatorname{erf} \frac{a + x}{2\sqrt{\alpha t}} \right] \quad (5.9.12)$$

where "erf" refers to the error function defined by:

$$\operatorname{erf}(x) = \frac{2}{\sqrt{\pi}} \int_0^x e^{-t^2} dt \quad (5.9.13)$$

In order to provide a temperature distribution similar to Figure 5.9.3A with a zero temperature at  $x = 0$ , a combination of a positive and a negative heat pulse such as illustrated in Figure 5.9.4A is necessary. The temperature distribution in the infinite body due to such a combination is obtained by:

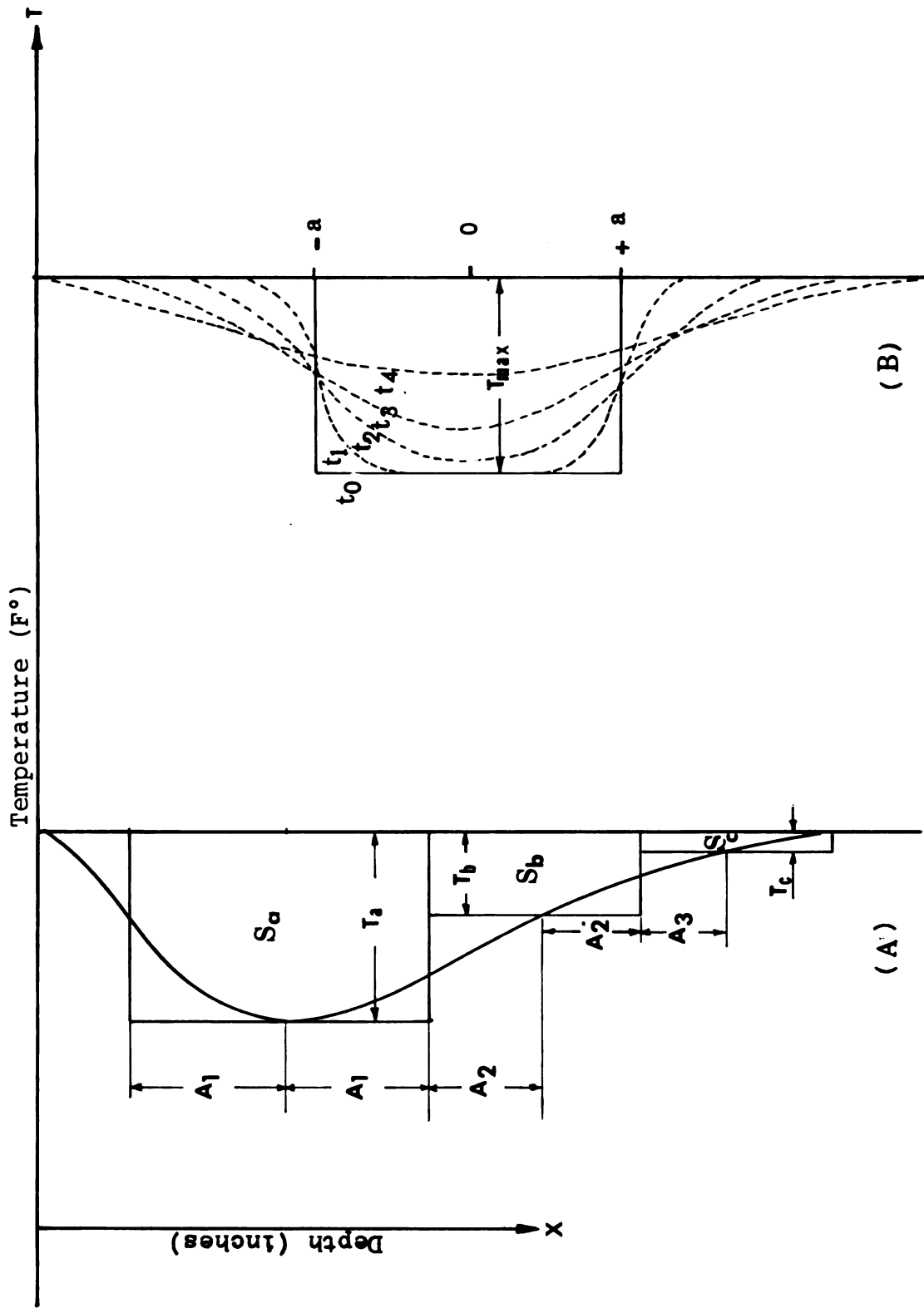
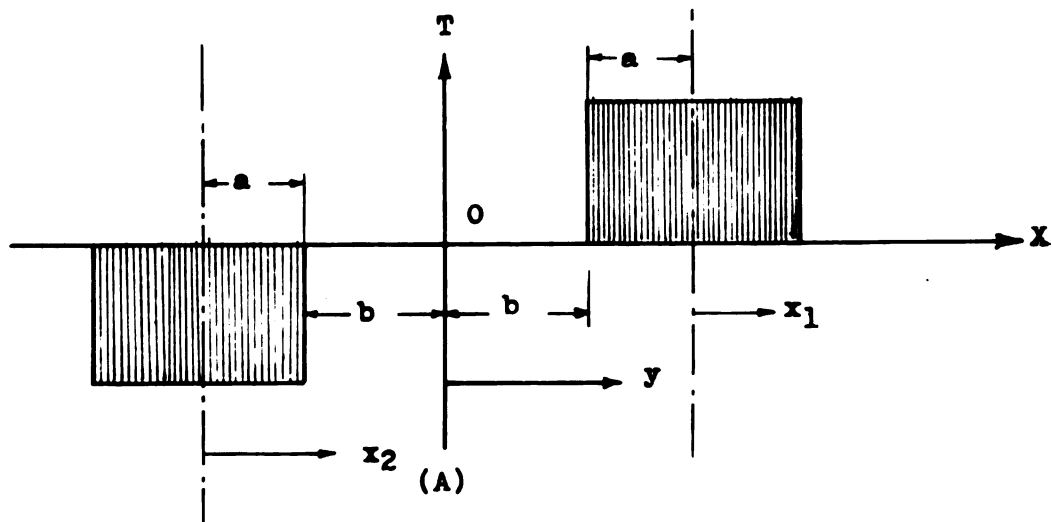
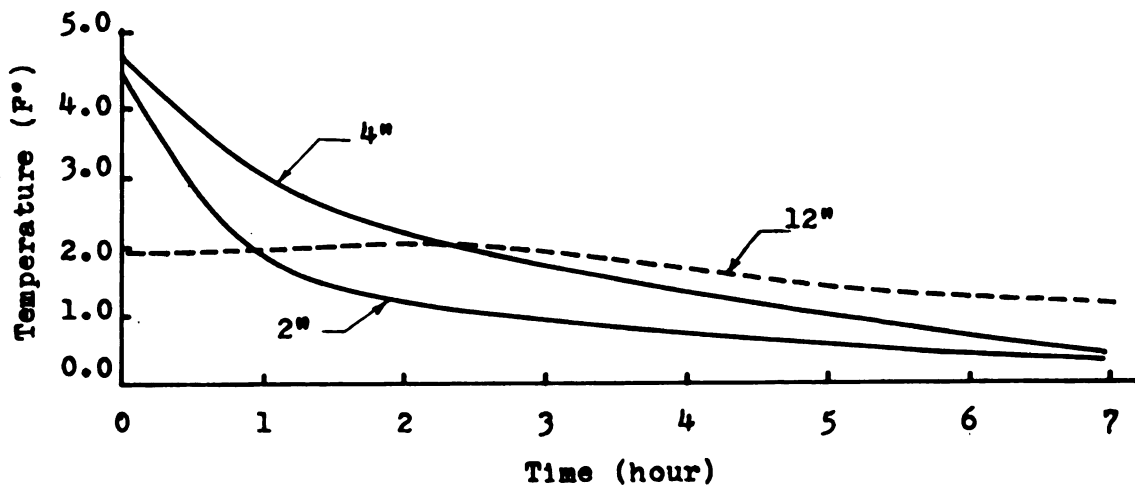


**Figure 5.9.3 Transient temperature distribution for rectangular-shaped temperature pulses**



Combination of Two Rectangular-Shaped Temperature Pulses.



Correction Temperature for Initial Condition

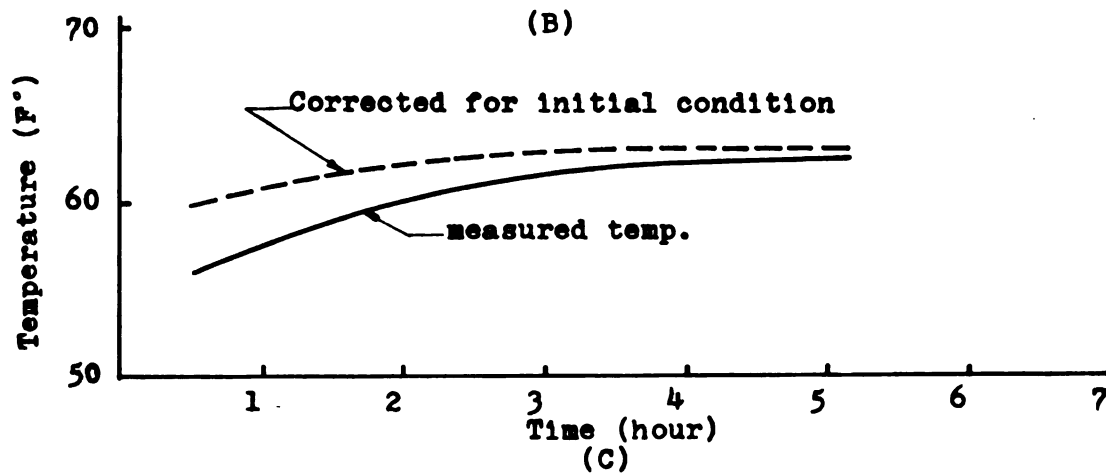


Figure 5.9.4 Combination of temperature pulses and correction temperatures

$$\frac{T - T_1}{T_{\max} - T_1} = \frac{1}{2} \left[ \operatorname{erf} \frac{|a - x_1|}{2\sqrt{\alpha t}} + \operatorname{erf} \frac{a + x_1}{2\sqrt{\alpha t}} - \operatorname{erf} \frac{|a - x_2|}{2\sqrt{\alpha t}} - \operatorname{erf} \frac{a + x_2}{2\sqrt{\alpha t}} \right] \quad (5.9.14)$$

where  $x_1$  and  $x_2$  are the distances of a point from the center of the pulses, respectively. There would be a point in the domain such as point 0 in Figure 5.9.4A, with a zero temperature due to the combined effect of the sources. The pavement may be assumed as a semi-infinite body with a surface at point 0.

The values of  $x_1$  and  $x_2$  are defined in terms of the variables  $a$ ,  $b$ , and  $y$ , and Equation 5.9.14 is brought into a convenient form for tabulation such as:

$$\begin{aligned} \frac{T - T_1}{T_{\max} - T_1} = \frac{1}{2} & \left[ \operatorname{erf} \frac{\left| 1 - \frac{y - b - a}{a} \right|}{2\tau_a^{1/2}} + \operatorname{erf} \frac{1 + \frac{y - b - a}{a}}{2\tau_a^{1/2}} \right. \\ & \left. - \operatorname{erf} \frac{\left| 1 - \frac{y + a + b}{a} \right|}{2\tau_a^{1/2}} - \operatorname{erf} \frac{1 + \frac{y + a + b}{a}}{2\tau_a^{1/2}} \right] \end{aligned} \quad (5.9.16)$$

where

$$\tau_a = \frac{\alpha t}{a^2}$$

Equation 5.9.15 may be written simply as:

$$\frac{T - T_1}{T_{\max} - T_1} = f\left(\tau_a, \frac{y}{a}, \frac{b}{a}\right) \quad (5.9.16)$$

which is a function of three variables  $\tau_a$ ,  $y/a$ , and  $b/a$ . This equation was programmed for numerical solution on the IBM 1800.

The values of the error function are calculated by a sub-routine denoted as "Subroutine ERF." The input are the values of the variables  $\tau_a$ ,  $y/a$ , and  $b/a$ . This program calculates the values of  $T - T_1/T_{\max} - T_1$  called "correction factor" which are printed as the output. Figure 5.9.5 shows the values of correction factor for  $y/a = 3.0$ .

Measured temperature correction is plotted as a function of time for various depths of the pavement in Figure 5.9.4B. In order to assume a uniform initial temperature, the first few measured temperatures should be corrected. Figure 5.9.4C illustrates measured, as well as corrected temperature distribution, due to a single temperature pulse.

Usually the area  $ST_2$  is composed of several temperature pulses, such as shown in Figure 5.9.3A. Thus, the combined effect of these temperature pulses should be used as the correction for initial conditions. According to Equation 5.9.11, the combined effect of temperature pulses can be obtained by:

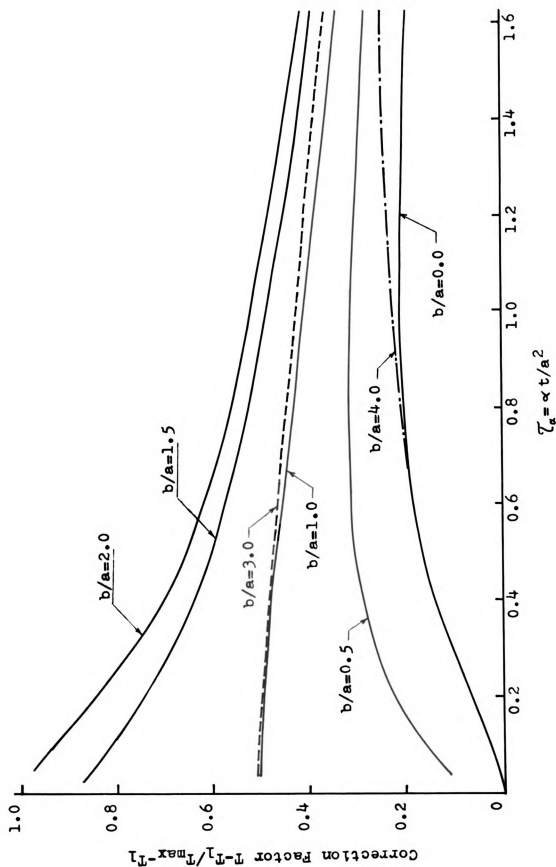


Figure 5.9.5 Correction factor for a single rectangular-shaped temperature pulse  
( $y/a = 3.0$ )

$$T_2(x,t) = T_{\max}^a \phi_a(x,t) + T_{\max}^b \phi_b(x,t) \\ + T_{\max}^c \phi_c(x,t) + \dots \quad (5.9.17)$$

or more simply

$$T_2(x,t) = \sum_{i=a}^n T_{\max}^i \phi_i(x,t) \quad i = a, b, c, \dots, n \quad (5.9.18)$$

where  $\phi_i(x,t)$  is the reduction factor  $T - T_1 / T_{\max} - T_1$  obtained by Equation 5.9.15 and  $T_{\max}^i$  is the maximum amplitude of temperature pulses.

Sometimes the temperature pulses are located on both sides of uniform temperature  $T_1$ . In these cases, the algebraic sum of  $T_{\max}^i \phi_i(x,t)$  should be considered. A temperature pulse located below the uniform temperature  $T_1(x,t)$ , is treated as negative and above  $T_1(x,t)$ , as positive.

Each pulse is specified by three variables:  $b/a$ ,  $y/a$ , and  $\alpha t/a^2$ . The variable  $b/a = B$  is constant while  $y/a$  and  $\tau\alpha$  are functions of position and time respectively. For each value of  $y/a$  which represents specific position in the pavement, various values of  $\tau\alpha$  should be calculated.

A program has been written to calculate  $\tau\alpha$  as well as  $\phi_i(x,t)$  for various values of  $a$  and  $t$ . A listing of the computer program and the input is given in Appendix 2. This program uses the previous program called PHI ( $\phi$ ) as

a subroutine to calculate the  $T_2(x,t)$  defined by Equation 5.9.17.

The program outputs all the values of  $\tau_a$ ,  $T_2(x,t)$ ,  $\phi_i(x,t)$ , and  $b/a$  for various values of  $y/a$ . A sample of output is tabulated and is given in Table 5.9.1.

#### 5.10 Computer Program

It was necessary to write a program utilizing Equation 5.2.19 to calculate thermal diffusivity. The program is written in FORTRAN IV and can be run on most computers although it is written to be run on the IBM 1800. If another system is used, it may be necessary to change the input and output statements.

Equation 5.2.19 is brought into a form suitable for electronic computation. Since temperature measurements are not made continuously with time, but at discrete times (which is the most common case), then the numerical integration in the Laplace transform is replaced by a summation over time. This summation is denoted by sum (ITC, IS) in the program. For the first thermocouple which is used as a driving boundary condition, sum (1,IS) represents the summation in the Laplace transform.

The variable names used in the program were abbreviations of words employed in the discussion of the method. These variables were utilized in the program within the limitation of the computer language. Measured temperatures were denoted by  $T(JJ,N)$  and defined by



Table 5.9.1 Correction factor and combined effect of temperature pulses

Time Steps	$\tau_a = t/a^2$		$\phi_1(x,t)=T-T_1/T_{\max}-T_1$		$T_2(x,t)$ ( $^{\circ}\text{F}$ )	
	$b/a=0.7$	$b/a=3.0$	$b/a=0.7$	$b/a=3.0$		
	$y/a=0.7$					
	1	0.64	0.76	0.35	0.03	-1.83
	2	1.28	1.51	0.22	0.07	-1.24
	3	1.92	2.27	0.15	0.08	-0.91
	4	2.56	3.02	0.11	0.08	-0.71
	5	3.20	3.78	0.08	0.07	-0.57
	$y/a=1.33$					
	1	0.64	0.75	0.56	0.08	-2.98
	2	1.28	1.51	0.36	0.14	-2.09
	3	1.92	2.26	0.25	0.15	-1.57
	4	2.56	3.02	0.19	0.15	-1.24
	5	3.20	3.78	0.15	0.13	-1.01
	6	3.84	4.53	0.12	0.12	-0.84
	$y/a=4.0$					
	1	0.64	0.75	0.12	0.58	-1.79
	2	1.28	1.51	0.19	0.43	-1.80
	3	1.92	2.26	0.20	0.36	-1.72
	4	2.56	3.02	0.19	0.31	-1.60
5	3.20	3.78	0.18	0.27	-1.45	
6	3.84	4.54	0.17	0.25	-1.33	
7	4.48	5.29	0.15	0.23	-1.21	
8	5.12	6.05	0.14	0.21	-1.11	
9	5.76	6.80	0.13	0.19	-1.01	
10	6.40	7.56	0.11	0.18	-0.94	

Equation 5.2.5 represented by  $T(IA,IB)$ .  $S(J)$  and  $x(J)$  are the Laplace transform parameter and depth dimensions respectively. The symbols  $E$ ,  $ZH$ ,  $ASUM$ , and  $AA$ , are clearly defined in the list of the program. The values of these variables are calculated based on input data and are printed as the output. Subsequent operations produced values for the numerator and denominator of the Equation 5.2.19, and finally, "ALPHA," the thermal diffusivity was calculated.

This program may be used to calculate the air heat transfer coefficient of  $(h_c)$  defined by Equations 5.8.10b and 5.8.10c. The heat transfer coefficient  $(h_c)$  may also be obtained by some additional operations which utilized the obtained value of thermal diffusivity as the input Equation 5.8.10b or 5.8.10c and calculated  $(h_c)$ . This process may be done by writing the mentioned equations in a proper form acceptable for the computer and using the result as the subroutine of the main program.

Thermal conductivity of asphalt concrete may also be obtained by an additional operation which multiplies the volumic specific heat by "ALPHA" to produce the resulting thermal conductivity in BTU/ft hr °F. Output from the program is in tabular form. Both the program and a sample of the output are included in Appendix 1.

### 5.10.1 Input

The environmental condition, as well as temperature data and a number of variables, are utilized as the data input for the program. The temperature data obtained both in the field and laboratory are utilized as the boundary conditions in the program. The list of the variables which are used in a suitable form for the program are given in Appendix 1. Daily, as well as data cumulative at the surface and at various depths of both a 7-inch and a 19-inch asphalt pavement, have been used as the temperature boundary condition to calculate thermal diffusivity of asphalt concrete under the field condition. Recorded temperature data during winter, spring, fall, and summer have been utilized to calculate thermal diffusivity relating to different seasons. Experimental temperature data have also been employed to obtain values of  $(\alpha)$  under the closed laboratory conditions. Both sets of temperature data provide an extensive range of temperature which is required in evaluating the value of thermal diffusivity as the function of temperature.

### 5.10.2 Output and Results

The program outputs all the values of  $e^{-st}$ ,  $\sum e^{-st} T'(x,t) dt$ , and  $T'(x,t)$  for all the time steps and various parameters  $s$ , and thermocouples. The program also calculates and prints the values of  $\chi(T'_j)/\chi(T'_0)$ , as well as logarithms and square logarithms values of

$\mathcal{L}(T'_j)/\mathcal{L}(T'_o)$ . Printed output also includes time steps, the sequence of time steps, the values of Laplace transform parameters, the thermocouple number, and the values of the numerator and the denominator of Equation 5.2.19.

The result of subsequent operations which calculate the values  $sx^2 / \ln^2 \frac{\mathcal{L}(T'_j)}{\mathcal{L}(T'_o)}$  and its summation for the parameter  $s$  and  $x$ , and finally the value of thermal diffusivity ( $\alpha$ ) are given sequentially in the list of output. Calculated thermal diffusivity of asphaltic concrete for various seasons and under different ambient conditions are given in Tables 5.9.2 and 5.9.3. The calculated thermal diffusivity of asphaltic concrete from experimental temperature data are given in Table 5.9.4.

Table 5.9.2 Calculated thermal diffusivity of wearing and binding courses from recorded temperature data ( $s = 4/t_{\max}$ ), simplified method

Case	Date	Ambient Condition	Surface Temp (F°)		$t_{\max}$ (hr)	Thermal Diffusivity (ft <sup>2</sup> /hr)
			Max	Min		
1	7.69	sunny	127	65	120	0.042
2	8.69	"	115	64	21	0.044
3	6.69	"	120	60	16	0.043
4	4.69	"	112	41	16	0.051
5	3.69	"	56	37	70	0.049
6	1.70	"	34	5	16	0.053
7	1.70	"	28	-2	118	0.054
8	8.69	cloudy	135	70	16	0.050
9	4.69	"	116	68	35	0.048
10	1.70	"	28	-3	16	0.062
11	1.70	"	36	10	118	0.059
12	7.69	rainy	118	73	16	0.060
13	3.69	"	33	20	16	0.055
14	7.65	sunny	131	68	70	0.052
15	7.65	(Alger)	123	69	68	0.052
16	1.65	"	29	6	96	0.056
17	1.64	"	40	-5	62	0.069

Table 5.9.3 Calculated thermal diffusivity of asphaltic concrete (entire pavement) from recorded temperature data ( $s = 4/t_{\max}$ ) simplified method

Case	Date	Surface Temp (F°)		$t_{\max}$ (hr)	Thermal Diffusivity (ft <sup>2</sup> /hr)		
		Max	Min		nonuniform I.T.	uncorrected I.T.	corrected I.T.
1	7.69	127	65	120	0.041	0.032	0.039
2	8.69	115	64	21	0.033	0.041	0.044
3	6.69	120	60	16	0.040	0.036	0.040
4	4.69	112	40	16	0.039	0.043	0.050
5	3.69	56	37	70	0.050	0.051	0.055
6	1.70	34	5	16	0.040	0.049	0.053
7	1.70	28	-2	118	0.080	0.072	0.060
8	8.69	135	70	16	0.050	0.061	0.050
9	4.69	116	68	35	0.049	0.058	0.047
10	1.70	28	-3	16	0.047	0.041	0.057
11	1.70	36	10	118	0.050	0.065	0.059
12	7.69	118	73	16	0.063	0.059	0.053
13	3.69	33	20	16	0.049	0.049	0.055
14	7.65	131	68	70	0.054	0.049	0.039
15	7.65	123	69	68	0.041	0.043	0.049
16	1.65	29	6	96	0.059	0.052	0.060
17	1.64	40	-5	62	0.059	0.078	0.063

Table 5.9.4 Calculated thermal diffusivity of wearing and binder courses from laboratory data ( $t_{\max} = 120$  seconds and  $s = 4/t_{\max}$ ), simplified method

Case	Condition	Surface Temp (F°)		Thermal Diffusivity (ft <sup>2</sup> /hr)
		Max	Min	
1.1	dry	146	118	0.039
1.2	"	146	118	0.042
1.3	"	146	118	0.039
1.4	"	146	118	0.038
2	"	130	97	0.041
3	"	124	80	0.042
4	"	117	75	0.051
5.1	"	80	5	0.048
5.2	wet	75	2	0.064
5.3	dry	85	-1	0.050
6.1	dry	26	-27	0.054
6.2	wet	25	-25	0.071
6.3	dry	32	-15	0.062

## CHAPTER VI

### PAVEMENT TEMPERATURE

#### 6.1 Temperature Distribution in Pavement

The main objective in the collection of the recorded field temperature data was to obtain temperature variation at various depths of the asphaltic pavement. It was realized that this temperature data was not adequate for this study. Necessary additional information had to be obtained in order to conduct a more comprehensive analysis of the simulated model. This additional data consisted of thermal properties of pavement materials, surface convection coefficient, solar radiation, and other environmental knowledge. The lack of information on thermal properties has been emphasized in earlier chapters.

In order to obtain a correlation between the observed and calculated temperature variation, a simulation model was required. This simulated model should be based on the basic heat transfer equations for radiation, conduction, and convection.

The problem in this study is a one-dimensional time-dependent boundary value problem of heat conduction



with temperature-variable thermal properties. The problem is nonlinear because of the temperature-dependent thermal properties of pavement material.

The recorded temperature of pavement may be utilized as the boundary condition to the simulated model to obtain the calculated temperature variation at various depths of the pavement.

One of the most important objectives of the simulation model was to predict pavement temperatures at various depths, in the simulated pavement, under the actual and the extreme conditions which the pavement might experience during its lifetime. The reasoning behind this condition is that during the period of data collection the coldest or hottest condition may not be reached; thus, the extreme temperature will be missed. For this reason a simulated model with a variable range temperature was required.

Most of the studies on the subject of temperature distribution in pavement have dealt with steady, stepped, or strictly sinusoidal boundary values (37), whereas as pavement exposed to daily change in temperature does not experience such convenient surface variation.

The purpose of this study was to define methods which may be utilized to analyze a realistic surface temperature history as the boundary condition to a simulated model for calculating theoretical values of temperature in a pavement.

## 6.2 Exact Solution Based on Periodic Surface Temperature

Daily, and annual variation of pavement surface temperature may be approximately represented by a steady periodic wave function according to the expression (13):

$$T(o,t) - T_i = (TA_d - TM_d) \cos \omega_d t \quad (6.2.1)$$

where  $T(o,t)$  is the pavement surface temperature at the time  $t$ , and  $T_i$ ,  $TM$ , are the initial and mean daily temperature at  $x = 0$ , respectively. Amplitude and angular frequency of surface temperature is denoted by  $(TA_d - TM_d)$  and  $\omega$ , respectively. The subscript "d" refers to daily temperature.

It is assumed that pavement is a semi-finite body with a sinusoidal surface temperature change; temperature at a depth  $x$  below the surface of pavement may be obtained by (13):

$$T(x,t) - T_i = (TA_d - TM_d) e^{-\sqrt{\frac{\omega d}{2\alpha}} x} \cos \left( \omega_d t - \sqrt{\frac{\omega d}{2\alpha}} x \right) \quad (6.2.2)$$

which is also periodic and its amplitude decays in an exponential manner by a damping factor  $e^{-\sqrt{\omega d/2\alpha} x}$ .

Further, the temperature at the depth  $x$  below the surface lags behind the temperature at the surface, and in proportion to  $\sqrt{\omega d/2\alpha} x$ .

In order to compare measured temperature data with the results of Equation 6.2.2, a possible value of  $\alpha = 0.04 \text{ ft}^2/\text{hr}$  for asphaltic concrete given in Table 4.4.1 should be selected and Equation 6.2.2 is solved for the temperature at a depth  $x$  below the surface.

Equation 6.2.2 is solved for annual and daily periods and surface temperature, and the calculated temperature distributions are plotted in Figures 6.2.1 and 6.2.2.

Since the temperature at a depth  $x$  below the surface is the function of daily and seasonal change, Equations 6.2.1 and 6.2.2 may be written in the following form to account for daily and seasonal changes:

$$[T(0,t) - T_i] = (TA_a - TM_a) \cos \omega_a t + (TA_d - TM_d) \cos \omega_d t \quad (6.2.3)$$

and

$$[T(x,t) - T_i] = (TA_a - TM_a) e^{-\sqrt{\frac{\omega_a}{2\alpha}} x} \cos(\omega_a t - \sqrt{\frac{\omega_a}{2\alpha}} x) \Big|_{\omega = \frac{2\pi}{24(365)}} + (TA_d - TM_d) e^{-\sqrt{\frac{\omega_d}{2\alpha}} x} \cos(\omega_d t - \sqrt{\frac{\omega_d}{2\alpha}} x) \Big|_{\omega = \frac{2\pi}{24}} \quad (6.2.4)$$

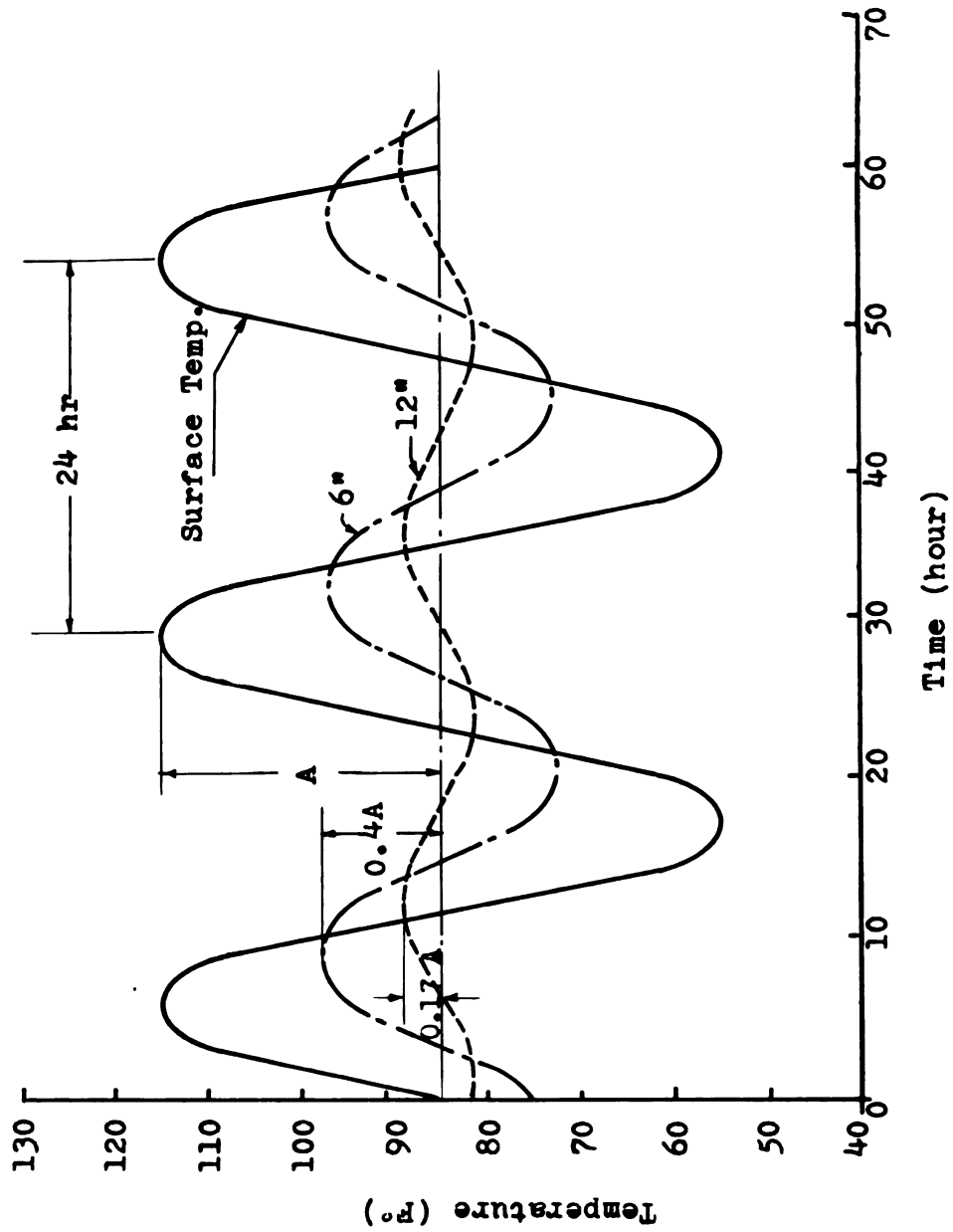


Figure 6.2.1 Daily variation of temperature (exact solution)

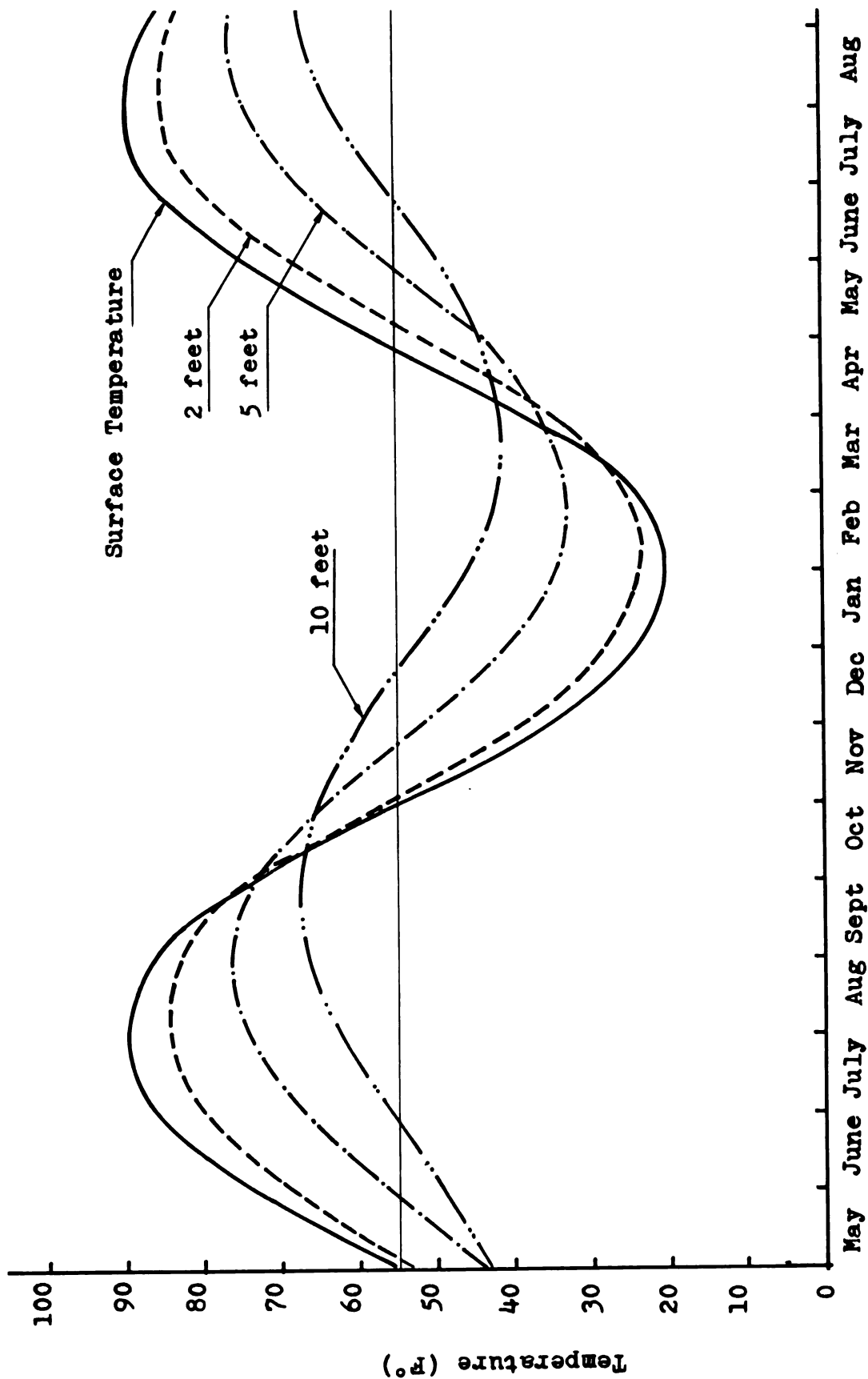


Figure 6.2.2 Annual variation of temperature (exact solution)

where  $TM_d$  and  $TM_a$  are the mean daily and annual surface temperatures, respectively.  $T_i$  is the initial temperature and  $TA_d$  and  $TA_a$  are the daily and annual temperature amplitude at the surface, respectively.

For the annual variation of the temperature, the angular frequency of the fluctuation is  $\omega_a = 2\pi/P = 2\pi/24(365)$  per hour for a period of one year or 365 days, while  $\omega_d = 2\pi/P = 2\pi/24$  per hour for a period of one day.

It may be observed that the first term on the right-hand side of Equation 6.2.4 represents the effect of seasonal temperature variation and the second term stands for daily fluctuation of temperature. For small values of  $x$  up to three feet, the second term dominates, while for large values of  $x$ , the effect of second term is negligible and the first term characterizes the temperature.

Neglecting the effect of seasonal temperature variation, daily variation of temperature lies within an envelope determined approximately by  $\pm e^{-\sqrt{\omega d/2\alpha} x}$ . These envelopes are actually the two exterior temperature distribution curves.

It was assumed in the foregoing that the surface temperature varies according to a simple harmonic sine curve. Such, however, is not the case in reality, instead, the surface temperature follows a complicated

temperature process which may be characterized as the sum of a series of partial oscillations.

The Fourier-series analysis has been proposed by Carson (14) in describing this phenomena and the surface temperature is assumed to vary according to the expression:

$$T(o,t) = F(t) = T_m + \sum_{m=1}^{\infty} (A_n \cos \frac{360}{P} nt + B_n \sin \frac{360}{P} nt) \quad (6.2.5)$$

where  $A_n$  and  $B_n$  are the Fourier coefficients determined through standard Fourier techniques.  $T_m$  and  $P$  are the mean temperature and the period of the cycle respectively, and  $n$  is the ordinal of partial oscillation.

### 6.3 The Integration Method (Volterra Integral Equation)

For a semi-infinite body such as a soil-pavement system with a time-variable surface temperature, the nonlinear heat conduction equation is transformed into an integral equation in the form (13):

$$T(x,t) = T_i + \frac{x}{2\sqrt{\pi\alpha}} \int_0^t T(\lambda - T_i) \frac{e^{-x^2/4\alpha(t-\lambda)}}{(t-\lambda)^{3/2}} d\lambda \quad (6.3.1)$$

where  $T(\lambda)$  is the known variable surface temperature and  $\lambda$  is a dummy time variable of integration.

Equation 6.3.1 may be solved for  $T(x,t)$  by a number of analytical methods (4). Monismith et al. (37) employed

this equation to determine the temperature distribution in a slab with sinusoidal surface temperature. In this study we employed the Runge-Kutta method (17) for integration and the Equation 6.3.1 was written in FORTRAN form and programmed. The recorded surface temperature was used as  $T(\lambda)$  in Equation 6.3.1 to calculate the temperature  $T(x,t)$ , at any depth  $x$  below the surface.

Difficulty was encountered using this method and the obtained value of the calculated temperature was not satisfactory. The conclusion is that this equation cannot be employed in this study and the application of the analytical methods given by Ames (4) for the solution of Equation 6.3.1 is not practical.

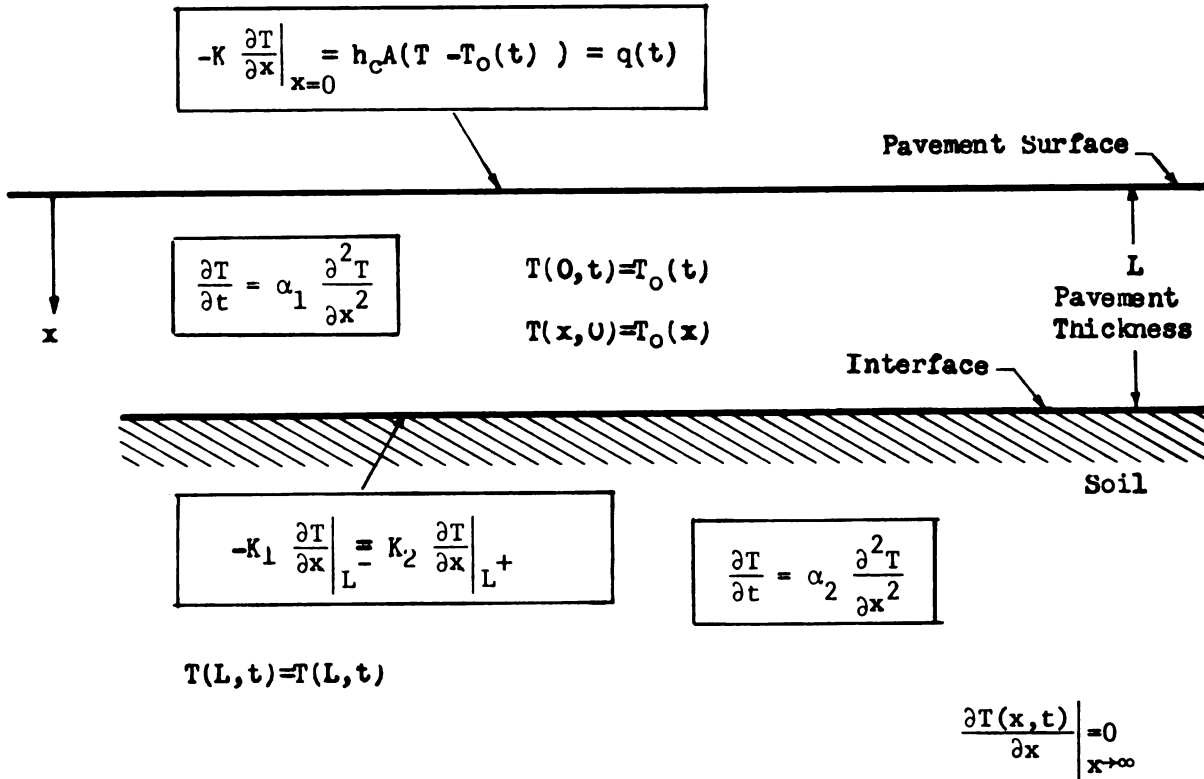
#### 6.4 Finite Difference Method

In this analysis it may be assumed that the pavement is a semi-infinite body with a time variable surface temperature and temperature-variable thermal properties. Nonlinear boundary conditions may also be treated. Figure 6.4.1a illustrates the geometry and the boundary condition of the soil-pavement system which was selected for the model. The related one-dimensional heat transfer equations and the prescribed boundary conditions are the following:

$$\frac{\partial}{\partial x} \left( K_1 \frac{\partial T}{\partial x} \right) = (\rho C_p) \frac{\partial T}{\partial t} , \quad T(x,0) = T_o(x) \quad 0 < x < L$$

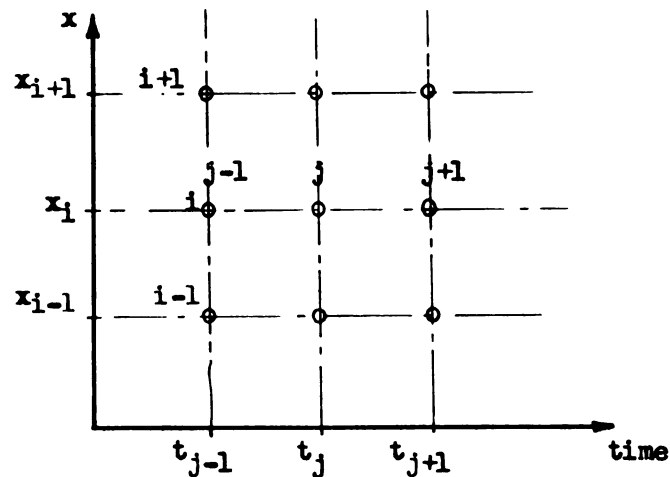
(6.4.1)





(A)

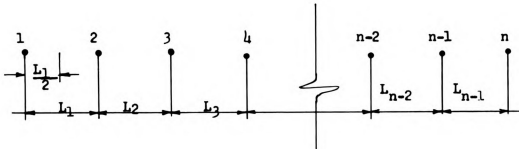
The Mathematical Model for the Soil-Pavement System



(B)

Representation of the nodal points in finite-difference method.

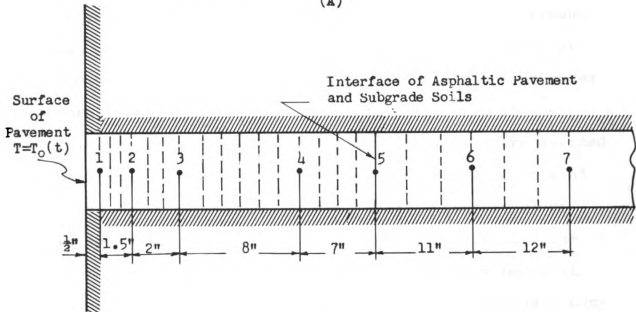
Figure 6.4.1 Soil-pavement system



Nodes 1 and n used as boundary conditions

Nodes 2 through n-1 used to improve difference approximation

(A)



(B)

Figure 6.4.2 Location of thermocouples, regions and nodes in the soil-asphalt system

$$-K_1 \left. \frac{\partial T(x,t)}{\partial x} \right|_{L^-} = K_2 \left. \frac{\partial T}{\partial x} \right|_{L^+}, \quad T(L^-,t) = T(L^+,t) \quad x = L$$

(6.4.2)

$$\frac{\partial}{\partial x} (K_2 \frac{\partial T}{\partial x}) = (\rho C_p)_2 \frac{\partial T}{\partial t}, \quad \left. \frac{\partial T(x,t)}{\partial x} \right|_{x \rightarrow \infty} = 0 \quad L < x < \infty$$

(6.4.3)

The surface temperature  $T(0,t)$  is assumed to be known and the heat flux  $q(t)$  has been calculated using experimental temperature data. The convective and radiative boundary condition may be employed. The pavement was divided into a number of equal thicknesses such as shown in Figure 6.4.2. Since the temperature fluctuates more in the upper layers of the pavement than in the lower layers, the regions in the upper layers are divided into smaller nodes than the lower regions. Each one of these subdivisions represents a finite control volume which may be denoted as a nodal point at (or near) the center of the volume. The first and the last nodes (1 and  $n$  in Figure 6.4.2A) are utilized as the boundary conditions, while the internal nodes (nodes no 2,3,4, ...,  $n-1$ ) are employed to improve the finite difference approximation. The temperature at the nodal point  $x_i$  at the time  $t_j$  is denoted by:

$$T(x_i, t_j) = T_i^j$$

(6.4.4)

Guided by the indexing scheme shown in Figure 6.4.1b, an approximation to Equation 6.4.1 at nodal point  $(x_i, t_{j+1/2})$  is shown by:

$$\left. \frac{\partial}{\partial x} \left( K \frac{\partial T}{\partial x} \right) \right|_i^{j+1/2} = \rho C_\rho \left. \frac{\partial T}{\partial t} \right|_i^{j+1/2} \quad (6.4.5)$$

Following the finite difference procedure, the resulting equation in finite difference form may be written as (48):

$$\begin{aligned} (\rho C_\rho)_i^j \frac{T_i^{j+1} - T_i^j}{\Delta t} = & \eta \frac{K_{i-1/2}^j (T_{i-1}^{j+1} - T_i^j) + K_{i+1/2}^j (T_{i+1}^{j+1} - T_i^{j+1})}{(\Delta x)^2} \\ & + (1-\eta) \frac{K_{i-1}^j (T_{i-1}^{j+1} - T_i^j) + K_{i+1/2}^j (T_{i+1}^j - T_i^j)}{(\Delta x)^2} \end{aligned} \quad (6.4.6)$$

where  $i$  indicates position and  $j$  indicates the time step.  $K_{i-1/2}^j$  is the thermal conductivity at a temperature equal to  $\left[ T_{i-1}^j + T_i^j \right] / 2$

• A forward difference, backward difference, or Crank-Nicolson technique is specified by setting the variable  $\eta$  to be equal to 0.0, 1.0, or 0.5, respectively (48).

Thermal properties of asphalt concrete are given in Tables 4.4.1 and 4.4.2. It can be assumed that the properties are constant for each seasonal temperature range. Equation 6.4.6 for constant  $K$  and  $\rho C_\rho$  may be written as:

$$\Delta_j T_i^j = r[\eta \delta_i^2 T_i^{j+1} + (1-\eta) \delta_i^2 T_i^j] \quad (6.4.7)$$

where  $r = \alpha \Delta t / (\Delta x)^2$  and,  $\Delta_j$  and  $\delta_i$  are the forward and central difference operators, respectively. Forward difference and second central difference of  $T_i^j$  are here defined as following:

$$\Delta_j T_i^j = T_i^{j+1} - T_i^j \quad (6.4.8)$$

$$\delta_i^2 T_i^j = T_{i-1}^j - 2 T_i^j + T_{i+1}^j \quad (6.4.9)$$

Equation 6.4.7 reduces to the solution of a set of algebraic equations which should be solved simultaneously. The result would be the calculated temperature at each nodal point as a function of time.

## 6.5 Computer Program

The process of simultaneously solving the set of equations 6.4.7, has been employed in the Property Program which may be used to obtain temperature at various depths of the pavement and underlying subgrade soils. (The computer program has been described in Chapter IV.) This program was run on the IBM 3600.

The program utilizes the pavement surface temperature as the time-dependent boundary condition to calculate temperature at various depths of the pavement. This program may be used to calculate temperature in a homogeneous as well as composite media and multilayered

bodies such as a soil-pavement system. In order to calculate temperature at various depths of a multilayer pavement, the thermal properties and the thickness of each layer should be given as the input to the program.

The latent heat of fusion was not taken into account, thus, the temperature is calculated if no change of state takes place; there is a method that can be used with the program to simulate phase-change, however.

#### 6.5.1 Input

The program requires two sets of main input; the initial and the boundary conditions. The initial temperature condition may be found by plotting the measured temperature of the pavement and subgrade soils versus depth at  $t = 0$ .

However, no information can be found for initial pavement temperature unless the pavement is monitored. The measured surface temperatures are utilized as the boundary condition to the model. The thermal properties of pavement and subgrade soils should be included in the input. As seen in Tables 4.4.1 and 4.4.2, the thermal properties of wearing course, binder course, and base course, are different. Consequently, the pavement should be divided into several regions with various thermal properties. The thermal properties of subgrade soils are assumed to be uniform in depth. The length of each region, the number of nodes in each region, and other

variables which were utilized as input in estimating properties are also included in the input.

#### 6.5.2 Output and Results

The program outputs the time step and calculated temperatures, for various locations. A sample of output which contains time steps, the measured surface temperature, and the calculated temperature at 2, 4, 8, 12, 15.5, and 19 inches below the surface of the pavement, is given in Tables 6.5.1 and 6.5.2. The calculated and measured temperatures are compared in Figure 6.5.1 for a few summer days. Calculated temperature at various depths of the pavement during a few summer days are plotted in Figure 6.5.2 (see the results and discussion in Chapter VII).

Table 6.5.1 Calculated temperature at various depths of the pavement during a few winter days

Time Steps	Measured Surface Temp	Location of Calculated Temperature				
		2"	4"	8"	12"	15.5"
1.5000	17.9500	20.5366	22.6745	25.7646	28.9998	31.0893
2.5000	16.3500	18.7730	21.4437	25.4958	28.4946	30.4242
3.5000	14.7500	17.3411	20.3233	24.8091	27.9655	29.8928
4.5000	13.2500	15.9891	19.1631	23.9960	27.3590	29.3786
5.5000	12.2500	14.8110	18.0190	23.1210	26.6999	28.8492
6.5000	11.5000	14.0815	17.1817	22.2750	26.0123	28.2985
7.5000	10.6000	13.1731	16.3153	21.4934	25.3332	27.7352
8.5000	10.1000	12.4786	15.5314	20.7322	24.6681	27.1710
9.5000	9.8000	12.0912	14.9799	20.0422	24.0213	26.6105
10.5000	9.4500	11.6594	14.4711	19.4375	23.4132	26.0624
11.5000	9.1500	11.2928	14.0205	18.8849	22.8458	25.5359
12.5000	8.9500	10.9787	13.6141	18.3790	22.3150	25.0336
13.5000	8.5500	10.6734	13.2718	17.9208	21.8193	24.5567
14.5000	7.8500	10.0573	12.7634	17.4715	21.3551	24.1056
15.5000	7.3500	9.4862	12.2074	16.9843	20.9005	23.6753
16.5000	7.1000	9.1437	11.7731	16.5025	20.4463	23.2565
17.5000	7.3500	9.0458	11.4685	16.0709	20.0069	22.8479
18.5000	7.9000	9.4068	11.5086	15.7498	19.6035	22.4563
19.5000	8.9500	9.9152	11.6689	15.5649	19.2662	22.0949
20.5000	10.5000	11.1026	12.3127	15.5487	19.0109	21.7785
21.5000	12.8500	12.5806	13.1772	15.7466	18.8693	21.5232
22.5000	15.2500	14.8076	14.7050	16.2101	18.8648	21.3482
23.5000	16.7500	16.1957	15.9482	16.8906	19.0280	21.2742
24.5000	17.2500	17.1702	16.9969	17.5811	19.3117	21.3082
25.5000	16.5000	16.9407	17.2962	18.1389	19.6443	21.4267
26.5000	15.0000	16.1139	17.0605	18.4128	19.9339	21.5890
27.5000	13.7500	14.9178	16.3252	18.3865	20.1126	21.7440
28.5000	13.5000	14.5238	15.8754	18.1847	20.1584	21.8521
29.5000	13.7500	14.5370	15.7169	18.0191	20.1281	21.9027
30.5000	13.5000	14.5889	15.7590	17.9479	20.0880	21.9166
31.5000	11.7500	13.5831	15.3107	17.8615	20.0590	21.9168
32.5000	9.0000	11.5760	14.1233	17.5259	19.9811	21.9021
33.5000	6.7500	9.4331	12.5147	16.8578	19.7674	21.8385
34.5000	5.5000	8.1076	11.2258	16.0232	19.3944	21.6891
35.5000	4.7500	7.1934	10.2373	15.2266	18.9274	21.4502
36.5000	4.5000	6.6905	9.5479	14.5282	18.4347	21.1478
37.5000	4.7500	6.6073	9.1757	13.9680	17.9607	20.8123
38.5000	5.0000	6.7656	9.0889	13.5733	17.5394	20.4718
39.5000	5.2500	6.8047	8.9940	13.2978	17.1888	20.1496
40.5000	5.7500	7.1207	9.0766	13.1013	16.8978	19.8576
41.5000	6.2500	7.4774	9.2510	13.0024	16.6662	19.5996
42.5000	7.2500	8.0425	9.5243	12.9805	16.4948	19.3802
43.5000	9.5000	9.4547	10.2607	13.0962	16.3882	19.2029
44.5000	12.5000	11.7768	11.7142	13.5050	16.3918	19.0804



Table 6.5.2 Calculated temperature at various depths of the pavement during a few summer days

Time Steps	Measured Surface Temp	Location of Calculated Temperature					
		2"	4"	8"	12"	15.5"	19"
1.5000	98.0000	84.4384	79.0909	77.6093	77.5063	77.5006	77.5000
2.5000	110.0000	99.2636	89.0228	79.5242	77.7481	77.5354	77.5040
3.5000	114.0000	105.8366	95.7154	83.3068	78.8285	77.7938	77.5513
4.5000	109.5000	105.9524	98.8224	86.7969	80.5786	78.4567	77.7399
5.5000	98.5000	99.7713	97.4228	88.9336	82.3971	79.4250	78.1294
6.5000	88.0000	91.2683	92.7873	89.1777	83.7513	80.4557	78.6774
7.5000	82.0000	85.3602	88.1617	87.9720	84.3460	81.2958	79.2747
8.5000	78.5000	81.7283	84.7096	86.2733	84.2694	81.8007	79.7994
9.5000	75.5000	78.8299	81.9941	84.5857	83.7939	81.9762	80.1734
10.5000	73.0000	76.2204	79.5761	82.9769	83.1174	81.9007	80.3779
11.5000	75.0000	75.5493	77.8724	81.4724	82.3323	81.6475	80.4293
12.5000	85.5000	80.8396	79.2688	80.5475	81.5475	81.2762	80.3544
13.5000	99.5000	91.3351	84.8888	81.1226	81.0604	80.8873	80.1904
14.5000	110.0000	100.8994	91.8649	83.4091	81.2494	80.6622	80.0054
15.5000	114.0000	106.7584	97.7296	86.5779	82.2017	80.7745	79.8999
16.5000	110.0000	106.7933	100.4527	89.5669	83.6589	81.2654	79.9612
17.5000	99.5000	101.0298	99.0998	91.3736	85.1748	82.0270	80.2169
18.5000	89.0000	92.5233	94.4368	91.4301	86.2754	82.8485	80.6221
19.5000	82.5000	86.4236	89.7035	90.0673	86.6654	83.4977	81.0766
20.5000	78.5000	82.2240	85.8618	88.1751	86.4067	83.8315	81.4662
21.5000	76.0000	79.3947	82.9532	86.2500	85.7439	83.8469	81.7140
22.5000	73.5000	77.1012	80.6787	84.4906	84.8842	83.6151	81.7986
23.5000	75.0000	75.9206	78.7225	82.8788	83.9491	83.2163	81.7352
24.5000	85.0000	80.9674	79.9121	81.7860	83.0246	82.7141	81.5534
25.5000	98.5000	90.8770	85.1145	82.1591	82.3893	82.2002	81.2901
26.5000	108.5000	100.1640	91.8119	84.2037	82.4136	81.8491	81.0102
27.5000	111.0000	105.0792	97.1408	87.1131	83.1880	81.8300	80.8107
28.5000	105.0000	103.5680	98.8806	89.7080	84.4398	82.1814	80.7765
29.5000	95.0000	97.0011	96.5121	90.9507	85.6828	82.7821	80.9311
30.5000	87.0000	90.1866	92.2783	90.5764	86.4558	83.4079	81.2222
31.5000	82.7500	85.6697	88.4390	89.2049	86.5899	83.8484	81.5465
32.5000	79.5000	82.8141	85.6954	87.5904	86.2271	84.0130	81.8035
33.5000	75.7500	79.4387	82.9562	85.9923	85.5941	83.9289	81.9384
34.5000	72.0000	76.2033	80.2538	84.3137	84.7965	83.6585	81.9433

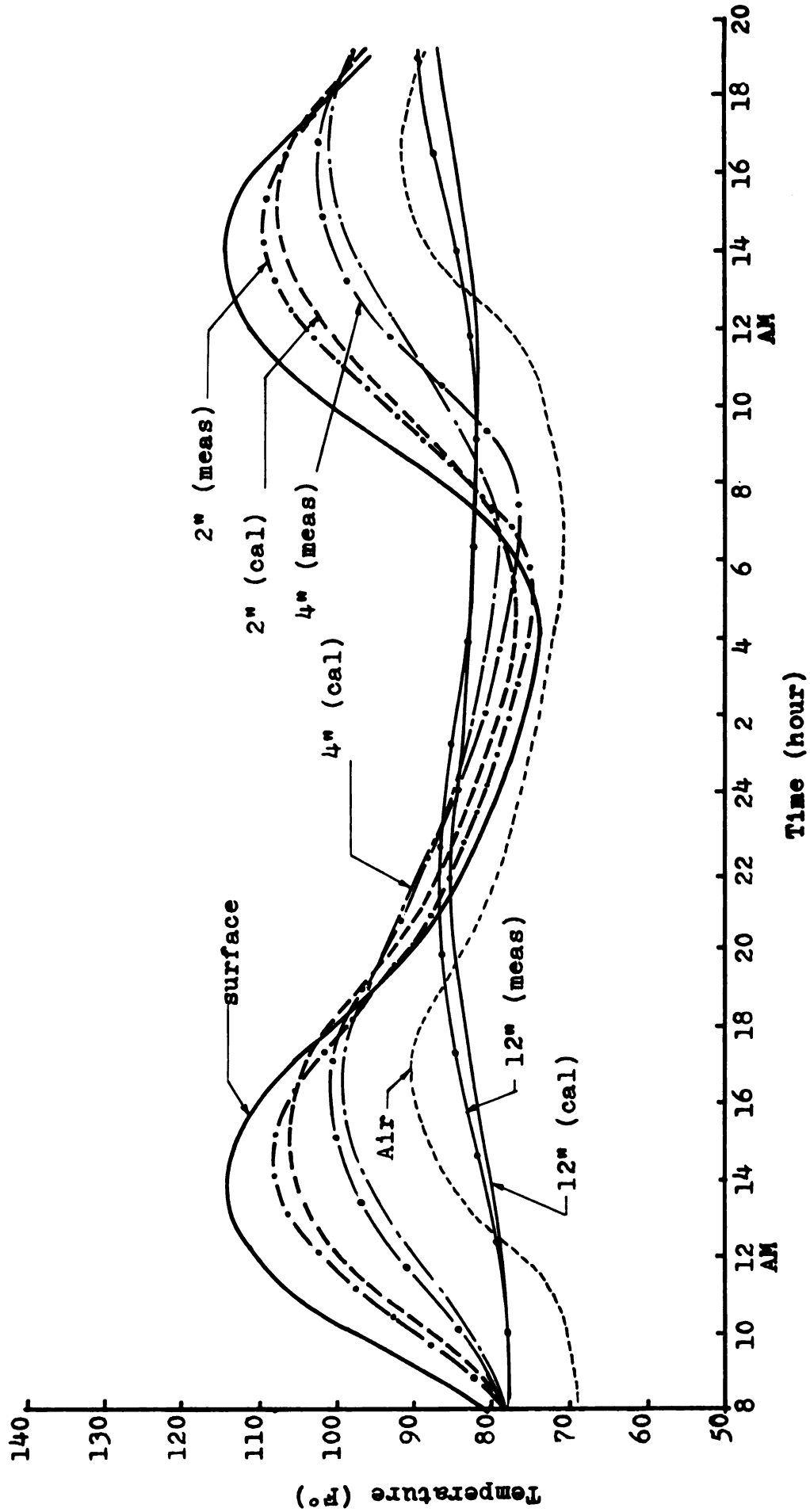


Figure 6.5.1 Calculated pavement temperature compared with measured temperature during the summer days

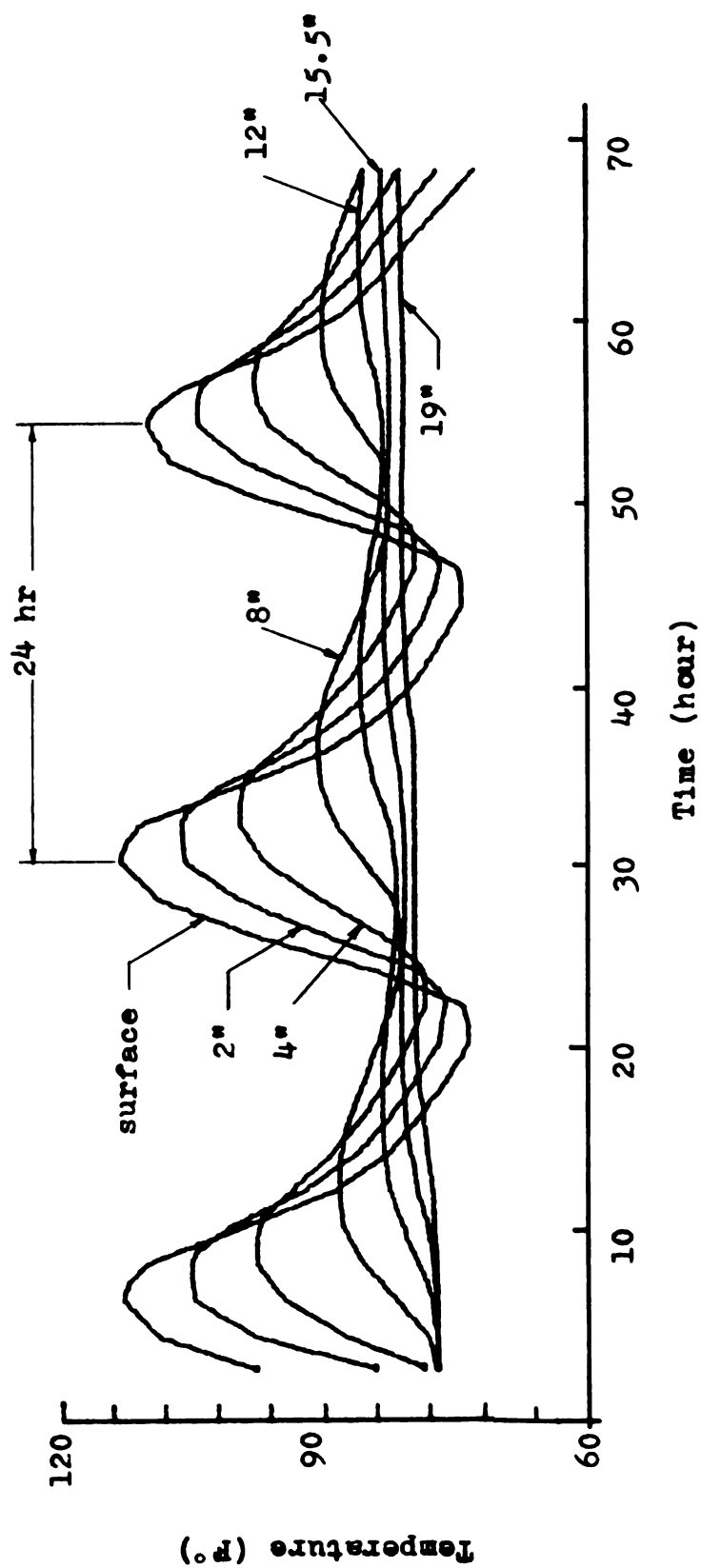


Figure 6.5.2 Calculated pavement temperature during summer (variable initial temperature)

## CHAPTER VII

### RESULTS AND DISCUSSION

The results and discussion are summarized under three headings: (1) Recorded Temperature Data, (2) Thermal Properties of Asphaltic Concrete, and (3) Pavement Temperature.

#### 7.1 Recorded Temperature Data

The analysis of temperature distribution data leads to the following observations.

During the summer months, the average temperature of the pavement decreases with increasing depth. However, during the winter months, this reverses. This may be observed from daily temperature distribution, as well as temperature profiles such as shown in Figure 5.9.2.

Temperature profiles were plotted from temperature distribution for several days during the summer, spring, and winter months. Available data in the section of literature review indicate that the soil beneath the asphalt pavement has approximately the same thermal properties as asphaltic concrete, thus it may be assumed that profile curves are

continuously smooth at the interface of soil-asphalt concrete.

During the summer months, temperatures ranging between 130°F and 140°F at the pavement surface occurred only 1 per cent of the time. During this period, the maximum temperature at a depth of 4 inches was 110°F and at 12 inches below the surface, 90°F.

It was observed that the surface and the few uppermost inches of pavement were greatly influenced by air temperature. However, at lower depths in the pavement, variations in temperature decreased, until a depth was reached at which the temperature was approximately constant. The deeper layers of the pavement remained fairly constant for a long period of time, while the surface layers fluctuated with the daily temperature cycles. This phenomena produced the crossing and overprinting of individual points. The recorded temperature data were usually congested especially during the cloudy and rainy days, since frequently the entire profile was at nearly the same temperature. Frequently it was impossible to determine the time of peak temperature at a given depth.

Time lag between maximum and minimum temperatures at various pavement depths was another interesting phenomenon which may be observed from daily temperature distribution curves. This time lag is not constant but increases with the depth of the recording in the pavement.

On a sunny summer day the maximum temperature occurred on the pavement surface at approximately 4:00 P.M., while the maximum temperature at a depth of 12 inches below the surface of the pavement was at 12:00 P.M., and at a depth of 19 inches maximum temperature occurred at 6:00 A.M. of the following day. The time lag of temperature was also true for winter days and minimum pavement temperature at each depth. Observation of daily temperature distribution supports the validity of the assumption of sinusoidal variation of daily air and surface temperature, which has been adapted by many investigators (28, 40).

The daily variation of the air and pavement surface temperature are graphically presented in Figures 2.7.6 and 2.7.7 for various seasons. These figures indicate that pavement surface temperature was generally warmer than air temperature during both summer and winter. This was due to solar radiation which has a greater heating potential than does the air in the summer and due to warmer pavement with negligible radiation input in the winter. This fact is also observed from curves of cumulative degree-days based on both air and pavement surface temperature (see Figures 2.10.1 and 2.10.2).

The observation of the temperature distribution in a 7-inch and a 19-inch pavement indicates that under the same surface temperature there is no significant difference between the temperature at depths of 2, 4, or 7 inches, and both sections behaved in the same manner. From the

observation of the Alger Road temperature data, we concluded that during the freezing season the temperature of subgrade soils beneath the asphaltic pavement was higher than in the underlying gravel section.

The higher temperature of the subgrade under the asphaltic pavement was mainly due to the absorption of solar radiation. A comparison between recorded temperature data at Bishop Airport and Alger Road, indicates that during the freezing seasons, under the same surface temperature, the temperature beneath the 19-inch full-depth pavement is higher than the 7-inch pavement.

The result of the evaluation of air and surface freezing index at the thermocouple installation site are illustrated in Figure 2.10.2. The values of freezing index derived from the annual climatological data for the Flint area during the last twenty years varies from year to year, but generally freezing indexes were higher than the value obtained from the recorded temperature data at Bishop Airport during 1969-70. The pavement surface freezing index was much less than the air freezing index. As a result, a small value of correlation factor "n" equal to 0.51 is obtained. The comparison between this value and the values recommended by Aldrich et al. (3) and Oosterbaan et al. (41) lead to the conclusion that the adoption of the obtained correlation factor would be entirely unjustified for the purpose of frost

depth prediction beneath the flexible pavements for central Michigan. The significant difference between the calculated air freezing index and the average of the air freezing index derived from the National Weather Service's records indicates the need for a more extensive and accurate study of pavement temperature variation for design purposes.

## 7.2 Thermal Properties of Asphaltic Concrete

Despite the vast quantities of recorded temperature data, very little were of use in thermal property determination. This was because not all of the recorded temperature data was discernible. The values of thermal property calculated from both the field and laboratory experimental temperature data by the nonlinear estimation method and simplified method discussed earlier, are presented in Tables 4.4.1, 4.4.2, 5.9.2, and 5.9.3.

The property calculated most independently was the thermal diffusivity  $\alpha$  since the heat flux need not be given to obtain  $\alpha$ . It should be pointed out that the pavement was not homogeneous but consists of several layers of asphaltic concrete with various aggregate sizes and asphaltic contents. The thermal properties of each layer were obtained by utilizing the temperature history of the upper and the lower interfaces. The temperature history of the upper boundary was used as the driving boundary condition and that of the lower one, as the data.



The estimated thermal property of the upper two layers (referred to as the wearing and the binder courses) are shown in Tables 4.4.2 and 5.9.2. Tables 4.4.1 and 5.9.3 give the thermal properties of the entire depth of the pavement obtained from temperature field data.

Calculated thermal properties for upper layers of the pavement, estimated from recorded temperature data, are more reliable than those of the deeper layers. This is because both methods used in the estimation of the thermal properties require a discernible temperature change within a given layer. For the top layers, the daily temperature cycle usually produces sufficient fluctuation, while this change does not occur daily or even monthly for deeper layers.

The values of thermal properties for upper layers of the pavement were more consistent than those for the lower layers, while these values for deeper layers exhibit a wider variation in magnitude. Generally the thermal diffusivity of the wearing and binder courses were higher than those of the base courses. The calculated values from field data appear to vary widely from day to day. However, certain of these variations are expected, due to various ambient conditions and seasonal changes. Calculated thermal properties are plotted versus temperature in Figures 7.2.1 and 7.2.2.

A comparison of the calculated thermal diffusivity from field and experimental data indicates the calculated

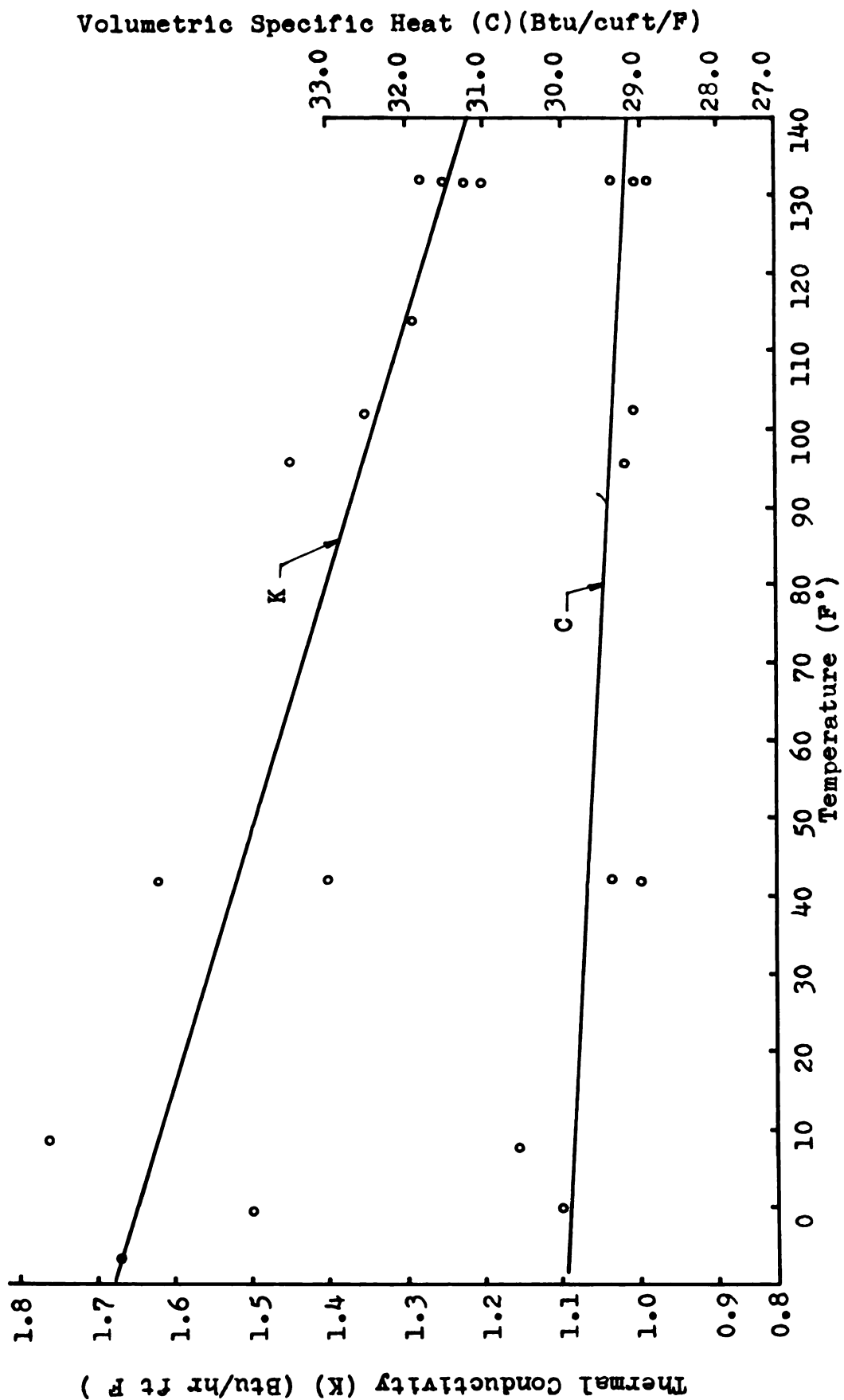


Figure 7.2.1 Calculated thermal conductivity and volumetric specific heat from laboratory data

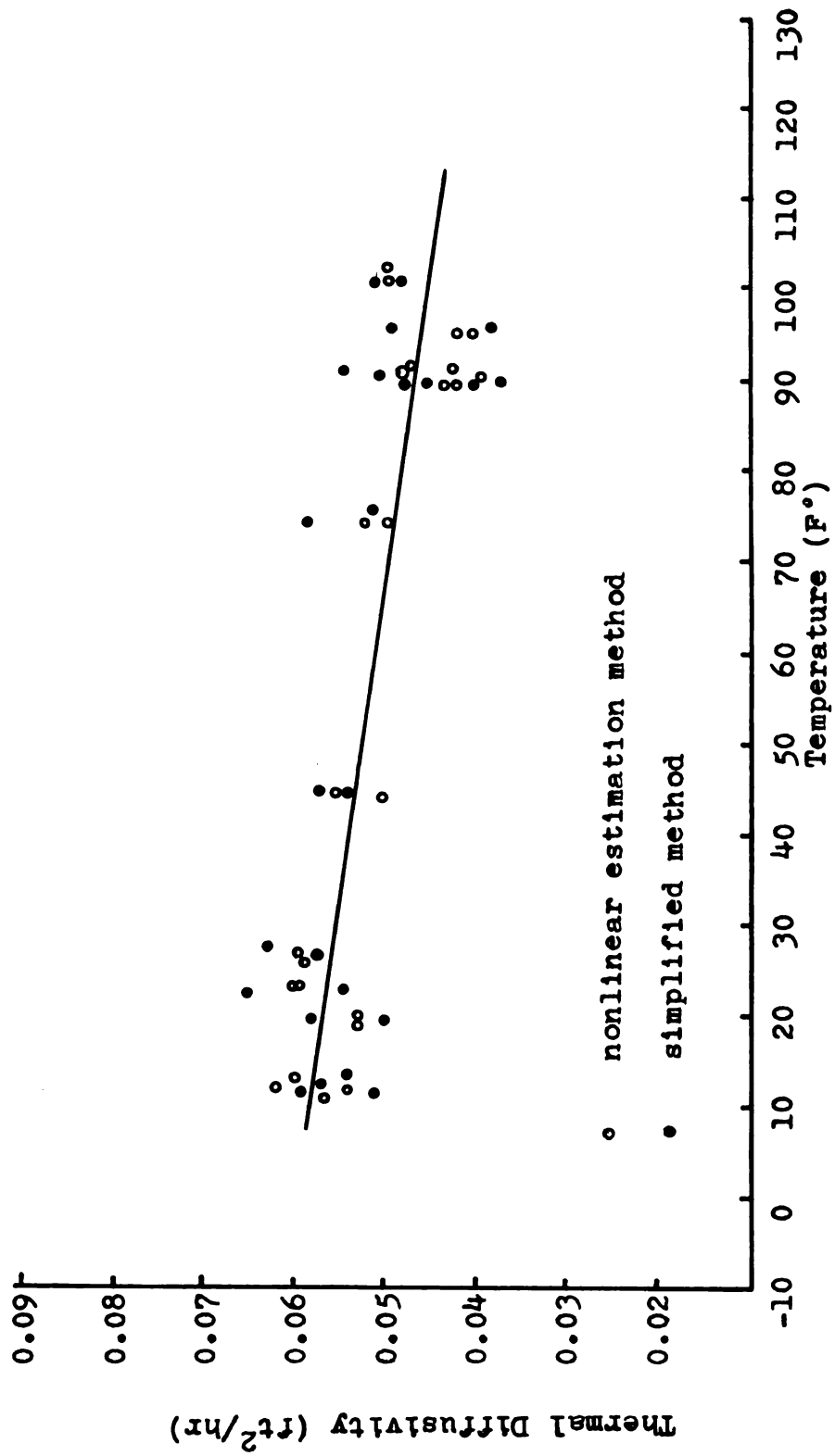


Figure 7.2.2 Calculated thermal diffusivity of asphaltic concrete from recorded field data

thermal diffusivity from field temperature data are slightly higher than those calculated from experimental data.

The discrepancy between the laboratory and field data may exist because the laboratory data was collected under a controlled condition while the recorded temperature data was obtained under the natural ambient condition. Laboratory conditions may be controlled to measure the effect of a single variable (e.g., moisture), under a specified form of heat transform, while in nature the processes of the inflow and outflow heat transfer do not lend themselves readily to theoretical heat transfer analysis. It should be pointed out, however, that the laboratory experimentations gave an explanation of the phenomena and thus provide a basis for interpreting field results. Moreover, the theory of heat transfer deals with a dry homogeneous substance subjected to a known heat source.

A comparison between the contents of Tables 4.4.1, 4.4.2, 5.9.2, and 5.9.3 indicates that there is not a significant difference between the calculated thermal properties by the two methods of calculation. The properties obtained by the nonlinear estimation method appear to be much more consistent than those calculated by the simplified method.

The nonlinear estimation method is an iterative search procedure which requires an initial estimation of

thermal properties as well as a considerable amount of computer time, while the simplified method does not. In terms of computing time, the simplified method is somewhat more advantageous than the nonlinear estimation method. The most important feature of nonlinear estimation method is its application to materials which have temperature-dependence thermal properties (7). Both methods eliminate the assumption of periodic surface temperature in estimating the thermal property of pavement materials. Pavement temperature under natural conditions may be utilized in both methods to estimate the thermal properties of pavement material. As a result, both methods have preference over the previously introduced method of estimating thermal properties which are limited to the periodic boundary condition (28, 40).

The estimation of thermal diffusivity by the simplified method is based on the assumption that the initial temperature is uniform. The discrepancy in the estimated thermal properties is due to the fact that the simplified method is quite sensitive to initial temperature. The lack of this condition being uniform necessitates the process of correcting the initial condition. The accurate correction for the initial temperature has been made, but a satisfactory mathematical treatment of the problem is time consuming and sometimes impractical.

The calculated thermal diffusivity of asphaltic concrete for the corrected and uncorrected initial condition is given in Table 5.9.3. A comparison between these two sets of values indicates that the correction for initial temperature is efficient. A criterion is derived for finding the optimum experiment as well as the location of the thermocouple and Laplace transform parameter "s" which is employed in the proposed method of estimation of thermal diffusivity. Further research is needed to consider the complex form of the Laplace transform parameter which reduces the effect of the initial condition in the estimation of thermal diffusivity.

In order to determine statistically whether the two sets of calculated thermal diffusivity differ significantly, their means and standard deviations should be compared. Since there were only two sets of data, the variance ratio test, known as the F-test, may be applied. The F value is calculated as (48),  $F = (s_1)^2 / (s_2)^2$ , where  $s_1$  and  $s_2$  are the estimated standard errors (variance) of sample 1 and 2, respectively. (Note that  $(s_1)^2$  should be greater than  $(s_2)^2$ .)

The critical values of F for various degrees of freedom and probability are given in the tabular form (pp. 306, ref. 48). The calculated variance ratio should not exceed the tabulated values for an insignificant

difference between two sets of data. The mean, as well as the variance of each set of data, are calculated and are given in Table 7.2.1. The calculated variance ratios are compared with the tabulated values at the 5 per cent level of significance in Table 7.2.1.

It is observed that for each set of data, the calculated F values were generally smaller than the tabulated values. The conclusion is that the two sets of calculated thermal properties do not differ significantly and they are in good agreement with a 95 per cent probability, though their mean values are different.

In the case of the obtained thermal properties from the laboratory temperature data, neither the mean values nor the results of the F-test show a significant difference between two sets of data calculated by two methods.

Similar conclusions as above were taken from the results of the F-test in comparing the values of thermal properties obtained by two methods under various ambient conditions and at two different locations. The results of the F-test are given in Table 7.2.1. Statistically, we can state that the data belong to the same population with a 95 per cent probability.

The thermal property values were determined for each test and the average value for all tests was used as the most realistic estimate. The average values of  $\alpha$

Table 7.2.1 Statistical comparison between the calculated thermal diffusivity of asphaltic concrete (analysis of the variance and F-test)

Pavement Course	Ambient Conditions	Mean Values		Variance ( $F^2 \times 10^{-6}$ )		Calculated F Values	Critical F Value
		Property Program	Alpha Program	Property Program ( $S_1$ ) <sup>2</sup>	Alpha Program ( $S_1$ ) <sup>2</sup>		
Wearing & Binder Course (Tables 4.2 & 5.8.2)	sunny	0.052	0.049	62.5	45.83	1.36	4.28
	cloudy	0.057	0.055	37.66	46.33	1.23	9.28
	rainy	0.062	0.058	8.00	13.00	1.60	161.4
	Alger Rd.	0.055	0.058	19.33	65.66	3.39	9.28
	sunny	0.049	0.049	73.83	77.33	1.05	4.28
	cloudy	0.051	0.053	8.33	25.66	3.08	9.28
Entire Pavement (Tables 4.1 & 5.8.3)	rainy	0.054	0.054	41.00	2.00	20.50	161.4
	Alger Rd.	0.049	0.053	51.00	120.00	2.35	9.28
	laboratory	0.049	0.049	75.56	115.90	1.60	4.16
Experi-mental Data (Tables 3.7.1 & 5.8.4)							



calculated by the nonlinear estimation method from recorded temperature data are 0.045 and 0.055 for summer and winter, respectively.

The obtained values from the simplified estimation method are 0.042 and 0.051. The calculated values of thermal properties by the estimation method were approximately 8 per cent higher than those of the simplified method. The calculated values of thermal conductivity,  $K$ , and volumetric specific heat,  $C = \rho C_\rho$  from experimental temperature and heat flux data are given in Table 3.6.2. The specific heat values  $C_\rho$  may be found from volumetric specific heat by utilizing the value of the density of asphaltic concrete. The density is relatively easy to measure and is much more insensitive to temperature change than either  $K$  or  $C_\rho$ , as mentioned in the section regarding the expansion coefficient of asphaltic concrete.

Though the small discrepancy is observed between the calculated thermal properties of asphaltic concrete by two methods, the obtained values are considerably higher than the assumed values (28, 2, 16). The accuracy of the values may be shown by comparing the calculated and measured pavement temperature distributions (see Figure 6.5.1). This result suggests the adoption of thermal diffusivity values considerably higher than the values which are generally in use in predicting the depth of frost penetration beneath flexible pavements for Central Michigan.

### 7.3 Pavement Temperature

The calculated temperature at various depths of the pavements are given in Tables 6.5.1 and 6.5.2 for summer and winter, respectively.

A good agreement was observed between the calculated pavement temperature by the finite difference method and the recorded temperature data both in summer and winter. For the purpose of comparison, the calculated and recorded pavement temperatures are plotted in Figure 6.5.1. The application of the finite difference method in calculating pavement temperature requires a realistic value of thermal properties of pavement material.

The results of the exact solution of Equation 6.2.2 indicate that the sine wave model for air and pavement surface temperature variation is a reasonable approximation in estimating subsoil temperature changes, as long as a proper sine wave frequency is selected. It was observed that the maximum depth at which daily variation of pavement surface temperature fluctuates is approximately between two to three feet, while the maximum depth of the annual variation does not exceed fifty to sixty feet. Below a depth of approximately three feet, temperature remains practically constant from day to day and is not subject to alternation due to change at the surface.

With the aid of the exact solution and finite difference methods, we may investigate the penetration

of periodic temperature waves in the pavement and underlying subgrades, the range or variation of temperature at various depths for the daily and annual changes, as well, as the rate of penetration and the time at which the maximum or minimum temperature may be.

## CONCLUSIONS

1. A full-depth pavement has the advantage of being a better insulator than asphaltic pavement.
2. The asphaltic pavements are good insulators that can stabilize the subgrade at a higher temperature than that of a gravel pavement during winter. Under the same surface temperature, the freezing line (32°F isotherm), generally penetrates to greater depths beneath the gravel section than the paved section.
3. There is little temperature variation at lower levels in the subgrade during a given twenty-four hour period, but several days of zero temperature does have a definite influence at all levels down to the subgrade.
4. The thickness of the pavement does not have a significant effect on the temperature of the upper-most inches of the pavement.
5. Snow has a significant insulating effect on the penetration of the frost depth and the subgrade

temperature remains at a higher temperature under a snow covered pavement.

6. The 140°F testing temperature of the standard Marshall Stability and Consistency Test is on the conservative side for the Central Michigan environment.
7. The temperature of 110°F should be considered for the laboratory testing temperature of lower course paving mixtures.
8. A simple method for calculating thermal conductivity,  $K$ , and specific heat,  $C$ , from the temperature and heat flux boundary conditions, is proposed.
9. A method is introduced to calculate the heat transfer coefficient  $h_c$  from recorded temperature data and thermal properties of pavement materials.
10. The nonlinear estimation procedure and the simplified method of calculating thermal properties of asphaltic concrete are satisfactory. Both methods are superior to the conventional methods which are limited to periodic surface temperature.
11. A good agreement is found between the calculated values of thermal diffusivity from field and laboratory temperature data.

12. It was found that thermal properties of asphaltic concrete are not constant, but vary with temperature. The thermal diffusivity of bituminous concretes obtained by two methods, was nearly equal and considerably higher than commonly assumed. For design purposes, values of thermal diffusivity of asphaltic pavement equal to 0.043 and 0.055 BTU/hr should be adapted for summer and winter, respectively. A value of 29.0 BTU/cu ft/°F should be adapted for volumetric specific heat of asphaltic concrete for both winter and summer.
13. The temperature in pavement and underlying soil subgrades may be accurately calculated using a modified Crank-Nicolson difference approximation applied to the heat conduction equation. A good agreement was found between the measured and calculated pavement temperatures.

#### Recommendations for Further Research

1. This study is the first step in evaluating the factors influencing the depth of the frost penetration beneath the pavement. Further research is needed in order to utilize the result of this study in developing a reliable method for predicting the depth of frost penetration for pavement design purposes.

2. The geographic area of this study was limited to two locations in central Michigan. In order to determine the validity of the result, this study should be extended to other locations and areas other than the state of Michigan.
3. The measurement of temperature data should be accompanied by the measurement of the moisture content of subgrade soils. It would be possible to install a continuous moisture content monitor of a resistivity type along with the thermocouples in the pavement and underlying subsoil to record the variation of moisture content at various depths. Variation of soil moisture is required in the estimation of thermal properties of subgrade soils as well as the study of the migration of moisture beneath pavements.
4. The process of data collection should be accompanied by the measurement of the solar radiation which is a governing factor in increasing the pavement surface temperature. Solar radiation data are required in studying the relationship between surface and air temperature.
5. The effect of latent heat of fusion is not taken into account, thus, the temperature is calculated if no change of state takes place. In practice, the problem involves the change of state due to

either melting or freezing. This study should be extended to include the effect of the latent heat of fusion in determining pavement temperature in freezing seasons.

6. The studies of the thermal properties of pavement material should be continued with emphasis being placed on the determination of the thermal properties of granular base and subbase materials.
7. The simplified method of estimating thermal properties is quite flexible and can be extended or modified with little difficulty. A few possible improvements and extensions are as follows:
  - a. The accuracy of the procedure may be improved by weighting the measured temperature data which are utilized as the boundary condition and data. The assumed value of weighting factor equal to one was selected for simplification.
  - b. The procedure should be extended to eliminate the assumption of uniform initial temperature.
  - c. In deriving a criterion for finding the optimum Laplace transform parameter, utilized in the simplified method, only positive and non-imaginary values of "s" are considered.



Further research is needed to consider negative, as well as complex forms of the Laplace transform parameters.

## BIBLIOGRAPHY

## BIBLIOGRAPHY

1. Abraham, H., Asphalt and Allied Substances, vol. 2, D. Van Nostrand Company, New York, N.Y.
2. Aldrich, Hart, P., Jr., "Frost Penetration Below Highway and Airport Pavements," Bulletin 135, Highway Research Board, 1956.
3. Aldrich, H. P. and Paynter, H. M., Analytical Studies of Freezing and Thawing of Soils, First Interim Report, Artic Construction and Frost Effects Laboratory, Corps of Engineers, 1953.
4. Ames, W. F., Nonlinear Partial Differential Equation In Engineering, Academic Press, New York, 1965.
5. Barber, E. S., "Calculations of Maximum Temperatures from Weather Reports," Bulletin 168, Highway Research Board, 1957.
6. Beck, J. V., "Optimum Transient Thermal Properties," Unpublished paper.
7. Beck, J. V., "The Optimum Analytical Design of Transient Experiments for Simultaneous Determinations of Thermal Conductivity and Specific Heat," Ph.D. Dissertation, Mechanical Engineering Dept., Michigan State University, East Lansing, Mich., June 1964.
8. Beck, J. V. and Dhank, A. M., "Simultaneous Determinations of Thermal Conductivity and Specific Heat," ASME Paper No. 65-HT-14. Presented at the ASME-AICHE Heat Transfer Conference, Los Angeles, Cal., August 1965.
9. Beskow, G., "Scandinavian Soil Frost Research of the Past," Highway Research Board, Proceedings, 1947.

10. Birch, F. and Clark, H., "The Thermal Conductivity of Rocks and Dependence Upon Temperature and Composition," Amer. Jour. Sci., 238, 1940.
11. Callendar, H. L. and McLeod, C. H., "Observations of Soil Temperature with Electrical Resistance Thermometers," Transactions, Royal Society of Canada, Second Series, vol. 2, sec. III.
12. Carlson, H. and Kersten, M. S., "Calculation of Depth of Freezing and Thawing Under Pavements," Bulletin 71, Highway Research Board, 1953.
13. Carslaw, H. S. and Jaeger, J. C., Conduction of Heat in Solids, Clarendon Press, Oxford, 1959.
14. Carson, J. E., "Analysis of Soil and Air Temperatures by Fourier Techniques," Journal of Geophysical Research, vol. 68.
15. Chudnoviskii, A. F., Heat Transfer in the Soil (translated from the Russian), Israel Program for Scientific Translations, Jerusalem.
16. Departments of the Army and the Air Force, Calculation Methods for Determination of Depths of Freeze and Thaw in Soils, Department of the Army Technical Manual TM 5-852-6, Department of the Air Force Manual AFM 88-19, 1966.
17. Erwin Kreyszig, Advanced Engineering Mathematics, John Wiley and Sons, New York, N.Y., 1962.
18. Farouke, P. T., "Physical Properties of Granular Materials with Reference to Thermal Resistivity," Highway Research Record, 128, Highway Research Board.
19. Fewell, R. B., "Cold Quantities in West Virginia," Master of Science Thesis, Civil Engineering Dept., West Virginia University.
20. Finn, F. N., "Factors Involved in the Design of Asphaltic Pavement Surface," National Cooperative Highway Research Program, Report 39, Highway Research Board, 1967.
21. Fowle, F. E., Journal of Astrophysics, vol. 42, 1915.
22. Gemant, A., "How to Compute Thermal Soil Conductivity," Heating, Piping, and Air Conditioning, January, 1952.

23. Gilman, G. D., "The Freezing Index in New England," Special Report 63, Corps of Engineers, U.S. Army, 1964.
24. Heley, W., "A Field Evaluation of the Thermal Properties of West Virginia Highway Materials," unpublished report, 1967.
25. Hogbin, L. B., "The Heat Capacity of Some Road Materials," Res. Note No. RN/4082/LBR, Brit. Road Res. Lab., November 1961.
26. Hooks, C. C. and Goetz, W. H., "Laboratory Thermal Expansion Measuring Techniques Applied to Bituminous Concrete," Report to U.S. Army Engineers, Waterways Experiment Station, Vicksburg, Miss., by Purdue University, August 1964.
27. Johnson, A. W. and Lovell, C. W., "Frost Action Research Needs," Bulletin 71, Highway Research Board.
28. Jumikis, A. R., The Frost Penetration Problem in Highway Engineering, Rutgers University Press, New Brunswick, New Jersey, 1955.
29. Kallas, B. F., "Asphalt Pavement Temperature," Highway Research Record No. 150, Highway Research Board.
30. Kimball, H. H., Monthly Weather Review, vol. 55, 1927; vol. 56, 1928; vol. 59, 1931.
31. Kersten, Miles S., "Thermal Properties of Soils," Experiment Station Bulletin No. 28, University of Minnesota, Institute of Technology, 1949.
32. Mack, C., "Physical Chemistry," in Bituminous Materials: Asphalts, Tars, and Pitches, vol. I, A. J. Hoiberg, ed., Interscience, 1964.
33. Makowski, M. W. and Mochlinski, K., "An Evaluation of Two Rapid Methods of Assessing the Thermal Resistivity of Soil," Proceedings, Institution of Electrical Engineers, vol. 103, part A, 1956.
34. Manz, G. P., "Study of Temperature Variation in Hot Mix Asphalt Base, Surface Course and Subgrade," Highway Research Record, 150, Highway Research Board.

35. Mickley, A. S., "The Thermal Conductivity of Moist Soil," Trans. American I.E.E. Tech. Paper 51-326.
36. Mitchell, L. J., "Thermal Expansion Tests on Aggregates, Neat Cement and Concrete," Proc. ASTM, vol. 53, 1953.
37. Monismith, C. L., Secor, G. A. and Secor, K. E., "Temperature Induced Stresses and Deformation in Asphalt Concrete," Proceedings of the Association of Asphalt Paving Technologists, vol. 34, 1965.
38. Moulton, L. K., "Prediction of the Depth of Frost Penetration in West Virginia for Pavement Design Purposes," Ph.D. Dissertation, West Virginia University, 1968.
39. Necati, Ozisik M., Boundary Value Problems of Heat Conduction, International Textbook Company, Scranton, 1968.
40. O'Brien, J. D., "Thermal Properties of West Virginia Highway Materials," Master of Science Thesis, Civil Engineering Dept., West Virginia University.
41. Oosterbaan, M. D. and Leonards, G. A., "Use of Insulating Layers to Attenuate Frost Action in Highway Pavements," Highway Research Record No. 101, Highway Research Board, 1965.
42. Penner, E., Canadian Journal of Earth Science, 7.982, 1970.
43. Przybycien, F. E., "Bituminous Pavement Temperature Related to Climate," Highway Research Record No. 256, Highway Research Board, 1968.
44. Scott, R. F., Heat Exchange at the Ground Surface, Cold Regions Research and Engineering Laboratory, U.S. Army Material Command, Report 11-A1, 1964.
45. Saal, R. N. J., "Physical Properties of Asphaltic Bitumen," Chapter 2 in The Properties of Asphaltic Bitumen, ed. by J. P. H. Pfeiffer, Elsevier Publishing Company, Inc., New York.
46. Trott, J. J., "An Apparatus for Recording the Duration of Various Temperatures in Roads," Road and Road Construction, vol. 41, no. 491, pp. 342-345, 1963.

47. Troxell, G. E. and Davis, G. E., Composition and Properties of Concrete, McGraw-Hill, New York, 1956.
48. Draper, N. R. and Smith, H., Applied Regression Analysis, John Wiley and Sons, Inc., New York, 1966.
49. Özişik, M. Nicati, Boundary Value Problems of Heat Conduction, International Textbook Co., New York, 1968.
50. Martinus, VanRooyen and Winterkorn, Hans F., "Theoretical and Practical Aspects of the Thermal Conductivity of Soils and Similar Granular System," Highway Research Board Bulletin 168, 1957.

## APPENDIX 1



## APPENDIX 1

### LIST OF INPUT AND DEFINITION OF TERMS USED IN "ALPHA" PROGRAM

Card 1   FORMAT (3 F 10.0, 3 I 10)

Case, Date, DT, NTIME, NTC, NS

CASE-Case number, any number desired

example 2.0

DATE-date or any number

example 6.24

DT-Time steps of measuring data

example 1.0 hour

NTIME-Number of times of data

For example, we might have measurements at

0.0, 1.0, 2.0, 3.0, hours, hence, NTIME=4

NTC-Number of thermocouples when data is given

example: for two internal thermocouples, NTC=2

NS-Number of Laplace transform parameters

For example: parameter s might have values of

0.1, 0.2, 0.3, hence, NS=3

Card 2 FORMAT (8 F 10.5)

X(I), I=1, NTC

X(I) = depth dimension which is denoted in the vertical distances between the thermocouples.

For example, if thermocouples are located at the surface and at 2", 4", and 8" below the surface of the pavement,

X(I)=0.0 0.166 0.333 0.666

Card 3 FORMAT (8 F 10.5)

S(J), J=1, NS

S(J) = values of Laplace transform parameter.

For example, parameter s might have values of 0.1, 0.2, 0.3, S(J) = 0.1 0.2 0.3

Card 4 FORMAT (8 F 10.5)

T (JJ,N), JJ=1, NTC, N=1, NTIME

T (JJ,N) = represents the temperature measured by JJ thermocouples at N different times. Each set of thermocouples data should be stacked together and placed one behind the other

Card 5 FORMAT (8 F 10.5)

TI (IT), IT=1, NTC

TI = initial temperature distribution

It is assumed that the temperature is uniform throughout the pavement. If it is not so, it should be corrected for initial

condition according to section 5.8.

For example:

$TI(IT) = 45.0 \ 45.0 \ 45.0$

```

// JOB
// FOR KAVI
*NONPROCESS PROGRAM
*10CS(CARD,1443 PRINTER)
*LIST SOURCE PROGRAM
*ONE WORD INTEGERS
C PROGRAM ALPHA
C THIS PROGRAM CALCULATES THERMAL DIFFUSIVITY UTILIZING LAPLACE TRANSFORM.
C * * * * *
C DIMENSION T(7,150),X(7),S(15),TI(7),SUP(7,10)
1 CONTINUE
  READ(2,100) CASE,DATE,DT,NTIME,NTC,NS
  IF (CASE) 1000,1000,2
2 CONTINUE
100 FORMAT (3F10.5,3I10)
   WRITE(3,101)
101 FORMAT (6X,CASE,6X,DATE,6X,DT,5X,NTIME,7X,NTC,8X,NS)
   WRITE(3,102) CASE,DATE,DT,NTIME,NTC,NS
102 FORMAT (2F10.5,3I10)
   READ(2,110) (X(I),I=1,NTC)
110 FORMAT (8F10.0)
   WRITE(3,111)
111 FORMAT (6X,X(1),I=1,NTC)
   WRITE(3,112) (X(I),I=1,NTC)
112 FORMAT (8F15.5)
112 FORMAT (F10.5,2(10X,F10.4),4X,F10.2,2I10,F10.2)
   READ(2,110) (S(J),J=1,NS)
   WRITE(3,120)
120 FORMAT (6X,S(J),J=1,NS)
   WRITE(3,112) (S(J),J=1,NS)
   DO 130 JJ=1,NTC
     READ(2,110) (T(JJ,N),N=1,NTIME)
     WRITE(3,113)
113 FORMAT (6X,T(JJ,N),N=1,NTIME)
     WRITE(3,112) (T(JJ,N),N=1,NTIME)

```

```

130 CONTINUE
   READ(2,110) (TI(IT),IT=1,NTC)
   WRITE(3,114)
114  FORMAT(6X,TI(IT),IT=1,NTC)
   WRITE(3,112) (TI(IT),IT=1,NTC)
   DO 161 IA=1,NTC
   DO 160 IB=1,NTIME
     T(IA,IB)=T(IA,IB)-TI(IA)
140 CONTINUE
141 CONTINUE

   DO 199 J=1,NS
   DO 199 I=1,NTC
     SUM(I,J)=0.0
199 CONTINUE
   WRITE(3,201)
201  FORMAT(6X,TIME,16X,E,16X,SUM(ITC,IS),5X,S(IS),7X,ITM,7X,ITC)
   DO 200 IS=1,NC
     TIME=0.0
   DO 200 ITM=1,NTIME
     TIME=TIME+DT
     PS=(S(IS)*TIME)
     IF (PS-6.5) 202,202,200
202  DO 200 ITC=1,NTC
     E=EXP(-S(IS)*TIME)
     SUM(ITC,IS)=SUM(ITC,IS)+E*T(ITC,ITM)
     WRITE (3,115) TIME,E,SUM(ITC,IS),C(IS),ITM,ITC,T(ITC,ITM)
200 CONTINUE
   DO 200 IS=1,NS
   DO 200 ITC=2,NTC
     SUM(ITC,IS)=SUM(ITC,IS)/SUM(1,IS)
   WRITE(3,205)
205  FORMAT(6X,SUM(ITC,IS))
   WRITE(3,112) SUM(ITC,IS)
   SUM(ITC,IS)=ALOG(SUM(ITC,IS))
   WRITE(3,207)

```

```

207 FORMAT(6X,SUM(ITC,IS))
   WRITE(3,112)SUM(ITC,IS)
   SUM(ITC,IS)=SUM(ITC,IS)*SUM(ITC,IS)
   WRITE(3,209)
209 FORMAT(6X,SUM(ITC,IS))
   WRITE(3,112)SUM(ITC,IS)
300 CONTINUE
   ASUM=0.0
   WRITE(3,301)
301 FORMAT(5X,S(IS),10X,ALPHA)
   DO 400 ISS=1,NS
   DO 400 ITCS=2,NTC
   ZH=(S(ISS)*X(ITCS)*X(ITCS)/SUM(ITCS,ISS))
   ASUM=ASUM+ZH
   WRITE(3,303) S(ISS),ZH
303 FORMAT(F10.5,F15.10)
400 CONTINUE
   AA=NS*(NTC-1)
   WRITE(3,401)
401 FORMAT(10X,AA)

   WRITE(3,112)AA
   WRITE(3,499)
499 FORMAT(10X,ALPHA)
   ALPHA=(ASUM/AA)
   WRITE(3,112) ALPHA
   GO TO 1
1000 CONTINUE
   CALL EXIT
   END

```

// XEQ KAV1

\*CCFND

1.00 8.69  
0.00 0.1667

0.0057

85.00 98.00 107.0  
79.0 76.0 74.0  
105.0 95.00 88.00  
88.00 99.00 106.0  
90.00 77.00 73.00  
80.00 88.00 89.00  
86.00 93.00 79.00  
103.0 102.0 97.00  
82.05 90.00 98.0  
82.05 80.00 78.00  
74.00 74.00

35

109.0 104.0  
76.0 88.00  
83.00 80.00  
107.0 101.0  
97.00 101.0  
76.0 77.00  
91.00 87.00  
101.0 99.0

2

94.0  
100.0  
77.00  
93.00  
102.0  
83.00  
83.00  
95.00

1

88.0  
108.0  
75.00  
87.00  
95.00  
90.00  
81.00  
90.00  
83.0  
110.0  
77.0  
84.00  
90.00  
98.0  
78.00  
86.00

## APPENDIX 2





```

// JOB
// FOR KAVI
*NONPROCESS PROGRAM
*LOC(CARD,1443 PRINTER)
*LIST SOURCE PROGRAM
*ONE WORD INTEGERS
C      THIS PROGRAM CALCULATES CORRECTION FACTOR AS WELL AS COMBINED EFFECT OF
THE TEMPERATURE PULSES ACCORDING TO EQUATION (5.8.17)
C      *      *      *      *      *
C      ALPHA=THERMAL DIFFUSIVITY
C      AMP=AMPLITUDE OF TEMPERATURE PULSE
C      A=WIDTH OF TEMPERATURE PULSE
C      NK,NY=NUMBER OF VARIABLES
C      PHI1=CORRECTION FACTOR
C      ERF=ERROR FUNCTION
C      DIMENSION TA(20),Y(10),B(10),AMP(10),A(10)
      READ (2,301) NK,NY
301 FORMAT (2I10)
      READ(2,100) ALPHA,DT,TIMX
      READ(2,100) (Y(J), J=1,NY)
      READ(2,100) (B(K), K=1,NK)
      READ(2,100) (AMP(K), K=1,NK)
      READ(2,100) (A(K), K=1,NK)
100 FORMAT (2E10.2)
      TIME=DT
      DO 303 J=1,NY
110 CONTINUE
      T=0.0
      DO 300 K=1,NK
      TA(K)=ALPHA*TIME/(A(K)*A(Y))
      CALL PHI(TA(K),Y(J),B(K),PHI1,NK,NY)
      T=(T+AMP(K)*PHI1)
      WRITE(2,501) TA(K),T,PHI1,B(K),Y(J)
501 FORMAT(1H,5(5X,F10.5))

```

```

300 CONTINUE
TIME=TIME+DT
IF(TIME-TIMX)110,110,304
304 TIME=DT
302 CONTINUE
CALL EXIT
END

// FOR
*ONE WORD INTEGERS
*NONPROCESS PROGRAM
SUBROUTINE PHI(TA,Y,B,PHI1,NK,NY)
X1=2.0-Y+B
YY=2.0*SQRT(TA)
Z1=X1/YY
CALL EPF(Z1,AA,DUMY)
WRITE(3,502) AA
502 FORMAT (1H,(5X,F10.5))
X2=Y-B
Z2=X2/YY
CALL EPF(Z2,BB,DUMY)
WRITE(3,502) BB
X3=-(Y+B)
Z3=X3/YY
CALL EPF(Z3,CC,DUMY)
WRITE(3,502) CC
X4=2.0+Y+B
Z4=X4/YY
CALL EPF(Z4,DD,DUMY)
WRITE(3,502) DD
PHI1=0.5*(AA+BB+CC+DD)
WRITE(3,502) PHI1
RETURN
END

// FOR
*ONE WORD INTEGERS

```

```

*NONPROCESS PROGRAM
SUBROUTINE ERF (X,ERFX,ERFC)
  M=3
  IF(X) 10,11,11
10 X=-X
  AK=-1.0
  GO TO 12
11 AK=1.0
12 CONTINUE
1 FORMAT(6X,44H ERF ARG. GREATER IN ABSOLUTE VALUE THAN 8500)
3 IF(X+.85E+04)2,3,2
3 IF(X+.85E+04)2,4,4
2 WRITE(M,1)
  STOP
4 ZZZ1 =(((((.430638E-4*X+.2765672E-5)*X+.1520143E-3)*X+.92705272E-7
1E-2)*X+.422820123E-1)*X+.705230784E-1)*X+1.0)*.16
  ERFC=1.0/ZZZ1
  ERFX=1.0-ERFC
  ERFX=AK*ERFX
  RETURN
  END

```

ERF000001

ERF000002  
ERF000003  
ERF 0ERF000006  
ERF000007  
ERF000008  
ERF000009  
ERF000010

```

// XEQ KAVI
*CCEND
0.04      1.0      10.0
0.7       1.32     4.0
0.7       3.0
-5.0      -2.0
0.25      0.23

```